OPTICAL ABSORPTION IN DIELECTRIC CRYSTALS

G. D. JONES

A thesis submitted for the degree
of Doctor of Philosophy at the University of
Oxford.

St. John's College,
Oxford.

January 1964

ACKNOWLEDGEMENTS

I would like to express my gratitude to:

Professor B. Bleaney for extending to me the facilities of the Clarendon Laboratory.

Dr. W. Hayes for supervision and encouragement.

Mr. C. T. Sennett for freely making available his theoretical work on the hydride ion problem.

Mr. E. J. Jenkinson, Mr. H. Ridgewell and Mr. V. Rose for building items of apparatus.

Mr. H. Lock for invaluable assistance in the workshop.

Mrs. A. Hurrell for assistance with computing.

The whole staff of the Clarendon Laboratory for their help at various times.

Dr. F. A. Johnson, Dr. J. P. Russell and Mr. J. E. Quarrington of R.R.E. Malvern for advice on infrared spectroscopic techniques

The Commissioners for the Exhibition of 1851 for the award of an Overseas Scholarship (1960 - 1963).

ABSTRACT

When a defect is introduced into a lattice it modifies the lattice vibrations in two ways. First there is a modification of the amplitude of the vibrations as a function of frequency. This is greatest in the immediate vicinity of the defect and negligible at large distances from it. The second is that new frequencies of vibration may appear. These are the localised modes. If the impurity has a much lighter mass than any of the constituent atoms of the lattice the frequency of this vibration is considerably higher than any of the lattice frequencies and the amplitude of the mode falls off rapidly away from the defect. The resultant mode is well localised and is almost solely confined to the defect atom itself.

Localised modes of this type are a subject of investigation in this thesis. The particular system studied was that of substitutional hydride and deuteride ions in the alkaline earth fluorides. The localised vibrations of these defects were detected as absorption lines in the infrared spectra of these crystals. The fundamental, second harmonic and a third harmonic doublet were measured for both the hydrogen and deuterium impurities. The lines display a marked temperature dependence and this was measured in the temperature range 4°K to 300°K.

Mr. C. T. Sennett of this laboratory has developed a theory appropriate for localised vibrations of light impurity atoms in lattices and this was used to interpret the observations. The existence of harmonic lines indicated that the light atom is present as a negative

ion at a tetrahedral fluorine site. The deviation of the harmonic lines from exact harmonicity and the temperature shift of the peak position and width are attributed to anharmonic effects. The experimental data was sufficient to determine the magnitude of these anharmonic forces to terms quartic in the light ion's displacement.

Satellite lines are present around the main vibration lines and these are ascribed to perturbations of the light impurity ion by nearby lattice defects and, in the case of the more distant lines, to light impurity ions present in lattice sites of different symmetry. The light impurity ion thus can be used as a probe to investigate other defects in the fluorite lattice.

Broad sidebands occur equally spaced in frequency about the main line. These bands are interpreted as multiphonon combination bands arising from the simultaneous excitation or decay of lattice phonons with excitation of the local mode phonon. The frequencies of these bands were used to determine the frequencies of peaks in the density of states of various branches of the dispersion curves of the three alkaline earth fluorides. These impurity induced lattice bands are experimentally more accessible than the pure lattice combination bands and thus offer a simpler method of determining dispersion data for these crystals.

Nickel and cobalt ions can be introduced into lithium fluoride crystals in sufficient concentration for their optical absorption to

to be detectable. These ions substitute for the lithium and are thus octahedrally surrounded by six fluorine ligands. The measured spectra were interpreted on the basis of the crystal field theory of Tanabe and Sugano in the cubic field approximation. Spin-orbit coupling effects were included in the analysis.

Room temperature X-irradiation of pure lithium fluoride crystals results in the formation of intrinsic lattice defects of which the F and M centres are the most well established. The F centre consists of an electron bound to a negative ion vacancy while the M centre is believed to be a pair of F centres. Interesting phenomena are observed after irradiation of lithium fluoride crystals containing nickel and cobalt. The nickel impurity strongly suppresses the formation of both the F and M centres while the cobalt impurity has little effect. The specific effect of the nickel impurity is related to the strong electron trapping properties of this ion. This interpretation is consistent with earlier electron spin resonance measurements on the irradiated crystals.

While investigating the irradiation behaviour of pure and iron group impurity doped lithium and sodium fluoride crystals an absorption due to a V centre of the molecular F_2^- ion type was observed. This centre has been shown by Känzig (by electron spin resonance methods) to consist of an isolated hole located on two neighbouring fluorine ions.

The optical absorption of this centre in the two lattices differ in some respects. The frequencies are similar (28700 cm^{-1} for LiF and 27300 cm^{-1} for NaF), but the disorientation temperatures (at which the centres are just mobile) differ, being 114°K for LiF and 155°K for NaF.

Several

Several transition metal compounds exhibit antiferromagnetic ordering phenomena at low temperatures. These affect the frequency of optical absorption lines slightly and the onset of the ordering may be studied, in suitable cases, by the temperature dependence of the frequency of sharp optical absorption lines. Experiments of this type performed on MnF_2, $KMnF_3$ and $KNiF_3$ revealed a marked frequency shift of sharp absorption lines in the spectra of these substances near the Néel temperatures. The magnitude of such shifts is discussed.

The optical absorption of trivalent rare earth ions are characterised by the presence of groups of sharp weak lines which arise from transitions within the $4f^n$ configuration. In a suitable host lattice the rare earth ions may be present in cubic symmetry sites and the structure of the line groups is then readily amenable to analysis.

The optical absorption of holmium in calcium fluoride was investigated as a typical example of such systems. The line group positions were interpreted using the electrostatic and spin-orbit matrices for the

f^{10} configuration. The structure of the line groups indicated that the holmium ions were not in cubic symmetry sites, but were perturbed by the presence of adjacent charge compensating defects, and an analysis of this structure was not attempted.

The occurrence of the holmium in noncubic sites is consistent with the electron spin resonance observations which show that only 2% of trivalent holmium ions, namely those on cubic sites, undergo conversion into the divalent form.

An experimental study of various ferrous iron compounds revealed a large (approximately 1500cm^{-1}) splitting of the broad absorption band near 10000 cm^{-1} in all the compounds. This band arises from the $^5T_2(^5D) \rightarrow {}^5E(^5D)$ transition of the $3d^6$ configuration. This splitting cannot be due to spin-orbit coupling effects or, in the case of the cubic crystals, to low symmetry fields. It was attributed to a dynamic Jahn Teller distortion of the upper E_g level. The magnitude of such splitting is discussed on this model.

In analogy to the molecular F_2^- ion V centre of the alkali halides, a centre of similar type occurs in the alkaline earth fluorides. This was detected by J. W. Twidell of this laboratory using electron spin resonance methods. This centre possesses <100> symmetry in contrast to the <110> symmetry shown by the alkali halide centres and this is due to the different symmetries of the two lattices. An optical absorption band present at 28000cm^{-1} in irradiated crystals of calcium fluoride doped with thulium is tentatively assigned to these centres.

CONTENTS.

CHAPTER ONE.

OPTICAL ABSORPTION BY THE VIBRATIONS OF HYDROGEN AND DEUTERIUM IMPURITIES IN THE ALKALINE EARTH FLUORIDES.

1. INTRODUCTION.

In this chapter an investigation of the localised vibrations of hydrogen and deuterium present as substitutional impurities in crystals of the alkaline earth fluorides is described.

1.1 Crystal Structure of the Alkaline Earth Fluorides.

The fluorides CaF_2, SrF_2, BaF_2 belong to the space group O_h^5. The metal and two fluorine ions (F_1 and F_2) lie in face centred cubic lattices. The lattices of F_1 and F_2 are displaced along the body diagonal of the metal ion lattice by $\frac{1}{2}r_o(1,1,1)$ and $\frac{3}{2}r_o(1,1,1)$ respectively, where $2r_o$ is the lattice constant. Each metal ion is surrounded by four of both types of fluorine ions, the eight ions forming a cube about it. Each fluorine ion is at the centre of a tetrahedron of metal ions. Alternatively, the crystals may be considered to have a body centred structure; each metal ion is at the centre of a cube of eight fluorines and every second cube of fluorines is empty. (Figure 1).

1.2 Optical Properties of the Alkaline Earth Fluorides.

The alkaline earth fluorides are transparent from the far ultraviolet to the middle infrared. Of the three fluorides, calcium fluoride has the farthest ultraviolet transmission, being only surpassed

Fig. 1. The Fluorite Lattice.

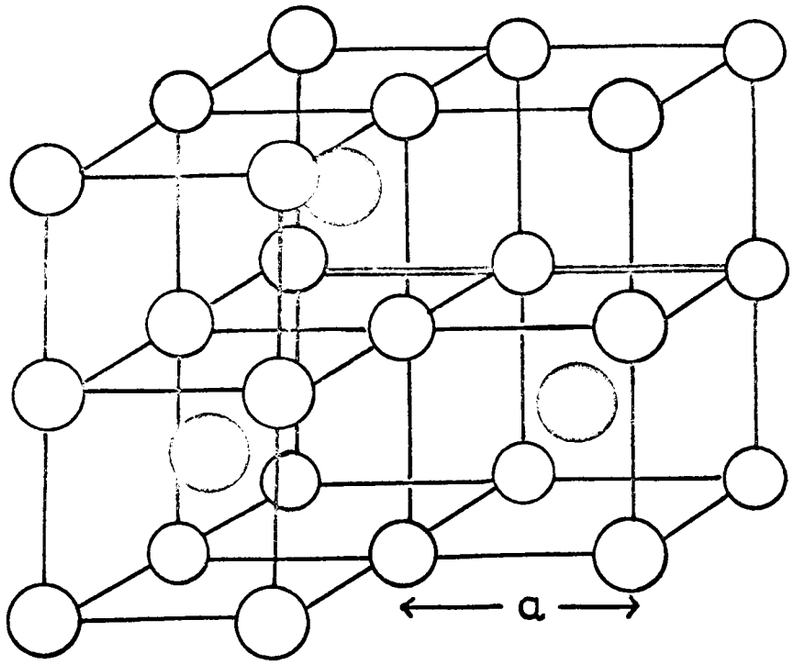

←unit cell dimension→

Ca^{2+} ○ F^- ○

a = fluorine – fluorine spacing

2a = 5·45 A° for CaF_2

= 5·78 A° for SrF_2

= 6·19 A°. for BaF_2

Cleavage planes are ⟨111⟩

Cleavage edges are ⟨110⟩

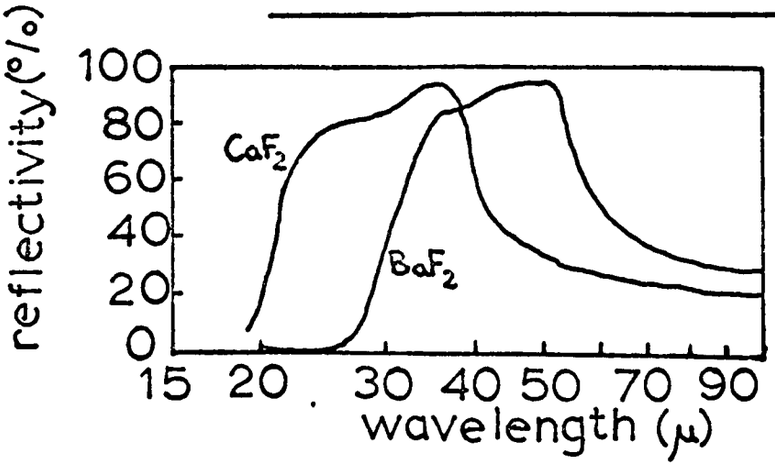

Fig. 2. Reflectivities of CaF_2 and BaF_2 single crystals obtained at the incident angle of 12°.
(Mitsuishi, Yamada and Yoshinaga, 1962)

in this respect by lithium fluoride, while barium fluoride has the farthest infrared. The absorption edges at room temperatures are given in tables 1 and 2.

On the ultraviolet side the transmission is restricted by electronic excitation; the exciton absorption maximum peak is about 20% higher in frequency than the absorption edge. Freytag (1960) has studied the frequency shift in the absorption edge with temperature for calcium fluoride.

On the infrared side the transmission is restricted by the onset of reststrahlen absorption, i.e. the absorption arising from atomic vibrations possessing a dipole moment. Lowering of the temperature causes the absorption coefficient to decrease on both sides of the reststrahlen absorption frequency and this is evident by the shift of the absorption edge to longer wavelengths (Table 2).

The reflectivity of the fluorides is low throughout the region of optical transparency, but attains high values in the dispersion region of large reststrahlen absorption. Mitsuiski, Yamada and Yoshinaga (1962) give the values of the reflection peaks as 34 μ for calcium fluoride and 45μ for barium fluoride, and absorption peaks as 37 μ for calcium fluoride and 52μ for barium fluoride. The reflection maximum lies at slightly shorter wavelengths than the absorption maximum (the Havelock formula; Born and Huang (1954) page 122). The reflection band has a subsidiary peak; the shape of the band is given in Figure 2.

TABLE 1. ABSORPTION EDGE IN THE VACUUM ULTRAVIOLET.

(Smakula (1962)).

Crystal	Absorption Edge (μ).
CaF_2	0.12
SrF_2	0.13
BaF_2	0.15

TABLE 2. ABSORPTION EDGE IN THE INFRARED.

(Kaiser et.al.(1962)).

Crystal.	Absorption Edge* at Room Temperature (μ)	Absorption Edge* at Liquid Nitrogen Temperature (μ).
CaF_2	11.8	12.4
SrF_2	13.7	14.7
BaF_2	15.2	16.4

* the absorption edge is defined here as the wavelength at which the crystal has an absorption coefficient of $10cm^{-1}$.

Raman absorption in calcium fluoride was first reported by Rasetti (1931). The temperature dependence of the position and halfwidth of the one single Raman line observed has been studied by Press (1950). At 40°C, the line has a frequency of 321.5cm and a width of 8.7cm^{-1}; at 280°C it is 312.2cm^{-1} with width 20.8cm^{-1}. Raman absorption in barium fluoride has been observed by Krishnan and Narayanan (1963). It consists of,a single line corresponding to a Raman frequency of 244,0cm^{-1}.

The most recent detailed experimental investigation of the infrared properties of the three fluorides is that of Kaiser et.al (1962). They measured the reflectivity of the crystals through the dispersion region and also examined the absorption of the crystals on the high frequency side of the reststrahlen absorption. The experimental data was analysed on classical dispersion theory using one strong and one weak resonance to fit the data. The strong resonance was identified as the transverse optical made of vibration for $\underline{k} \simeq o$; from this the corresponding longitudinal optical made was calculated by the Lyddane, Sachs, Teller relation.

The weak resonance frequency was interpreted as a two phonon combination band (transverse optical and acoustical). For calcium fluoride, it is close to the Raman line frequency, while in barium fluoride these two frequencies differ considerably. The results of the analysis are given in Table 3.

Fray, Johnson and Quarrington (1963) have determined the energies of the optical and acoustic branches of calcium fluoride from the

Table 3 Optical Frequencies for the Alkaline Earth Fluorides. (from Kaiser et.al. (1962))

Optical frequency	CaF_2	SrF_2	BaF_2
Transverse optical	257	217	184 cm^{-1}
Longitudinal optical	463	374	326 cm^{-1}
Secondary reflection peak	328	316	278 cm^{-1}

frequencies of two and three phonon summation bands observed in the absorption spectrum of calcium fluoride in the 5-22 micron region. Their results for the longitudinal and transverse optical made frequencies at $\underline{k} = o$ are in agreement with those of Kaiser et.al (1962). The values obtained for the frequencies of the branches of the dispersion curve at critical points in the frequency spectrum of the density of states are:

LO_1 $368cm^{-1}$

TO_2 $325cm^{-1}$

LO_2 $286cm^{-1}$

TO_1 $262cm^{-1}$

TA $149cm^{-1}$

The results given here for the optical properties of the pure alkaline earth fluorides will be further discussed in Section 6.2 and will be employed in the interpretation of the hydrogen impurity induced lattice absorption bands described in Section 8.2.

1.3 Previous work on the Infrared Absorption of Calcium Fluoride Crystals containing Impurities.

Bontinck (1958) investigated the reactions which occur when crystalline calcium fluoride is heated strongly in moist air and reported 4 infrared absorption bands (at 3650, 3580, 1480 and 1415 cm^{-1}) which he assigned to vibrations and torsions of the hydroxyl ion substituting for fluorine in the calcium fluoride lattice.

This conclusion has been criticised in part by Wickersheim and Hanking (1959) who attribute the 1480 and 1415 cm^{-1} bands to calcium carbonate impurity. They observed a further band at $880cm^{-1}$ also due

to carbonate. These three bands could be made to disappear by grinding away the outer faces of the crystals. Confirmation of the assignment of the 3650 and 3580 cm^{-1} as due to hydroxyl ion impurity was shown by deuteration; the 3600cm^{-1} lines then occurred near 2700cm^{-1}.

1.4 Analogous Work on the Infrared Vibrations of Hydrogen and Deuterium in the Alkali Halides.

Investigations, similar to the work carried out here on the alkaline earth fluorides, were first made by Schäfer (1960) on the localised vibrations of hydrogen in alkali halide crystals containing U centres.

The existence of U centres has been known for some considerable time. They were initially detected by the characteristic absorption band in the ultraviolet spectrum of alkali halides containing a small percentage of the corresponding alkali metal hydride. For potassium bromide this band occurs at 2280A°. The model for the U centre is that of a negatively charged hydrogen ion occupying a halide site. (Mott and Gurney (1950)). Considerable research has been done on the optical bleaching and thermal annealing properties of these centres and this has been summarised by Seitz (1953). Spin resonance work on the same centres has been described by Delbecq, Smaller and Yuster (1956) and the results discussed by Delbecq and Yuster (1956).

The localised vibrations of the U centres were first observed by Schäfer in the infrared absorption spectrum of alkali halide crystals containing U centres. For potassium chloride, he observed a line of frequency 490cm^{-1} and width 30cm^{-1} at room temperature, which narrowed on cooling to become 4cm^{-1} wide at pumped liquid nitrogen temperature

(57°K). Analogous lines were found in several other alkali halides.

Fritz(1962) studied the low temperature optical bleaching properties of the U centre vibrational lines, and observed the formation of an infrared band at approximately half the frequency of the U centre vibration. This band consisted of groups of lines possessing different annealing temperatures, and was attributed by him as due to vibrations of interstitial hydrogen atoms situated at varying distances from an anion vacancy.

A later paper by Fritz (1963) describes the observation of the corresponding localised vibration of deuterium in deuterated potassium chloride at a frequency of $360cm^{-1}$. Both this line and the hydrogen vibration line show a T^2 dependence of the halfwidth on temperature. Two side bands are also present about these lines; one at higher and one at lower frequency and at about equal spacing from the main line. The high frequency satellite shows little change on cooling, while the low frequency satellite's absorption decreases as $\exp\left(-\frac{w}{kT}\right)$ on cooling. For potassium chloride, w was approximately $60cm^{-1}$. These satellite bands were attributed to a simultaneous excitation (high frequency sideband) or decay (low frequency sideband) of a lattice phonon caused by an interaction of the localised light atom vibration with lattice vibrations.

Other work on the infrared absorption of U centres includes that of Mitsuishi and Yoshinaga (1963[a,b]) who observed the hydrogen and deuterium lines in potassium chloride. They reported slightly larger widths for the deuterium line compared to the hydrogen line at all temperatures. They also showed that the U centre, after bleaching to

less than half initial intensity by strong U light irradiation could be recovered at almost original intensity by heating the crystals to 200°C.

Price, Smart and Wilkinson (1963) have measured the U centre localised vibration frequencies in a wide range of hydrogenated and deuterated alkali halides. These frequencies were also calculated on the basis of the Born-Mayer theory of ionic interaction for these alkali halides.

A theoretical study of the broadening mechanism responsible for the strong temperature dependence of the line width of the U centre has recently been carried out by Hanamura and Inui (1963). Their proposed mechanism for the broadening is a fourth order anharmonic interaction in which a localised vibration mode decays into three lattice phonons. They obtained good agreement with experimental data. [redacted] They consider the contribution of the other possible anharmonic interactions to the broadening as negligible.

The localised vibration lines of H^- and D^- in the alkali halides have both similarities and differences to the spectra reported here for the same impurities in the alkaline earth fluorides.

The differences largely arise from differences in the respective crystal lattice structures and will be discussed, where appropriate, later.

2. PREPARATION OF HYDROGENATED AND DEUTERATE CRYSTALS OF THE ALKALINE EARTH FLUORIDES.

The work of Hall and Schumacher (1962) on the electron spin resonance spectrum of interstitial hydrogen and deuterium atoms in calcium fluoride has shown that it is possible to introduce hydrogen and deuterium into the fluorite lattice. They prepared their samples by first heating together pure calcium fluoride crystals and aluminium metal for several hours at 900°C in the presence of a few centimetres pressure of hydrogen (or deuterium) gas, and subsequently irradiating the crystals for four hours at room temperature with 30 kilovolt, 30mA X-rays. The resulting crystals appeared very black in reflection and were essentially opaque in transmission for pieces as thin as 1mm. They estimated that densities of interstitial atomic hydrogen as high as $10^{19}/cm^3$ could be obtained by this method. The paramagnetic centres were thermally stable to at least 50°C.

The first part of this method of preparation was employed here to produce substitutional hydride ions in the alkaline earth fluorides. Evidence will be presented later to justify the assumption that the observed infrared absorption lines are due to substitutional hydride ions on fluorine sites.

The starting material was crystals of the pure alkaline earth fluorides as supplied by Mervyn Instruments Ltd. These crystals had been grown from natural (or synthetic in the case of strontium and barium fluorides) materials previously purified by repeated recrystallisations, in a vacuum furnace by the Stockbarger method. 5% by weight of lead fluoride was added to the melt prior to the growing to remove any oxygen or similar impurities present.

Suitable pieces of the pure crystals as supplied were heated in the presence of aluminium metal in a quartz tube to 500°C in 30 minutes under high vacuum. Hydrogen or deuterium gas was admitted to a pressure of two thirds of an atmosphere and the temperature raised to 800°C and maintained for 8 hours. After cooling, the crystals were cleaved to size. For optical measurements two plane parallel faces were ground and polished on the crystals. These faces were usually <111> planes. Polishing methods were conventional and involved the successive use of 45,8,3 and ¼ micron grades of "Hyprez" diamond polishing compound on a paper lap.

The crystals were pink to colourless in the case of calcium fluoride, yellow-green to colourless in the case of strontium fluoride and dark green to colourless in the case of barium fluoride. There was no apparent correlation between the amount of hydrogen present and the intensity of colouration. The colour, in all cases, corresponds to that reported for weak additive colouration of the alkaline earth fluorides by the corresponding alkaline earth metal and occurs here in the samples which have not been completely decolourised by the hydrogen gas.

The density of hydride ions could be approximately calculated from the Smakula formula (Sedtion 5.5). It is estimated that densities of up to $10^{19}/cm^3$ have been obtained by this method of preparation.

During the course of this work, Görlich et. al. (1963) reported the observation of identical infrared lines to those reported here, in the room temperature absorption spectrum of calcium fluoride crystals which had been strongly additively coloured. Johnson (private communication) has observed the fundamental vibrational line of the hydride ion in

nominally pure calcium fluoride at 4°K. His results correspond to a hydride ion density of $4 \times 10^{15}/cm^3$.

Hall and Schumacher (1963) describe a weak paramagnetic resonance spectrum of interstitial hydrogen atoms in synthetic fluorite that had been heated either in a vacuum or in helium gas. Sierro (1962) has observed the same spectrum in natural fluorite.

Analogous observations have been reported for the substitutional hydride ions (U centres) in the alkali halides. Crandall (1963) has shown that weak U centres may be formed by heating additively coloured potassium bromide crystals in air.

It is evident that either fluorite initially contains hydrogen in some form or there is moisture present at some stage during the growing or subsequent heating of the crystal. The moisture could undergo reaction with the metal (aluminium or calcium) when heated producing hydrogen which diffuses into the crystal.

3. DESCRIPTION OF THE APPARATUS.

The infrared absorption spectra were measured on an infrared spectrometer incorporating a modified Leiss double monochromator.

The Leiss double monochromator has been described in detail by Roberts(1953). It was adapted for this work to use plane gratings. The first or foreprism section served no useful purpose in the infrared region covered in this work and was fitted with a plane mirror in the foreprism holder to direct the infrared radiation from the first to the intermediate slit. The second section was equipped with holders to take a range of gratings of dimensions either 2" x 3" or 3" x 3". A series

TABLE 4. GRATING SPECIFICATIONS.

Grating.	Dimensions.	Ruling (lines per inch).	Blaze Wave-Length.	Range covered	Higher order Filter
Merton NPL	3" x 2"	7500	3.5	3-3.5 3.5-4.5	Ge InAs.
Bausch and Lomb	3" x 3"	3750	6	4-7 7-8	InAs InSb
Merton NPL	3" x 2"	2500	10	7-12	InSb
Bausch and Lomb	3" x 3"	1850	12	7-16 11-20	InSb Ge* Inter-ference
Bausch and Lomb	3" x 3"	975	22.5	17-25	Ge* Inter-ference

* Germanium interference filter supplied by Optical Coating Inc., Santa Rosa, California. This filter was opaque (<o.1% transmission) to 10.5 μ and had a transmission exceeding 40% in the range 11 to 25 μ.

The other filters are bloomed semiconductor filters supplied by Grubbs Parsons Ltd.

TABLE 5. DEWAR WINDOWS.

Wavelength Range.	Outside Windows	Inside Windows.
3 to 7	Ca F_2	CaF_2
7 to 16	NaCl or KRS5	Cs Br.
16 to 25	KBr or KRS5	Cs Br.

of gratings covering the range 3 to 30 microns in first order throughout was available. Specifications of these gratings are given in Table 4. All unwanted higher order spectra were removed by use of the appropriate semiconductor or interference filter, which are also listed in Table 4. Curved slits were installed in place of the original straight slits and these partially compensated for aberrations in the spherical mirror optics.

The radiation source was a globar type constructed for a Morgan "crusilite" furnace element. For the near infrared, and alternative source available was a tungsten filament lamp with a magnesium oxide window.

The usual detector was a Golay pnuematic cell with a potassium bromide window which, with associated chopper and electronics, was supplied by Unicam Ltd.

The spectrometer was a single beam instrument and so a careful comparison between the crystal spectra and the background spectra was necessary to detect any absorption due to the crystal itself. This became difficult in the middle of the strong water absorption band at six microns and there it was necessary to resort to a tedious and time consuming "in-out" plotting of the absorption with wavenumber through the region of interest in order to extract significant spectral information such as peak position and halfwidth. Some attempt was made to reduce water absorption by use of drying agents in the monochromator, but the rather open arrangement of the dewar and detector optics prevented any worthwhile improvement being achieved.

For measurement of wavenumbers of the observed lines and for calibration

of the spectrometer, the accurately known absorption lines of the infrared spectra of water vapour, ammonia, methane, carbon monoxide, carbon dioxide and hydrogen chloride given in the International Union of Pure and Applied Chemistry Tables (1961) were utilised in the appropriate Spectral regions. Figures 3-7 show some typical gas calibration spectra and indicate the performance obtainable with the spectrometer. Resolution of better than $1cm^{-1}$ was achieved throughout the spectral range 3 to 18 microns.

For low temperature spectral measurements a dewar based on the design of Roberts (1953) was built. This dewar is shown in Figure 9. . It has several advantages over the usual type, namely:-

(1). The crystal specimen may be moved out of the path of the radiation beam while at low temperatures. This enables low temperature "in-out" spectra to be plotted and eliminates errors that could arise through the use of a reference spectrum run sometime before or after the recording of the low temperature spectrum. It also allows compensation for any absorption due to the dewar windows as well as that due to atmospheric water vapour and carbon dioxide.

(2). Cooling of the crystal was by helium exchange gas. The crystal on its mount was placed in a small chamber fitted with infrared transmitting windows capable of withstanding cooling to x low temperatures. A few millimetres pressure of helium gas was sufficient to cool the crystal in a matter of minutes to within 1°K of the temperature of the liquid refrigerant. This method of cooling removes any necessity for clamping the crystals onto a copper block in contact with the refrigerant, and relying on thermal conduction to cool them. The method also ensured

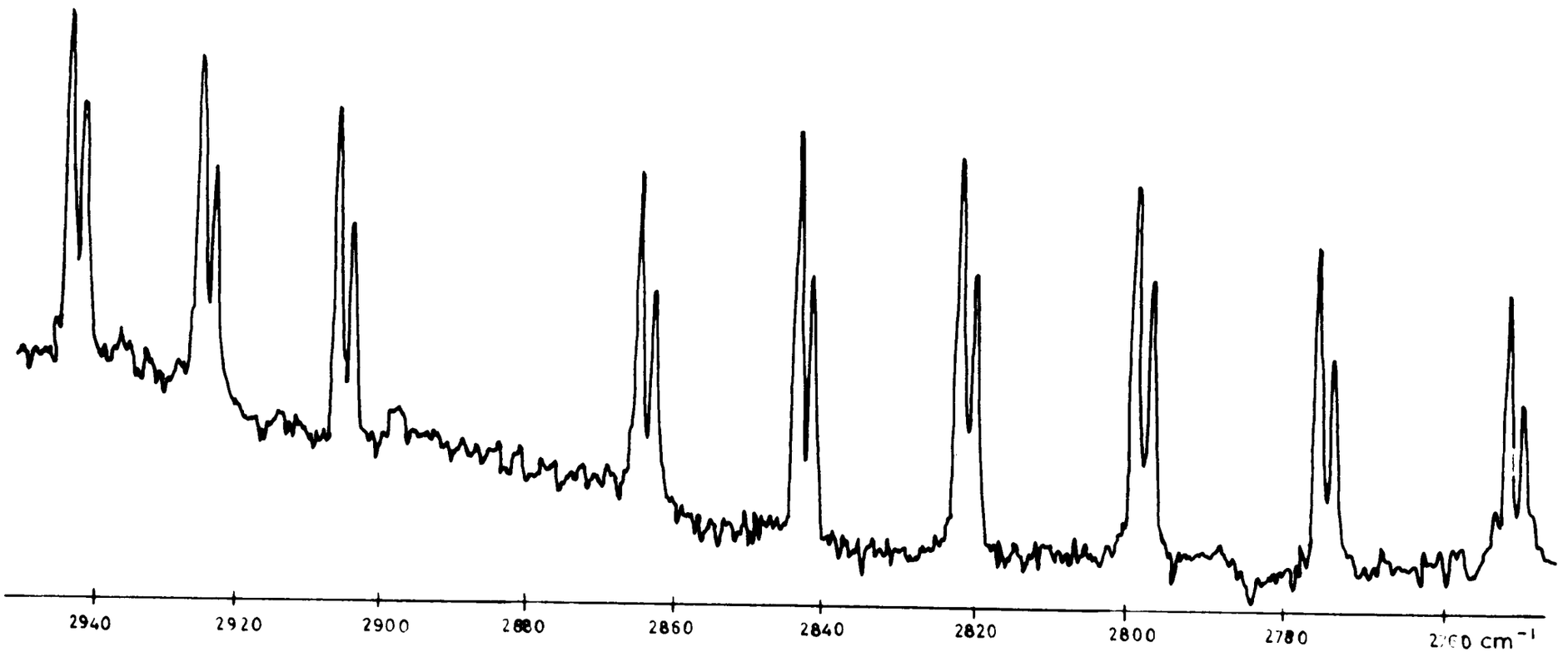

FIGURE 3 Spectrometer recording of the 3·5μ absorption band of hydrogen chloride using a 3·5μ, 7500 line/inch grating in first order

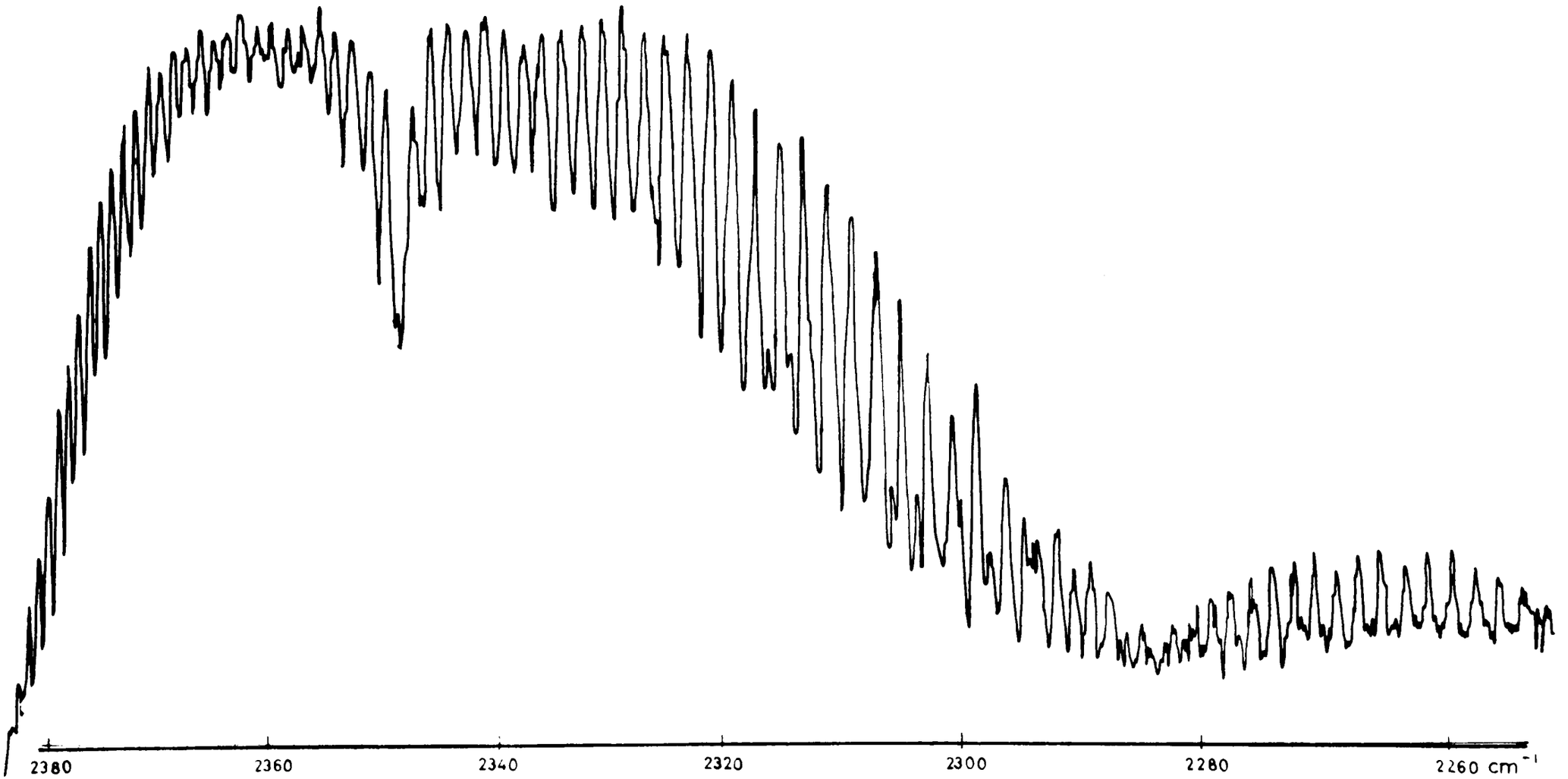

FIGURE 4 Spectrometer recording of the 4·3μ atmospheric carbon dioxide band, using a 3·5μ, 7500 line/inch grating in first order.

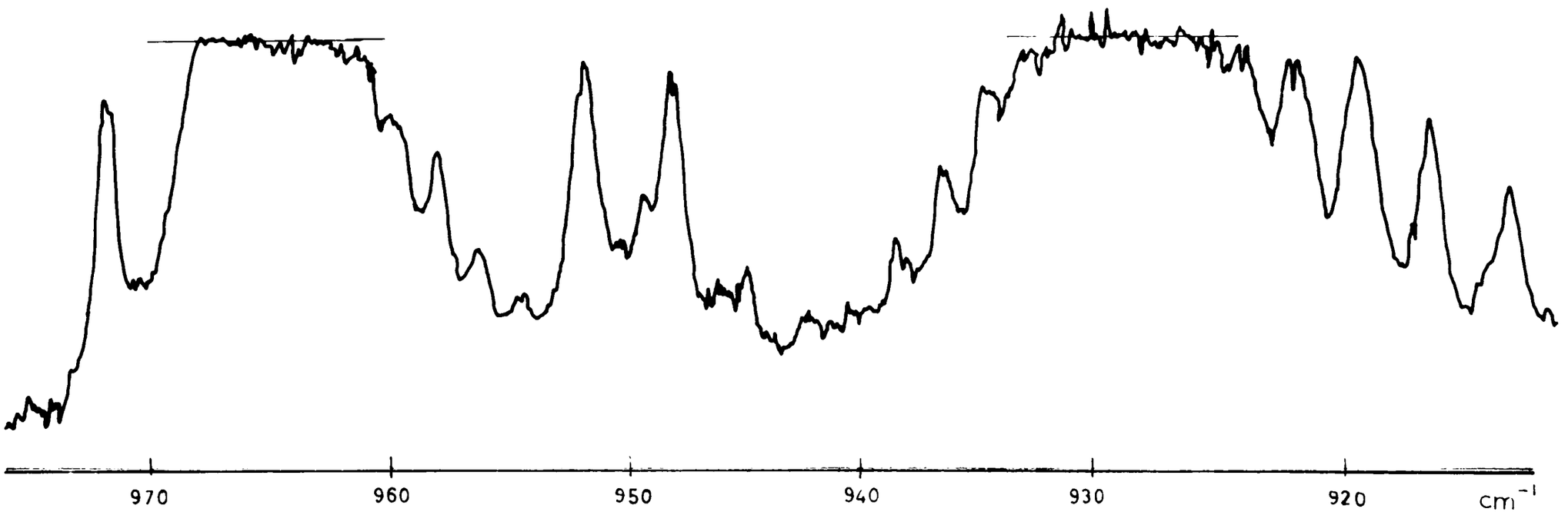

FIGURE 5 Spectrometer recording of the 10·5μ ν_2 absorption band of ammonia, using a 12μ, 1850 line/inch grating in first order.

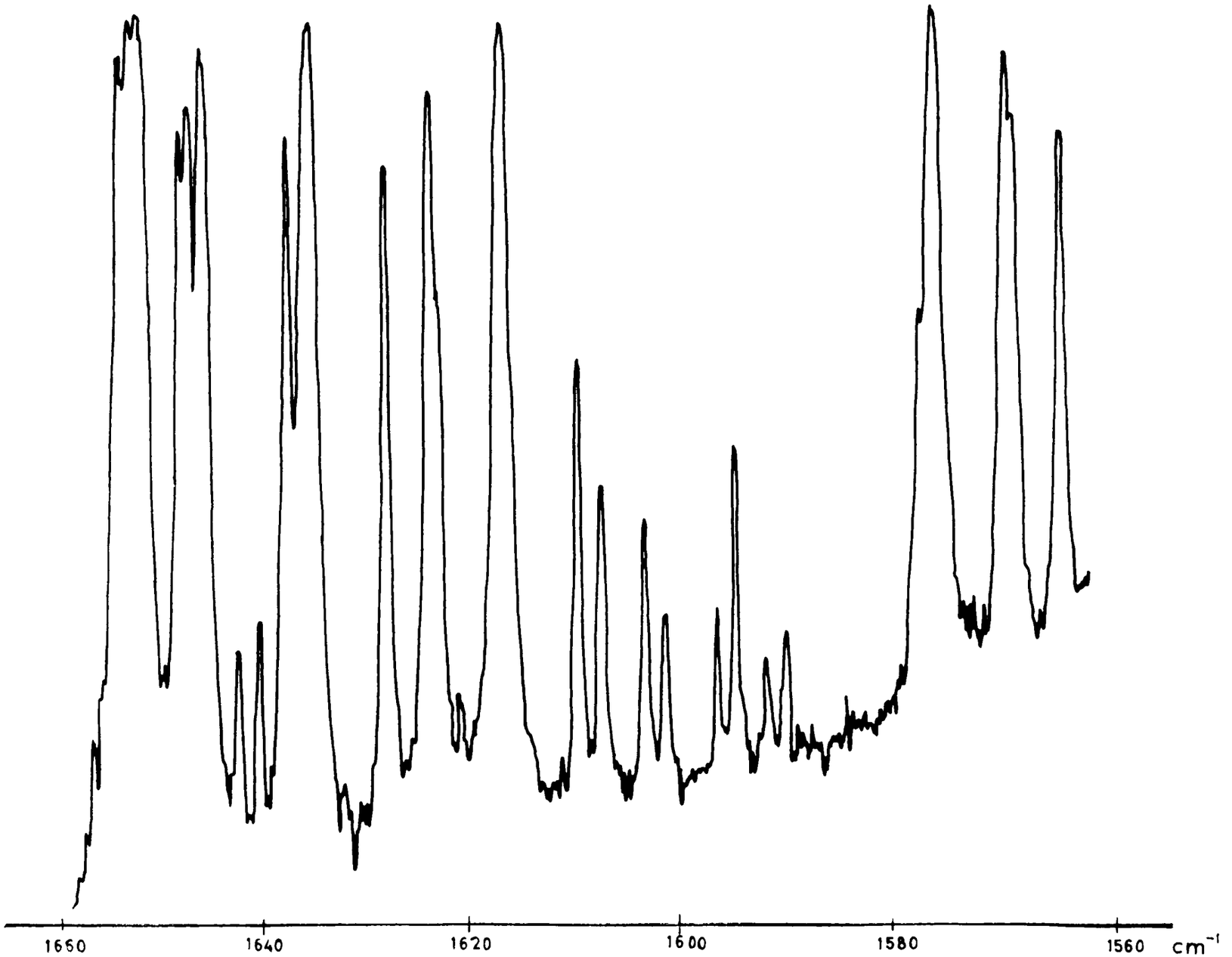

FIGURE 6 Spectrometer recording of atmospheric water-vapour absorption near 1600 cm^{-1}, using a 6μ, 3750 line/inch grating in first order.

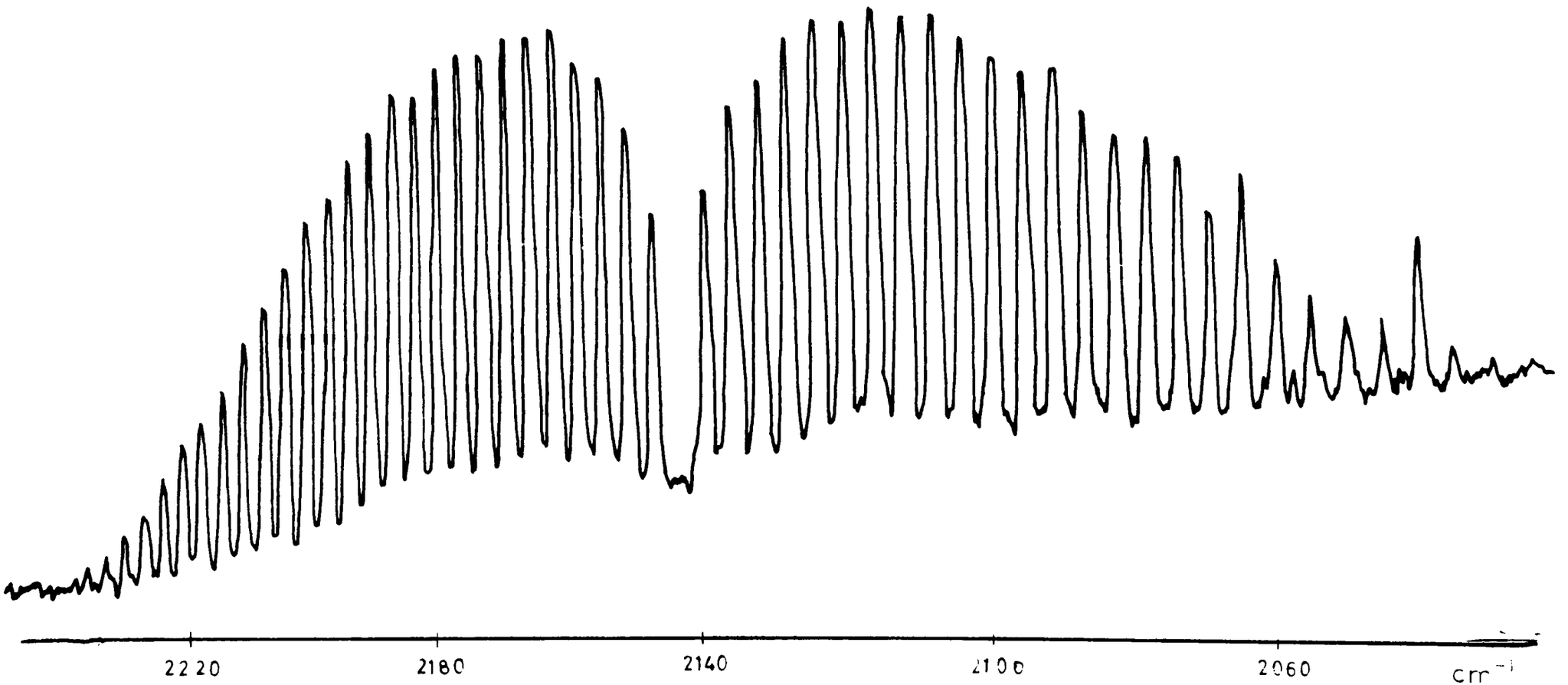

FIGURE 7 Spectrometer recording of the 4.7μ absorption band of carbon monoxide, using a 6μ, 3750 line/inch grating in first order

that thick crystals (such as the 6.9cm total thickness specimen used for detection of the third harmonic of the localised vibration of deuterium in calcium fluoride) were cooled despite their size.

An obvious disadvantage of the dewar is the need to provide low temperature infrared transparent windows for the helium exchange gas chamber. Four windows in all, instead of the usual two, are thus required in this dewar and the two inner windows have to be fitted to a suitable coolable and demountable vacuum seal. Such a seal has been described by Roberts (1954,1959) and was used in this dewar. The only modification was the substitution of P.T.F.E. gaskets for the polythene ones specified. These were not quite as satisfactory in their vacuum sealing properties, but did not crack after one or two cooling cycles as the polythene gaskets often did.

The absorption due to the two extra windows was kept low by a suitable choice of window material. A typical selection is given in Table 5. It was usually necessary to repolish the sodium chloride and potassium bromide windows after each low temperature run, particularly as any slight tendency of the dewar to cool these windows aggravated their hygroscopic nature. However, these alkali halide windows were preferable to those of KRS5 because of their lower reflection loss.

The dewar was continually evacuated during use by a 70 litre/second "Edwards" diffusion pump. This had sufficient speed to cope with any slight leaks of helium exchange gas, which sometimes occurred, through the low temperature window seals into the dewar vacuum space.

In the temperature variation experiments in which the observed line

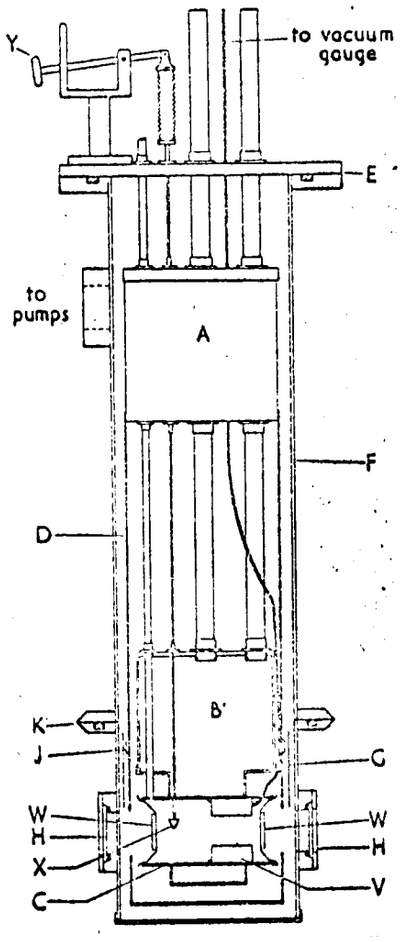

Fig: 9 Schematic layout of absorption cell with specimen holder removed. (Roberts, 1955)

had to be plotted out for various temperatures between 4°K and room temperature, there was sufficient thermal inertia in the exchange gas chamber and the crystal mount to maintain the temperature to within ±10°K of the required value for the time required (10-15 minutes). The temperature of the crystal was monitored by a gold + 2.11% cobalt alloy verus copper thermocouple with one junction at liquid nitrogen temperature and the other junction fixed to the crystal mount. This thermocouple was initially calibrated using the fixed points of water, dry ice, liquid nitrogen and liquid hydrogen.

The performance of the Golay detector was adequate for most of the spectral measurements. One exception was in the case of the fundamental vibration frequency of deuterium in calcium fluoride lattice/is large and where the absorption of the calcium fluoride there the spectrometer sensitivity(and resolution)is only marginal. To improve the performance of the spectrometer for this particular measurement a zinc doped germanium alloy photoconductive detector was constructed. This detector utilises the second impurity level of zinc at 0.095 eV above the valence band of germanium; the first level at 0.035 eV is compensated by addition of an n type impurity to the alloy; usually antimony. The detector has a response peaking at 12μ and will only operate at temperatures below 40°K. The required alloy was supplied by Mullards Ltd.

For the experiments here the detecting element was mounted in a holder just behind the doped calcium fluoride crystal in the same cryostat and so was operated at the same temperature as the crystal, viz. 20°K or 4°K. With this arrangement for the detector, liquid nitrogen temperature spectra could not be recorded. However, the elimination of the three

[illegible] that

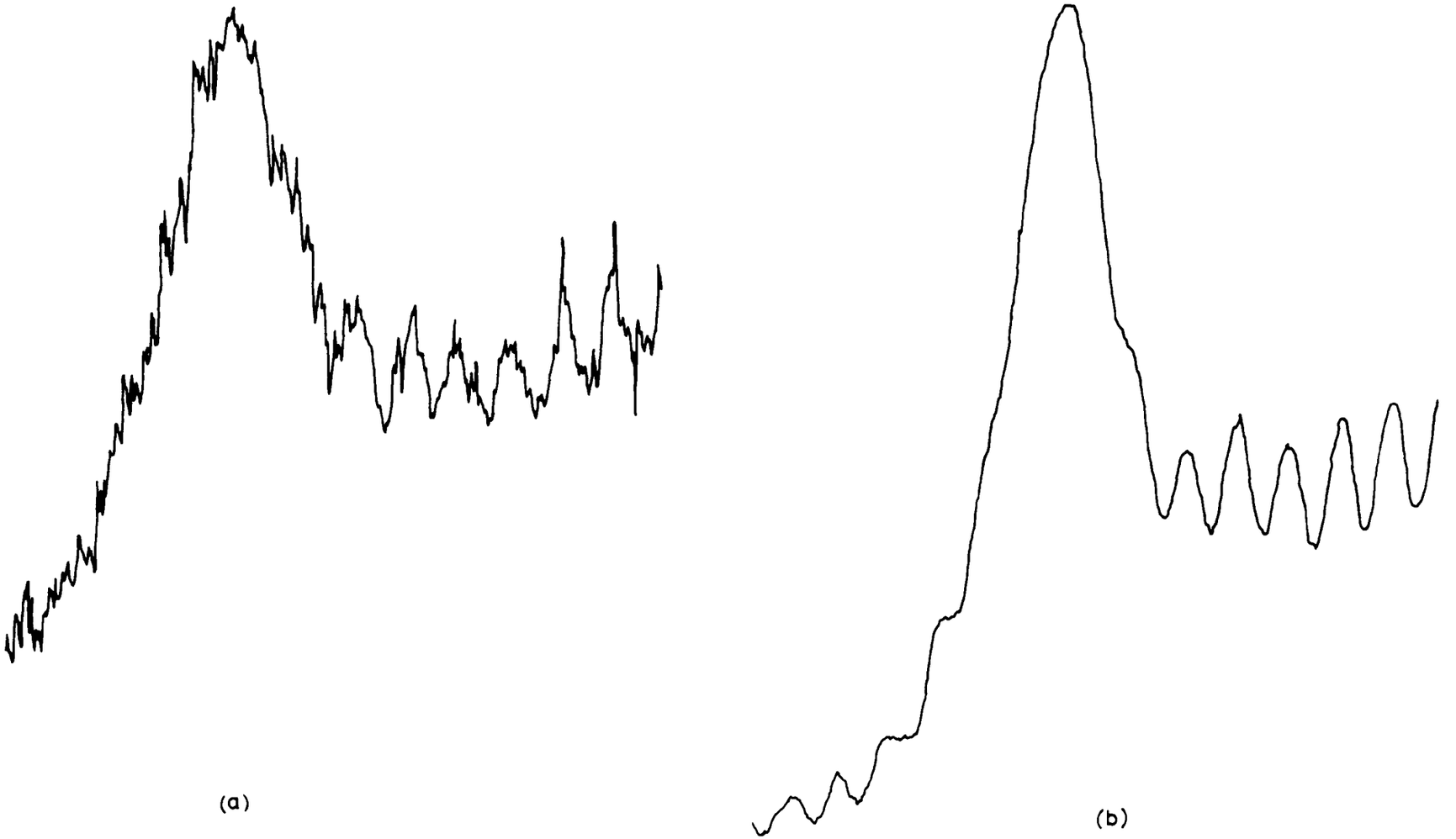

Fig 10 Recordings of the fundamental frequency of the localised vibration of deuterium in calcium fluoride at 20°K
(a) with the Golay detector
(b) with the zinc doped germanium detector
The small bands are 15μ atmospheric carbon dioxide absorption lines

windows that would be necessary were a separate cryostat used for the detector, was considered necessary for the attainment of maximum ultimate sensitivity.

The method of preparing the detecting element is as follows:

(1). The optimum size is first calculated. The cross section must be identical in size to the image from the spectrometer. The depth of the specimen depends on the absorption coefficient of the particular alloy for radiation of wavelengths where it has peak response. It is chosen as the best compromise between too great a depth, where the back section beyond the absorption depth acts as an electrical shunt, and too small a depth which results in a very high detector resistance (hundreds to thousands of megohms), which renders subsequent signal amplification difficult.

The size of detecting element used here was 5mm x 1mm x 5mm deep. This had a resistance of 200 megohms at liquid hydrogen temperature.

(2) The required specimen is cut to shape with a diamond saw. The surfaces are then polished with various grades of "Hyprez" diamond polishing compound to a mirror finish, etched with C.P.4. etch and washed in deionised water.

(3). The contacts are made of an indium alloy containing 0.5% gallium. Suitably sized pieces of alloy are pressed into the ends of the specimen and diffused on by heating the whole specimen to 400°C in an atmosphere of hydrogen.

(4). Platinium wires are soldered ontp the contacts using the same indium alloy as solder and clean Baker's fluid as flux.

(5). The contacts are checked for ohmicity. The resistance must be

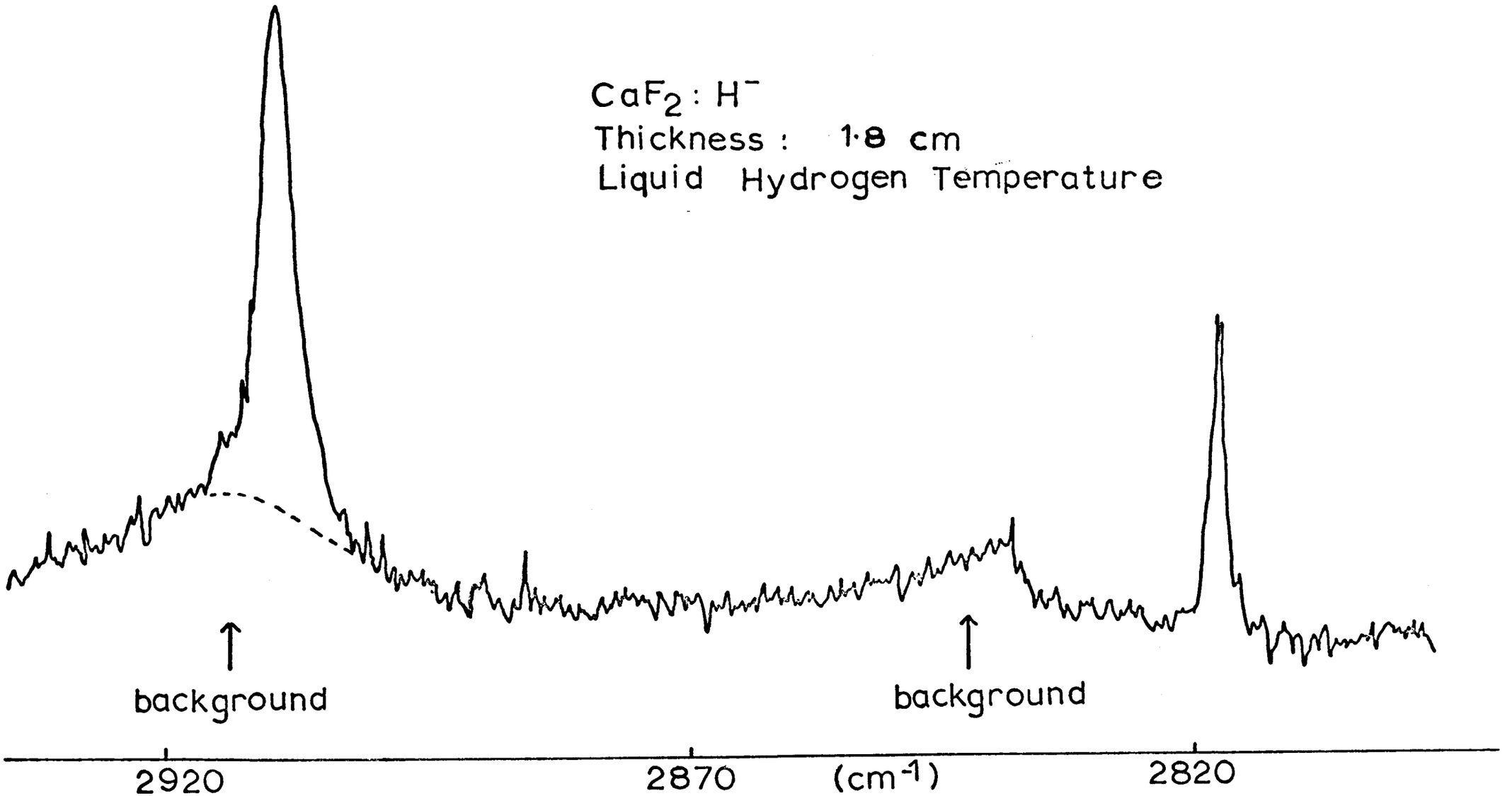

Fig. 11 The two third harmonic lines of the localised vibration of hydrogen in calcium fluoride recorded at 20° K.

temperature.

(6). The specimen is mounted on the holder and washed in a stream of deionised water for several hours. The latter operation is important in minimising $^{1}/f$ noise due to surface contamination. (Hollin and Russell,1963). In the particular detector used here, the specimen was mounted in a small integrating chamber goldplated on the inside. The design of suitable chambers has been discussed by Morton, Schultz and Harty (1959). The specimen used also possessed the wedgeshaped back section, recommended by these authors, to internally reflect any radiation incident on the back face. Such shaping confines the radiation within the specimen for a distance up to approximately three times the actual specimen depth. The high impedance lead was brought out through a Kovar seal direct to the imput of a cathode follower unit mounted on the outside of the dewar. This unit was battery operated to reduce hum problems and stringent precautions were necessary to avoid pickup through earth loops, etc. The output from the cathode follower was at low impedance and was fed into a 650 c/s transistorised tuned amplifier and phase sensitive detector unit and then to the recorder.

The detector was three times more sensitive than the Golay detector on an absolute comparison. However, the gain in overall sensitivity was greater because the photoconductive detector uses a 650 c/s chopped radiation system and so is noticeably free from the low frequency vibration and microphony troubles of the 10 c/s Golay system. Its noise spectrum was also more favourable to the use of high damping.

Figure 10 shows the spectrum of the fundamental frequency of the localised vibration of deuterium in calcium fluoride as measured with

TABLE 6. PEAK POSITION AND LINEWIDTHS OF THE LOCALISED VIBRATION LINES OF HYDROGEN AND DEUTERIUM IN THE ALKALINE EARTH FLUORIDES.

Material and Impurity		Room Temperature		Liquid Nitrogen Temperature		Liquid Hydrogen Temperature	
		Peak Position	Line Width* (cm^{-1})	Peak Position	Line Width* (cm^{-1})	Peak Position	Line Width* (cm^{-1})
CaF_2	H^-	957.8±0.6	8.7	965.1±0.3	1.0	965.6±0.5	0.7[t]
		1903 ±1	21.2	1919.0±0.3	1.5	1919.8±0.3	0.9
		2888 ±2	35	2910.8±0.6	4.5	2912.2±0.5	3.0
		-	-	2825.4±0.6	2.3	2825.6±0.8	1.3
	D^-	689.0±1	6.5	694.0±0.5	2.2	694.3±0.5	2.2
		1374 ±1	12.3	1383.9±0.5	4.0	1384.5±0.4	3.6
		2075 ±2	22	-	-	2093 ±1	5.4
		-	-	-	--	2047 ±1	7
SrF_2	H^-	885.3±0.5	8.3	892.8±0.3	2.0	893.2±0.2	1.7
		1759 ±2	23.2[a]	1775.0±1	3.3	1775.9±0.5	2.2
	D^-	635.8±0.4[a]	5.4[a]	638.8±0.4[a]	3.1[a]	640.4±0.3[a]	2.5[a]
		1266.8±1	14	1275.9±0.7	3.5	1276.5±0.7	2.7
BaF_2	H^-	798.2±0.5	14	806.3±0.5[a]	9[a]	806.7±0.2[a]	8.8[a]
		1580 ±2	24.6	1594.9±0.8	7.0	1596.2±1	5.0
	D^-	-	-	-	-	-	-
		1142 ±2	15.4	1150.7±1.5	10.5	1151.7±0.8	10.0

*Linewidths ±0.5cm^{-1} at room temperature and ±0.3cm^{-1} at low temps.

[t]resolution limited linewidth [a] measured by H. Macdonald.

the Golay and the Zinc doped germanium detector under similar experimental conditions. The other lines on these spectra are those of the fifteen micron atmospheric carbon dioxide band.

4. EXPERIMENTAL RESULTS.

4.1. The Main Vibrational Lines.

Absorption measurements were made on the doped crystals in the wavelength range 3 to 18 microns at temperatures from 4°K to room temperature and the results are given in Table 6. For calcium fluoride the fundamental, second harmonic and a third harmonic doublet of the localised vibrations of both hydrogen and deuterium were observed, while for strontium fluoride and barium fluoride only the fundamental and second harmonics were obtained. The third harmonics were not detected due to the lack of suitably thick and heavily doped crystals. The recording of the third harmonic doublet of hydrogen in calcium fluoride is shown in Figure 11.

The effect of temperature on the absorption lines was investigated between 4°K and room temperature. Both the position and width depend markedly on the temperature. For example, for hydrogen doped calcium fluoride the line width of the second harmonic changes from 21cm^{-1} at room temperature to 0,9cm^{-1} at liquid hydrogen temperature, while the peak position shifts from 1903 to 1919.8cm^{-1}. Figure 12 shows the temperature dependent spectral characteristics of this line.

A detailed study was made on the temperature behaviour of several of the lines.

FIGURE 12 Variation of the second harmonic line of the localised vibration of hydrogen in calcium fluoride with temperature.

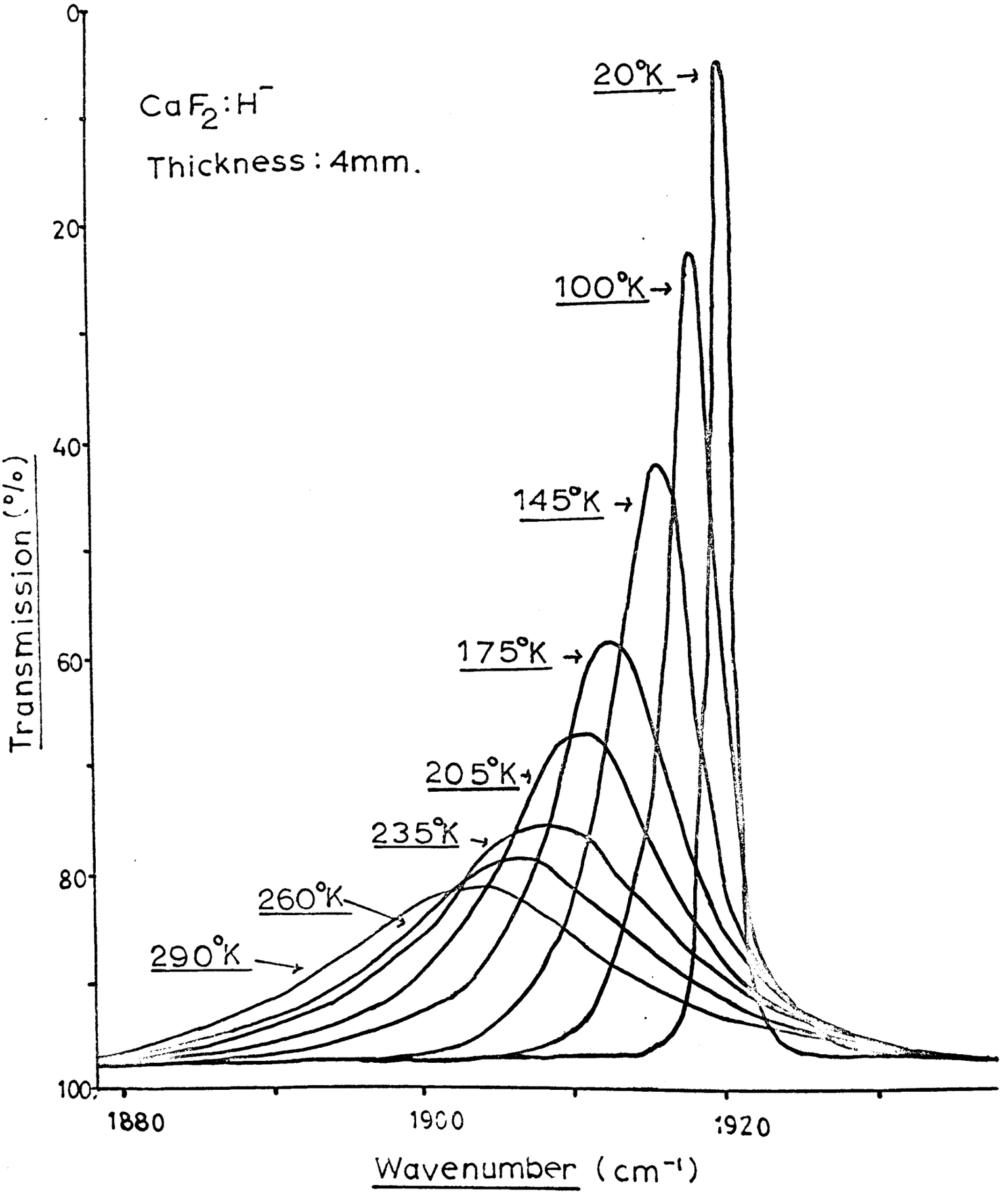

The temperature variation of the line widths shows a T^2 dependence and this is shown in Figures 13 and 14 where halfwidth $\Delta\nu$ is plotted against temperature on a logarithmic scale for the lines studied. A relation of the form: $\Delta\nu \sim T^n$ will give straight lines of slope n on such a plot. The actual values obtained for the exponents are listed in column 2 of Table 7.

Below 80°K, the change in line width is small and the linewidth itself, reaches a limiting value at 20°K. Further cooling to 4°K produces no further decrease in width. Values of the widths for the three temperatures; room, liquid nitrogen and liquid hydrogen are given in Table 6.

The residual linewidth will cause a deviation of the apparent exponent, n, of the temperature dependence from 2 to lower values. For example, in the case of the one third harmonic line of hydrogen in calcium fluoride studied the apparent value of the exponent is 1.5. This arises solely from the large residual linewidth of this line.

The residual linewidth can be estimated as the value required to give an accurate T^2 dependence to the remaining linewidth in the 100-300°K range. These values are tabulated in Table 7 and, for comparison, the observed residual linewidths (widths at 20°K) are also given. The agreement is fairly good in nearly all cases and substantiates the conclusion that the temperature dependence of the lines is, apart from the zero temperature width, accurately T^2.

The peak position of the lines shows a linear temperature

Table 7. Temperature Dependence of the Linewidth and the Estimated Residual Widths.

Line	Observed value for the exponent n in: $\nu = KT^n$	Calculated value for K in 10^{-3} cm^{-1}/°K^2 units	Estimated residual width from deviation of temperature dependence from T^2 in 140-290°K range	Residual Linewidth (=observed linewidth at 20°K)
Fundamental of CaF_2:H^-	1.8	0.32	0.5	0.7*
Second harmonic of CaF_2:H^-	1.9	0.75	0.6	0.9
Third harmonic of CaF_2:H^-	1.45	1.07	3.8	3.0
Second harmonic of CaF_2:D^-	1.8	0.54	1.5	3.6
Second harmonic of BaF_2:H^-	1.5	0.75	4.3	5.0

* machine resolution limited linewidth

Table 8. Intensity Ratio of Various Harmonic Lines

	CaF_2:Hydrogen	CaF_2:Deuterium
Fundamental / Second Harmonic	^{t}23±3 at 20°K (31*)	^{t}39±5 at 20°K
Second Harmonic / Total third harmonic	23±2 at 20°K	---
One third harmonic doublet line	5.7±0.5 at 77°K	5.7±1 at 20°K
other third harmonic doublet line	5.1±0.5 at 20°K	

*this has large error arising from the determination of the intensity of a weak second harmonic line which was plotted out of the 6 μ water band.
t "first method" results. Experiments showed that the variation of hydrogen or deuterium through these crystals was small.

dependence in the range 80°K to 300°K. This is shown in Figures 15 and 16.

The variation of the total integrated intensity with temperature was also studied. The intensity was evaluated as the product of the peak optical density and the halfwidth of the line. Errors arise from uncertainties in the base line of the absorption envelope and from the effects of finite spectral slit widths on the low temperature lines, which are almost or completely machine resolution limited. An approximate correction for the latter effect was estimated by the methods outlined by Brügel (1962) in as far as these were applicable. The resulting corrected relative intensities are presented plotted against temperature in Figure 17. In hydrogenated calcium fluoride, the intensity is almost constant over the range 80°K to 200°K and falls slightly outside this range.

The measurement of the ratio of the intensities of the different harmonic lines required the accurate determination of two lines of widely different intensities. Two methods were tried and both were subject to inherent inaccuracies. They were:-

(1). A thick crystal is used for measurement of the weaker harmonic line at a given temperature and a thin slice cleaved off it used for the measurement of the stronger harmonic line at the same temperature. By this means both lines can have approximately equal intensity and be of optimum size for an accurate evaluation of their intensity. The relative thicknesses can also be accurately measured. The final result for the harmonic ratio is invalidated if the concentration of

FIGURE 13 Variation of line-width with temperature for three harmonic lines of the localised vibration of hydrogen in calcium fluoride, on a logarithmic plot.

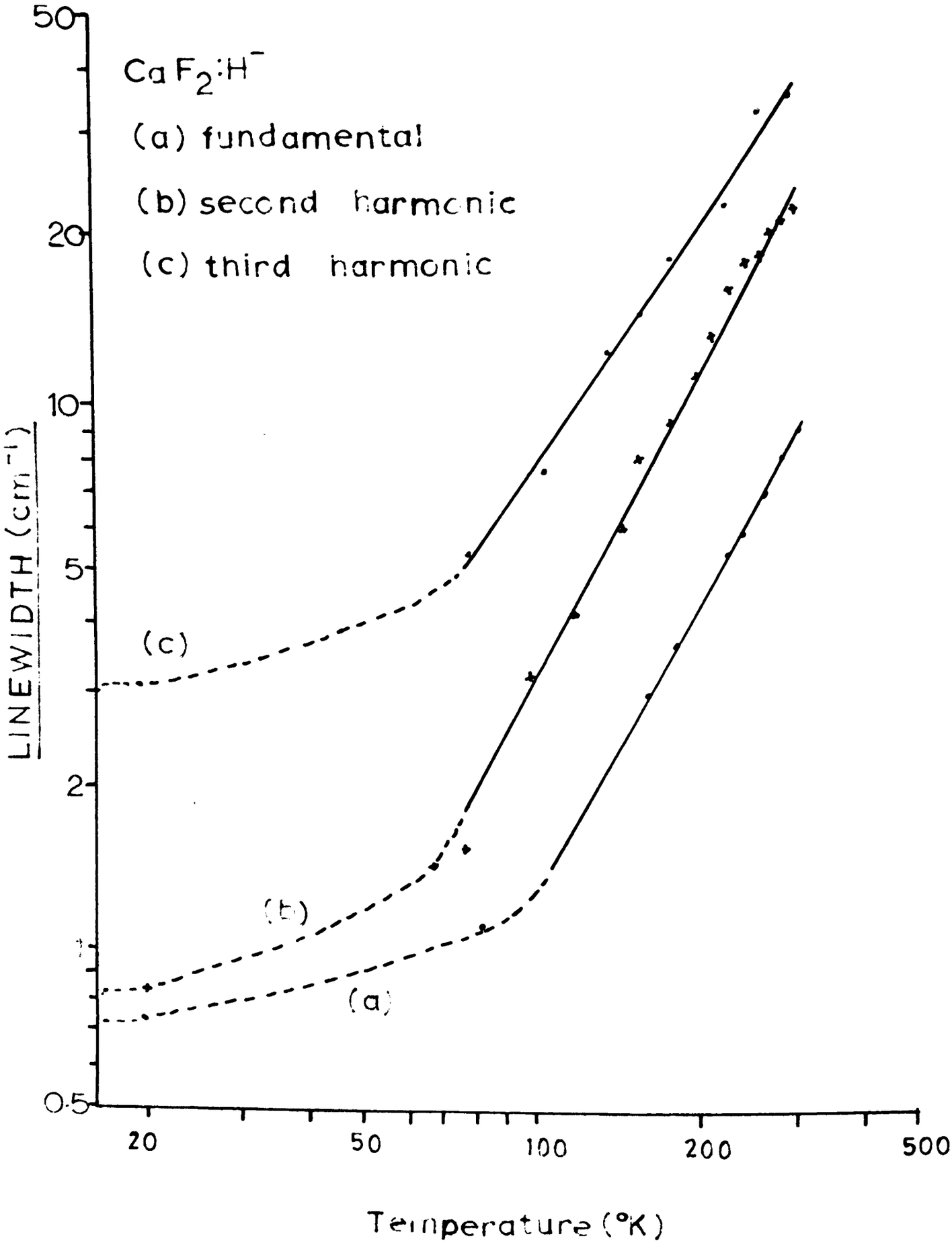

the hydrogen (or deuterium) through the crystal is appreciably nonuniform As it is more likely for the impurity to be present at greater concentration near the surface this method would tend to give too large a value for the intensity ratio.

(2). The same crystal is used throughout. The weaker harmonic line is measured at low temperature where it is narrow and of high peak optical density; the stronger harmonic line is measured at room temperature where it is broad and of low peak optical density. This method requires an accurate knowledge the variation of intensity of one of the lines with temperature.

For the case of the ratio of the fundamental to the second harmonic line of hydrogenated calcium fluoride the first method gives the value 23 and the second the value 31. The agreement is only fair. The second result is to be preferred as it uses the same crystal for both measurements.

Values for the various harmonic ratios is given in Table 8.

4.2. Satellite Structure.

Apart from the strong and prominent lines just described there are subsidiary lines which occur about the fundamental and second harmonics. These are clearly visible in crystals of sufficient thickness and light ion impurity concentration to have almost complete absorption of the main line.

Figures 18 - 23 show the satellite structure for several of the lines. It was not possible to observe similar structure around the fundamental of deuterium in calcium fluoride as a crystal of sufficiently

FIGURE 14 Variation of line-width with temperature for the second harmonic lines of deuterium in CaF_2 and hydrogen in BaF_2, on a logarithmic plot.

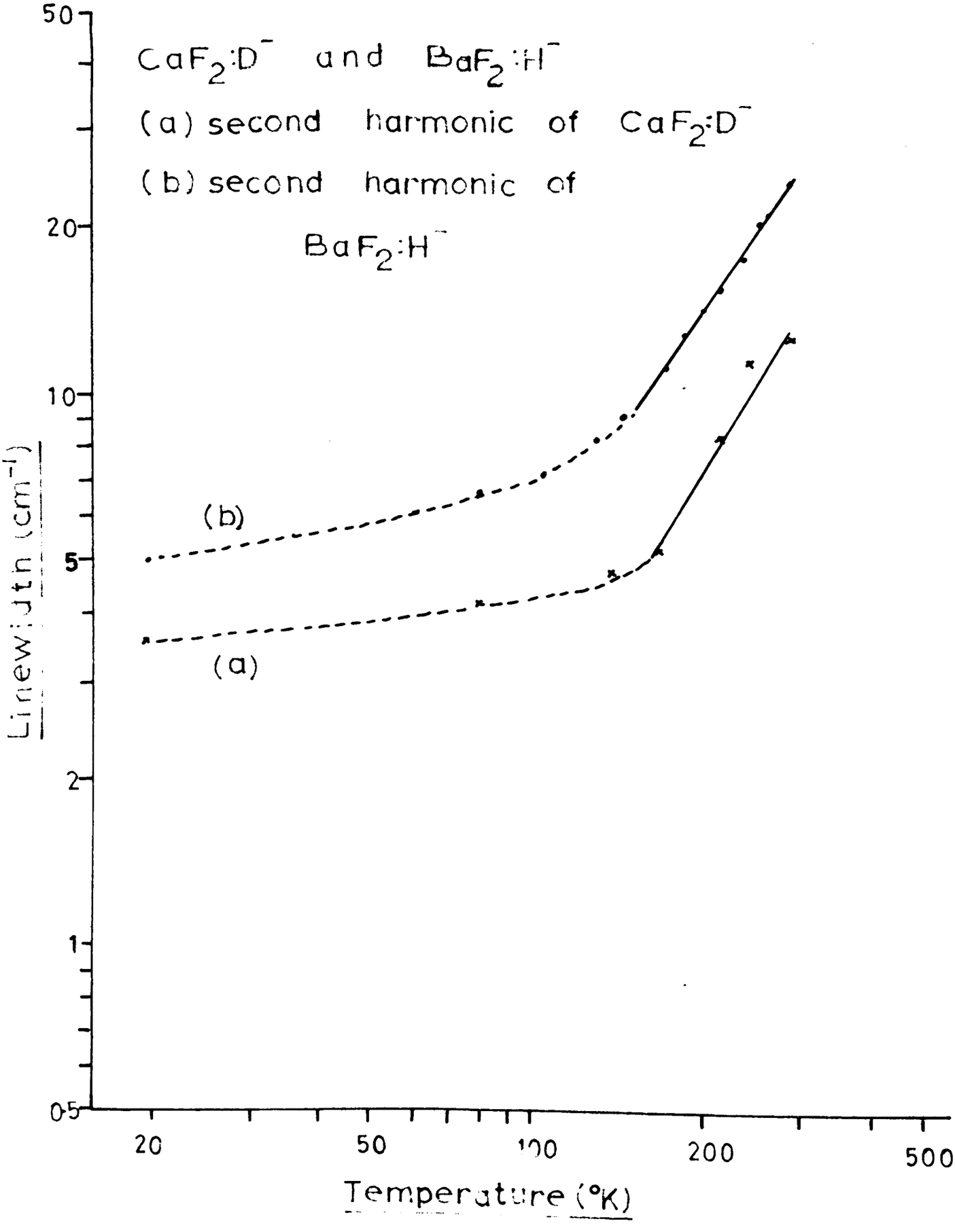

high total deuterium concentration has a thickness giving a prohibitively high lattice reststrahlen absorption.

The satellite structure falls naturally into two groups:

(1). Lines immediately around the main vibrational lines and which possess a marked temperature dependent width.

(2). Broad bands some 100cm^{-1} higher or lower in frequency; the high frequency ones of which sharpen only slightly on cooling.

It was not possible for the author to do more than a preliminary survey of these lines. A detailed study is being undertaken by H. Macdonald of this laboratory. [redacted] Various aspects of the lines, such as their dependence on impurity ion concentration, sample history and temperature are being investigated.

The results given here for the present state of the research are discussed later in Section 8.

4.3. The Effects of X-irradiation on the Infrared Spectra.

The resonance work of Hall and Schumacher (1962) shows that hydrogenated calcium fluoride crystals contain interstitial hydrogen atoms after room temperature X-irradiation. J.W. Hodby (private communication) of this laboratory has observed similar results for hydrogenated barium fluoride crystals.

After irradiation the crystals are black and opaque to approximately two microns wavelengths. Irradiation of a hydrogenated calcium fluoride crystal causes a decraese in intensity of the infrared lines. In a heavily hydrogenated crystal some additional lines appear in the 1000cm^{-1} region, while some of the existing satellite lines

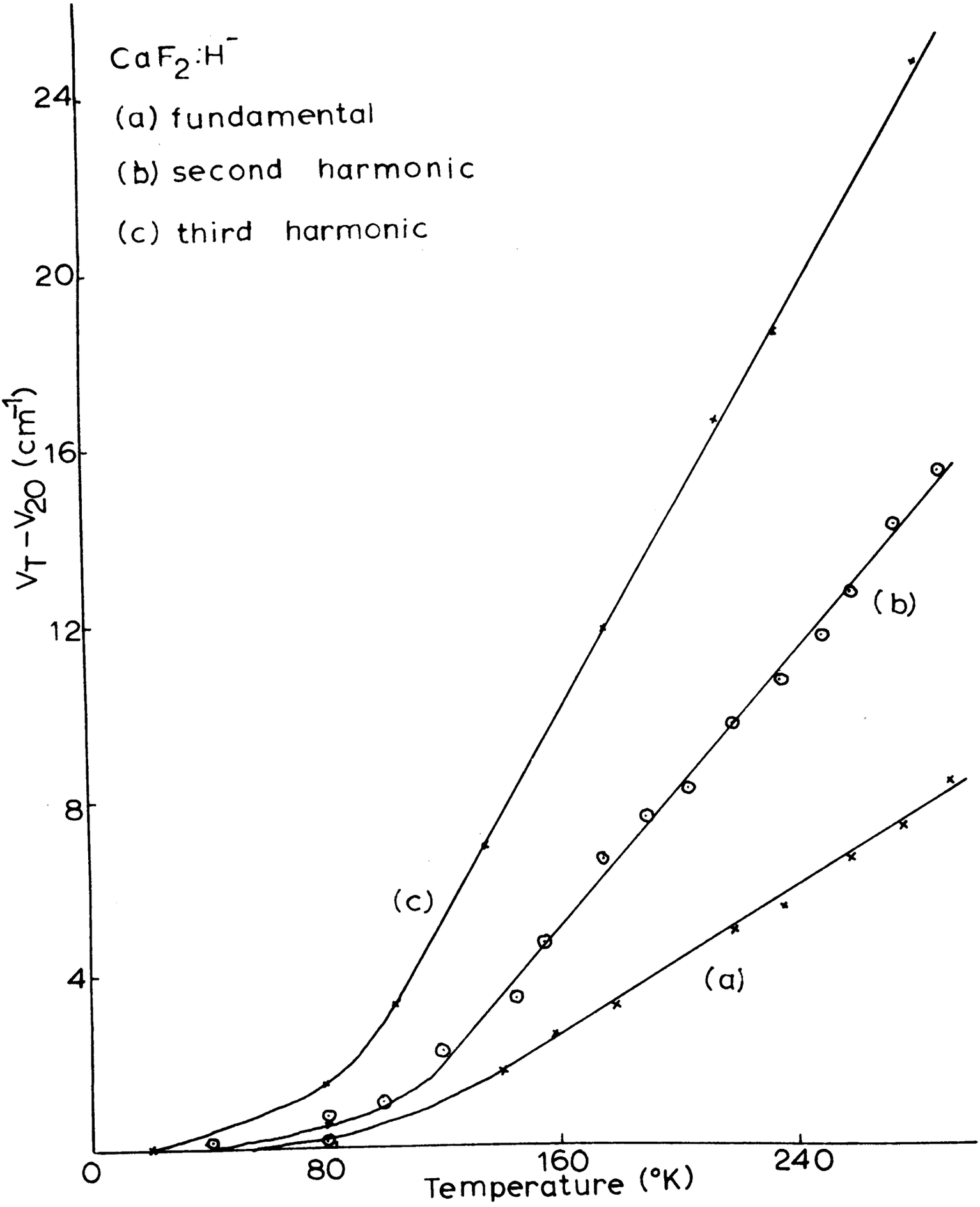

FIGURE 15 Variation of peak position with temperature for three harmonic lines of the localised vibration of hydrogen in CaF_2.

decrease in intensity. (Figure 26)(P.77) No new lines appear in the wavenumber range from 2400 to 1200 cm^{-1}. Heating of the crystal to 200°C for 15 minutes restores the original spectrum.

Heavily hydrogenated crystals were chosen for the irradiation studies as any absorption due to hydrogen atoms can only occur through the admixture of the hydrogen atoms wavefunction with that of its charged neighbours and so is expected to be weak. There is also the possible occurrence of lines due to interstitial hydride ions and the absorption of these will be relatively strong.

A study of the thermal annealing properties of the elctron spin resonance spectrum of interstitial hydrogen atoms was carried out by J.W. Twidell of this laboratory. He established a decay curve for the annealing process and this shows that the interstitial hydrogen atoms are stable for weeks at room temperature and decay to $\frac{1}{e}$th of their original concentration in 16 hours at 50°C, 1 hour at 100°C, 10 minutes at 150°C and 1½ minutes at 200°C. There thus appears to be an approximate correlation between the disappearance of the irradiation produced infrared lines and the disappearance of the electron spin resonance spectrum. However, an accurate one to one pulsed annealing experiment on both spectra is necessary to establish any definite correlation between the two spectra.

The irradiation results are discussed more fully in Section 8.1.

FIGURE 16 Variation of peak position with temperature for the second harmonic lines of deuterium in CaF_2 and hydrogen in BaF_2.

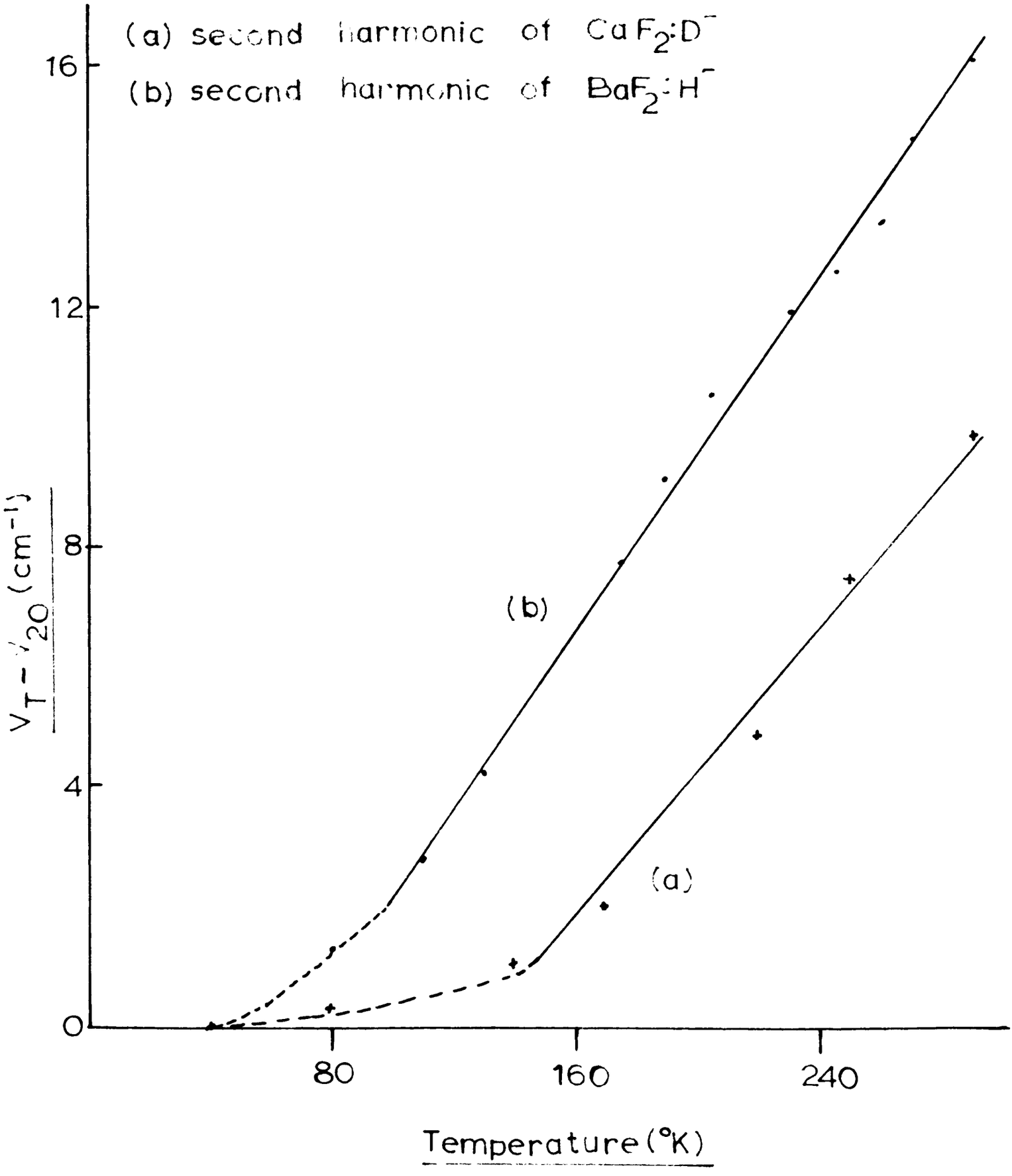

4.4 Optical Measurements in the Ultraviolet and Visible Regions.

The absorption spectra were recorded in the range 50,000 to 2,800cm^{-1} on a Unicam SP700 spectrophotometer.

At room temperature, the hydrogenated calcium fluoride crystals showed complete absorption in the region from 47,000 to the limit of the spectrophotometer at 50,000cm^{-1}, and also a band spectrum in the near ultraviolet and visible regions, vaying from sample to sample, and bearing no apparent relation to the intensity of the infrared absorption lines of the hydride lines.

This varying spectrum was identical to the "additive" colouring spectrum of calcium fluoride discussed by Görlich et.al. (1961) and is also possessed by calcium fluoride crystals that have been heated in oxygen. These bands presumably arise because of the incomplete removal of the additive colouration spectrum (produced by the action of the aluminium metal) by the hydrogen gas. They are responsible for the slight colouration of some samples described earlier in Section 2.

The only absorption that could be attributed directly to the hydrogen is the strong absorption in the far ultraviolet. Dr. P. H. Yuster of Argonne National Laboratories has run off a vacuum ultraviolet spectrum of one of the crystals to check whether the peak of this absorption lies beyond 50,000cm^{-1}. He found complete absorption of the crystal to 1600A° (66,700 cm^{-1}), the limit of his apparatus. Further work on this band requires very weakly hydrogenated crystals and is in progress. From the present results, it can only be concluded that any band analogous to the ultraviolet U band of the alkali halides

FIGURE 17 Variation of the total absorption with Temperature for several localised vibration lines.

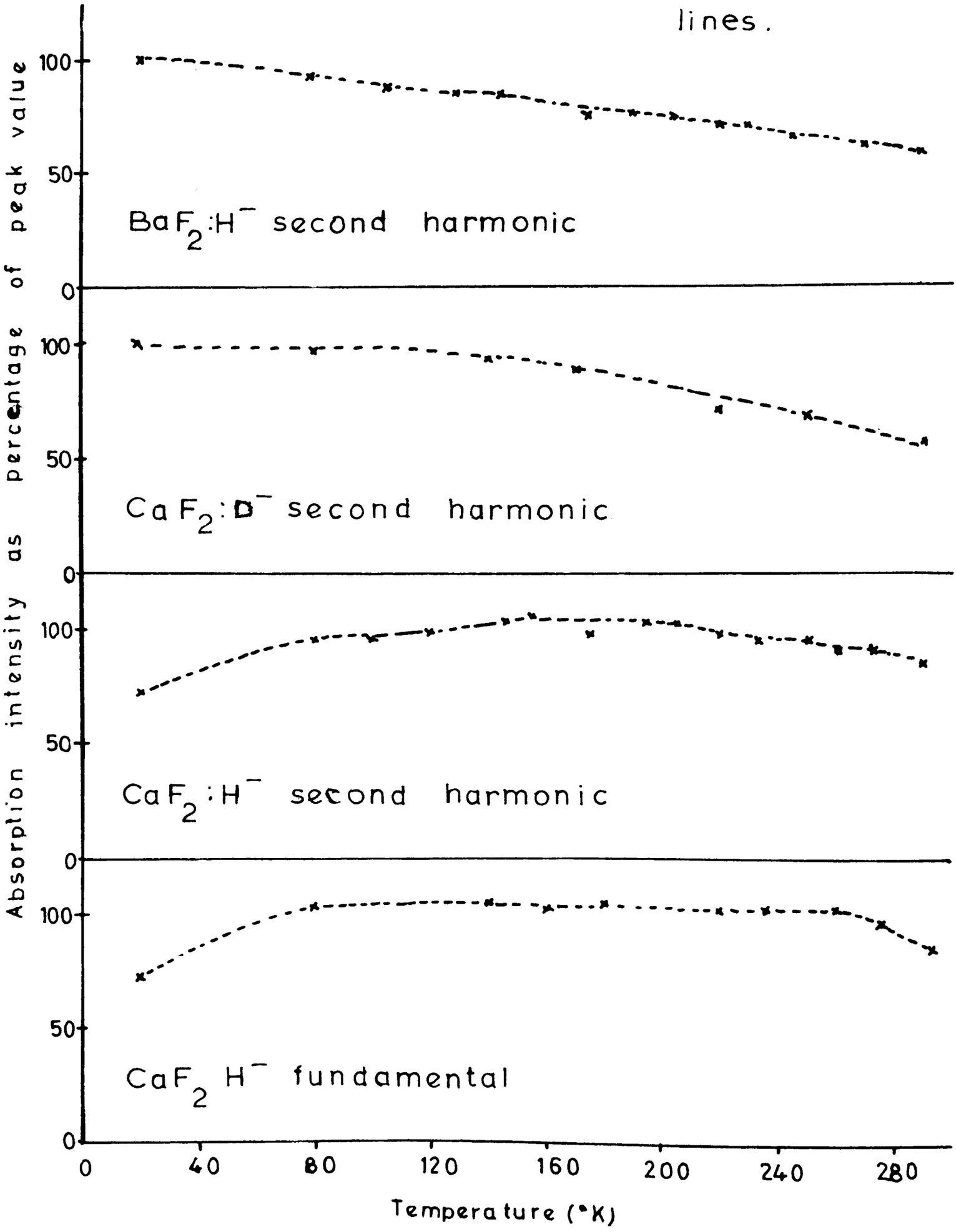

lies at frequencies in the vacuum region beyond 2000A°. Such a conclusion is consistent with the larger band gap of the alkaline earth fluorides compared to the alkali halides.

4.5 Irradiation Effects on the Ultraviolet and Visible Absorption.

Room temperature X irradiation of hydrogenated calcium fluoride crystals causes a rapid growth of colour centre bands at 27,000 and 17,000cm^{-1} and the crystal first becomes purplish then black.

Low temperature (77°K) X irradiation causes the growth of different bands at 25,600 and 23,000cm^{-1} and the crystal is yellow. On warming the crystal from 77°K these bands rapidly change. At 140°K the 25,600 cm^{-1} band shifts to 27,000cm^{-1} and the 23,000cm^{-1} band bleaches almost completely. A further band simultaneously builds up rapidly in intensity at 17,800cm^{-1}. The final spectrum is identical to the room temperature one above.

Both the room temperature and low temperature irradiation spectra are the same as that observed in oxygen treated calcium fluoride crysta ls and the first is characteristic of additively coloured calcium fluoride systems (Görlich (1961)). It appears that the hydrogen plays a similar part to oxygen in promoting additive colour centre formation on irradiation.

There was no irradiation effect that could be uniquely ascribed to the hydrogen itself. In particular, there was no obvious analogue to the U_1 and U_2 bands of the alkali halides, which are due to interstitial hydrogen ions and atoms respectively and are produced by ultraviolet irradiation into the U band.

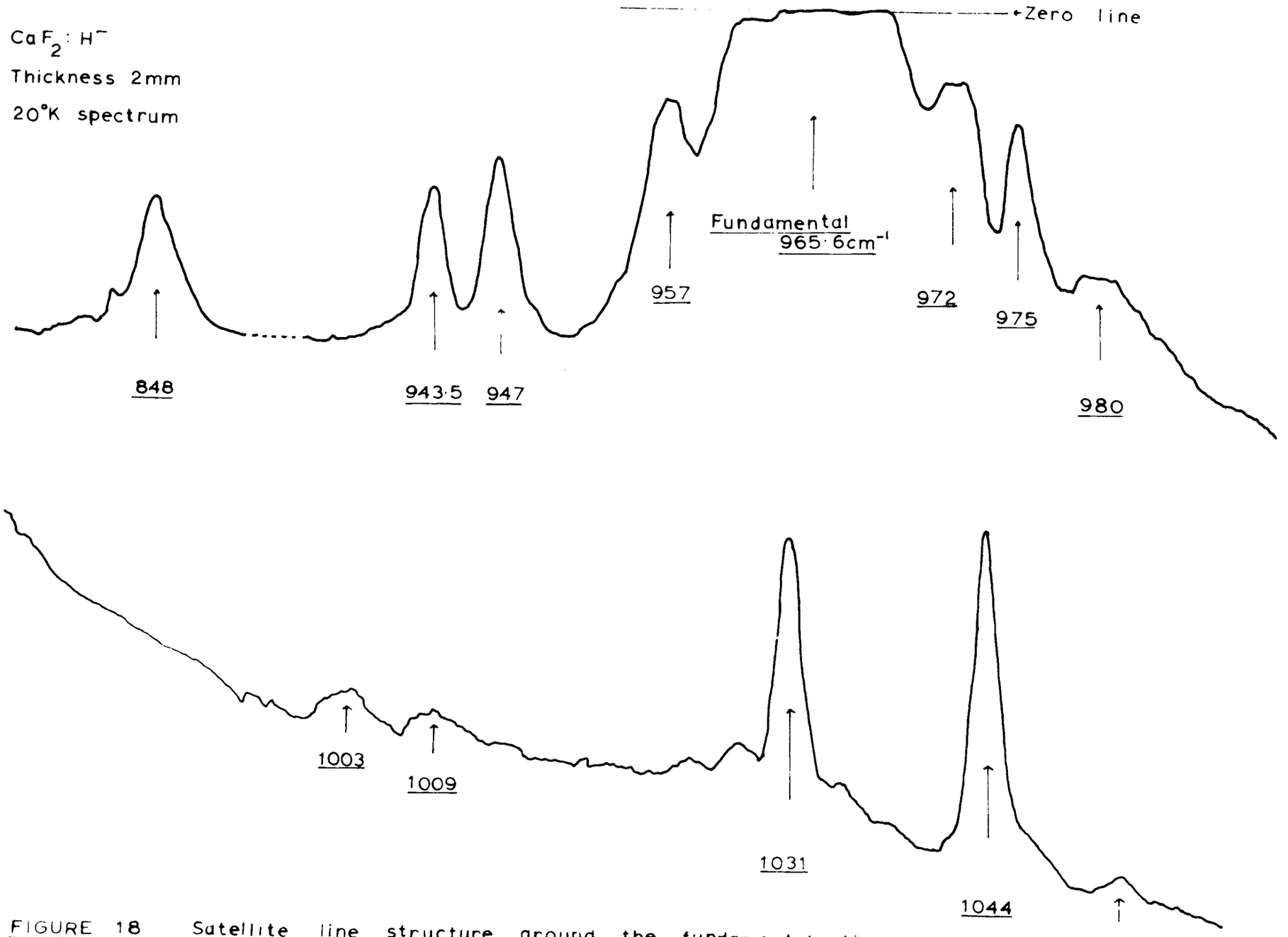

FIGURE 18 Satellite line structure around the fundamental line of the localised vibration of hydrogen in calcium fluoride

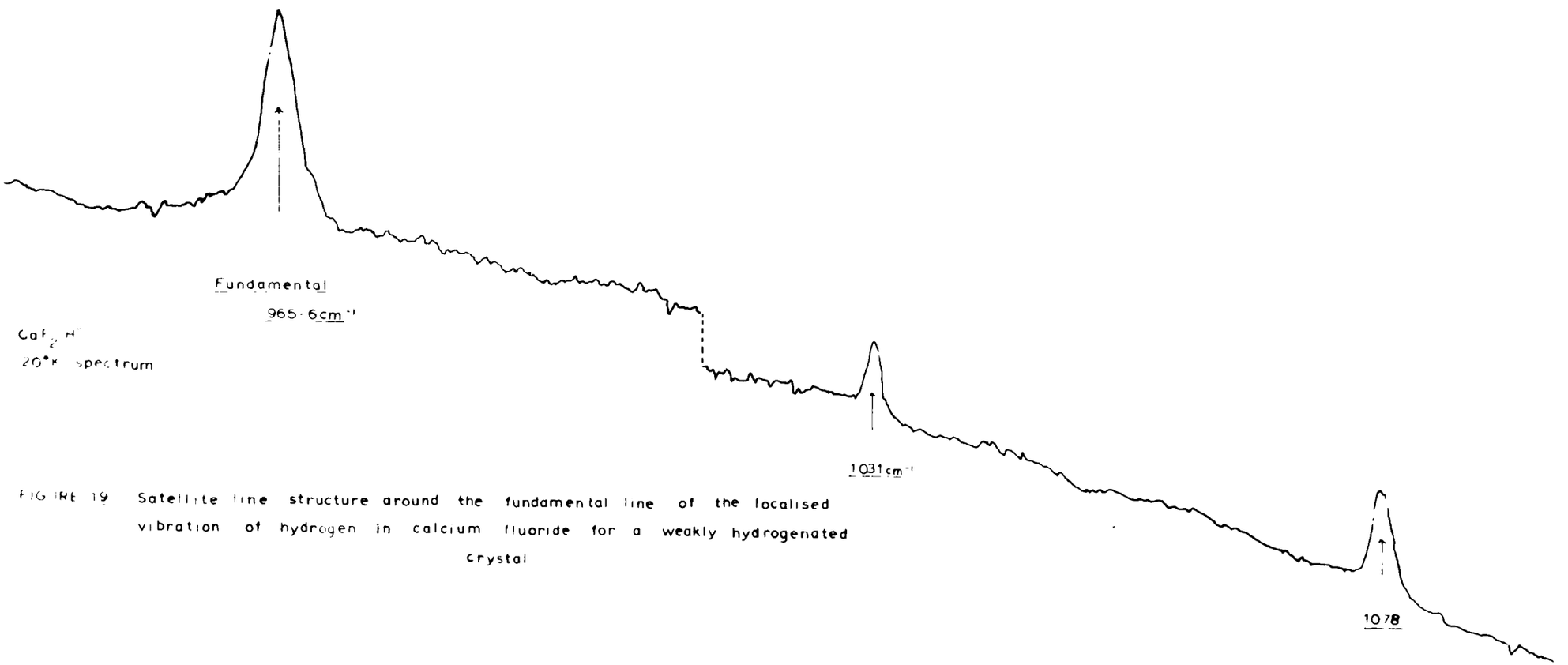

FIGURE 19 Satellite line structure around the fundamental line of the localised vibration of hydrogen in calcium fluoride for a weakly hydrogenated crystal

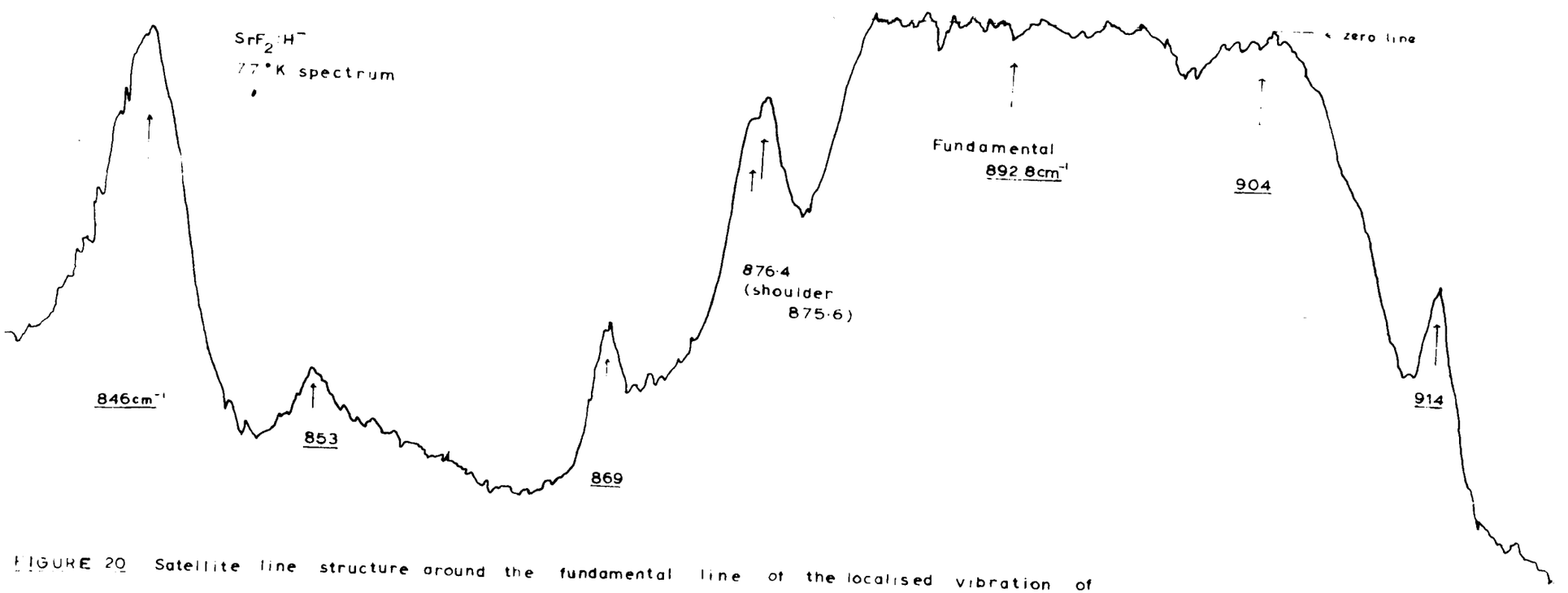

FIGURE 20 Satellite line structure around the fundamental line of the localised vibration of hydrogen in strontium fluoride.

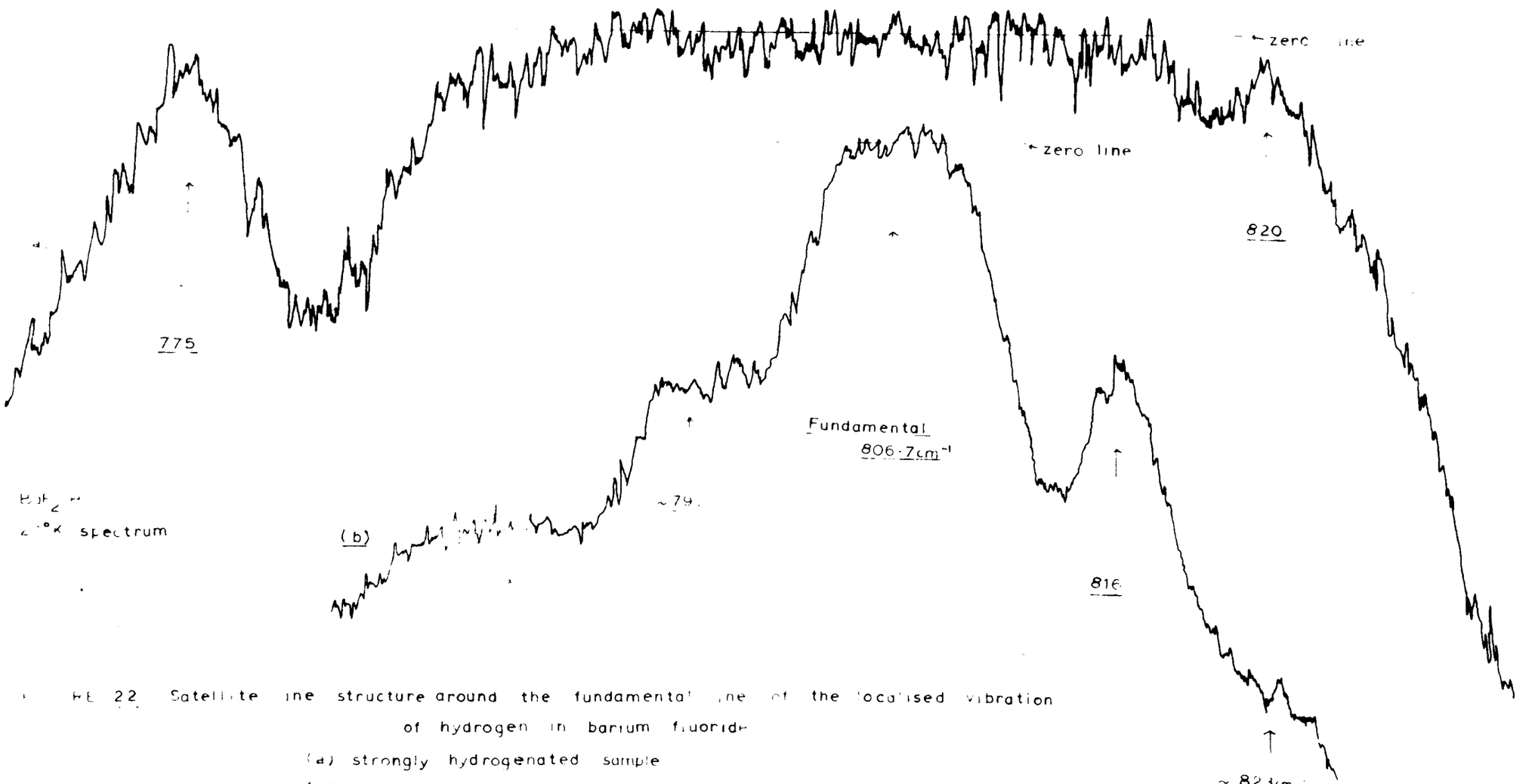

FIG 22 Satellite line structure around the fundamental line of the localised vibration of hydrogen in barium fluoride

(a) strongly hydrogenated sample

(b) weakly hydrogenated sample

Work on ultraviolet irradiation effects related to the above work is being carried out by H. Macdonald of this laboratory.

4.6. Stark Splitting of the Vibrational Lines.

It has already been assumed that the hydrogen is present as a substitutional impurity on the fluorine sites and a justification for this is to be given later.

An interesting confirmation of this assumption would be the observation of a Stark splitting of the infrared absorption lines. It can be seen that, in the fluorite lattice, the fluorine sites are the only ones not possessing a centre of symmetry and hence the only ones for which a first order Stark effect would be expected.

From energy considerations a splitting (and/or shift) of the lines by 1 part in 1000 would be given by an applied electric field of 100,000 volts/cm. This is an order of magnitude estimate. The widths of the fundamental and second harmonic lines of hydrogen in calcium fluoride are sufficiently narrow at low temperature ($<1 cm^{-1}$) for a 1 part in 1000 energy level perturbation to be just detectable as a definite splitting. Smaller splittings should also be evident in a broadening of these lines.

All experiments attempted were confined to the fundamental line, as the second harmonic line is in the 6 micron atmospheric water band.

The crystal was mounted between, and touching, two electrodes on a polythene plate. This was mounted in the dewar previously described. The required high voltage was supplied by a 0 to 20 kilovolt R.F. oscillator E.H.T. unit. The crystal was cooled by helium exchange

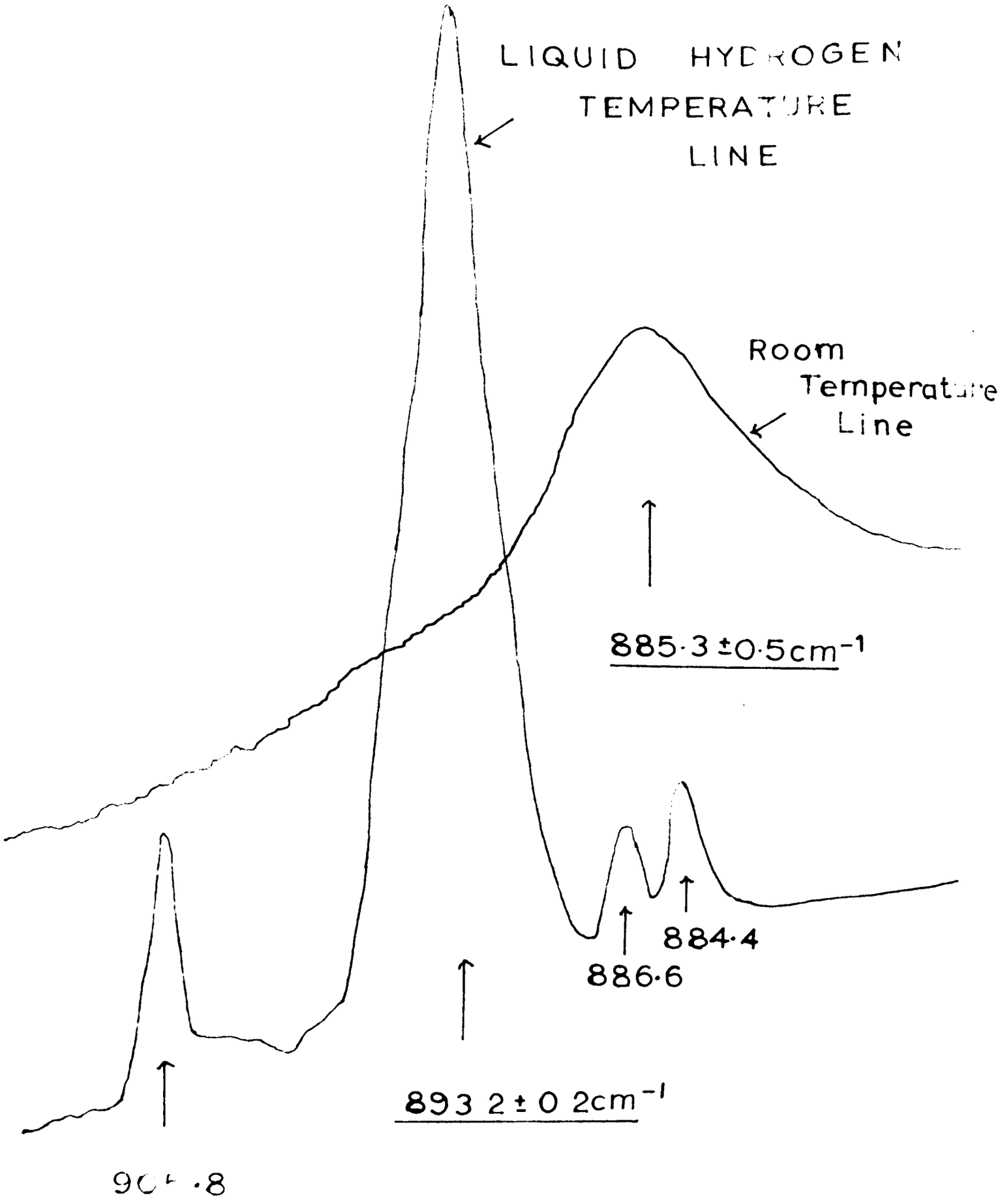

FIGURE 21 Satellite line structure around the fundamental vibrational line of hydrogen in strontium fluoride.

gas and this was pumped out immediately prior to the application of the electric field. The limiting field for breakdown of the crystal surface and/or the vacuum was about 100,000 volts/cm. The crystal itself has a considerably higher breakdown voltage limit. (Mott and Gurney (1950)).

Two different crystal orientations were studied; one with the electric field applied along a <111> axis and the other with it applied perpendicular to a <111> axis. In both cases, there is no observable splitting or broadening of the vibrational line even under maximum available applied electric field. Any splitting can, therefore, be no greater than $0,5cm^{-1}$ for an applied field of 80,000 volts/cm. Any shift in the line frequency was less than $0.2cm^{-1}$.

It has been suggested that the crystal mayhave enough ionic conductivity at low temperatures for it to polarise under the applied field and so cause a reduced electric field inside the crystal. However, a preliminary experiment, using a crystal with graphite painted on its edges to minimise this effect, showed no appreciable broadening either so the previous statement about the magnitude of the splitting is still valid.

Due to the crudeness of the model used for predicting the magnitude of the Stark splitting, nothing definite can be deduced, from the above negative result, about the site symmetry of the hydrogen impurity giving rise to the vibrational lines. The experiment has been inconclusive because of sensitivity limitations of the spectrometer. The actual width of the line achieved at 20°K was only $1cm^{-1}$ and this was caused by the necessity of using slit widths sufficiently wide to give an adequat e

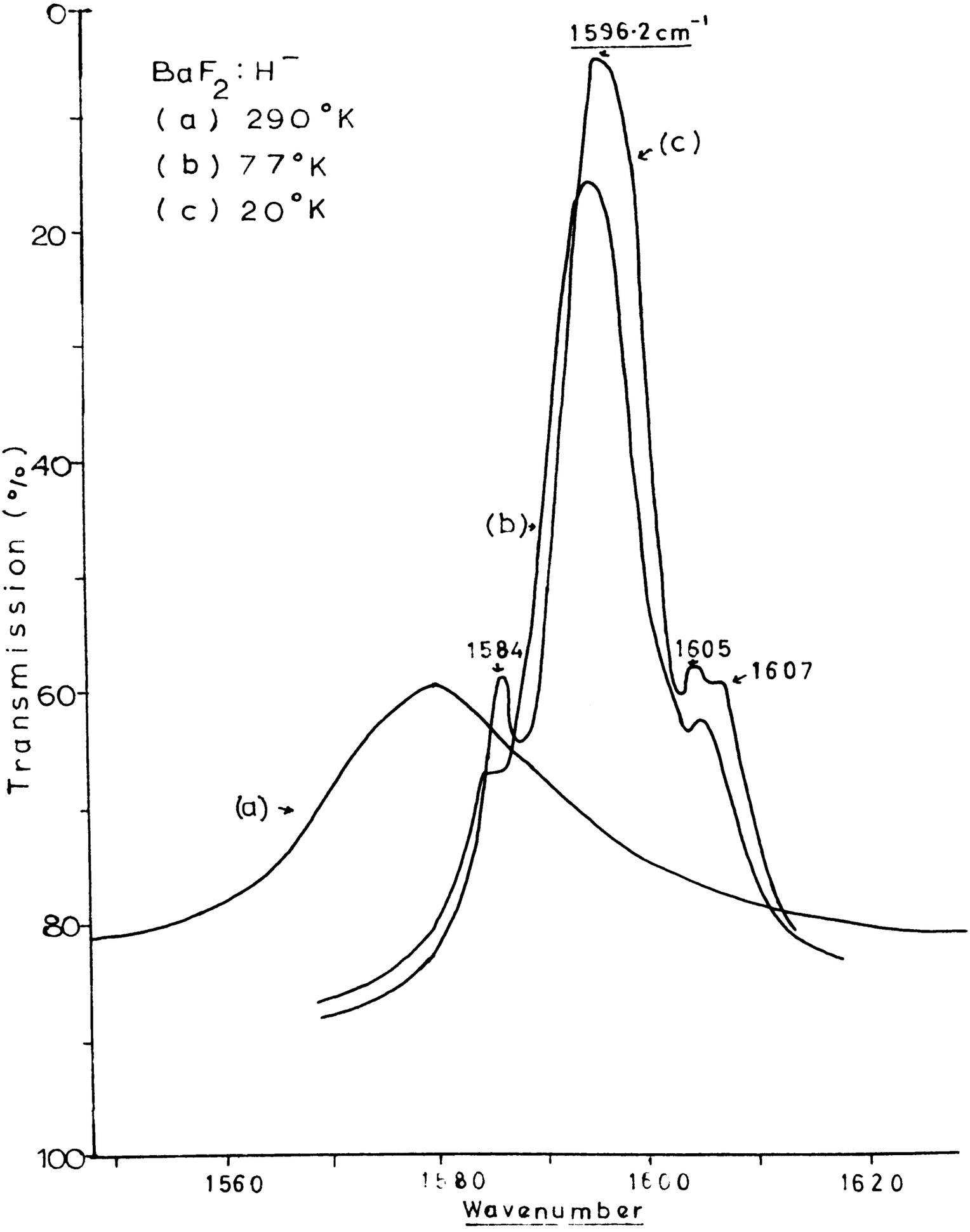

FIGURE 23 Satellite line structure on the second harmonic line of the localised vibration of hydrogen in barium fluoride

detector signal to noise ratio. The line itself is probably $0,5cm^{-1}$ x wide and, with a more sensitive spectrometer, a minimum incipient splitting of $0.25cm^{-1}$ should be detectable. Only when this limit has been reached could one deduce anything by this method about the site symmetry of the hydrogen impurity.

5. PRELIMINARY DISCUSSION OF THE RESULTS.

Phenomenological Treatment.

It is possible to rationalise several aspects of the observed infrared absorption lines on the basis of phenomenological theories and before considering the detailed theory of localised vibrations in crystal lattices such a treatment will be developed here.

5.1. Approximate Calculation of the Observed Frequencies.

The infrared absorption frequency w_o of a diatomic lattice is given by (Mitra (1963)):

$$w_o = \sqrt{\frac{\beta_o}{\mu_o}}$$

where β_o is the force constant of the lattice and μ_o the reduced mass of an elementary diatomic cell.

The introduction of light atoms as substitutional impurities in the lattice results in a frequency w_1 given by:

$$w_1 = \sqrt{\frac{\beta_1}{\mu_1}}$$

where β_1 is the force constant in the immediate neighbourhood of the disturbing atom and μ_1 the reduced mass of the disturbed elementary cell.

With the assumption of unchanged force constant:

$$\frac{w_1}{w_o} = \sqrt{\frac{\mu_o}{\mu_1}}$$

For barium fluoride, the mass of the barium atom (138) is much greater than that of a fluorine (19) and a reasonable approximation can be made by equating the reduced masses μ_o and μ_1 to the actual masses of the substituted and substituting atoms respectively. For the case of hydrogen impurity in barium fluoride:

$$\mu_o = 19 \text{ (fluorine mass)}$$

$$\mu_1 = 1 \text{ (hydrogen mass)}$$

W_o is taken as $184cm^{-1}$ which is the value of the transverse optical made frequency observable as the peak of the reststrahlen absorption in pure barium fluoride. With these values:

$W_1 = 800cm^{-1}$ and this is close to the observed frequency of $798cm^{-1}$ for the localised vibration of hydrogen in barium fluoride at room temperature.

For calcium fluoride one cannot make the approximation of equating the reduced mass of the diatomic cell to the actual mass of a fluorine ion as the mass of the calcium atom (40) is comparable to that of a fluorine (19). This is confirmed by the large discrepancy between the calculated value of $1120cm^{-1}$ and observed value of $960cm^{-1}$. Instead, one could consider the very crude model of a linear chain of alternate calcium and fluorine atoms. The reduced masses of a diatomic cell of this lattice are:

$$\mu_0 = \frac{760}{59}$$

$$\mu_1 = \frac{40}{41}$$

and $w_1 = 935cm^{-1}$, which is reasonably close to the observed room temperature value of $960cm^{-1}$.

TABLE 10. RATIO OF HYDROGEN TO DEUTERIUM FREQUENCIES FOR SEVERAL HARMONIC LINES OF THE LOCALISED VIBRATIONS OF HYDROGEN AND DEUTERIUM IN THE ALKALINE EARTH FLUORIDES.

Material	Localised Vibration Lines.	Room Temperature.	Liquid Hydrogen Temperature.
Calcium Fluoride.	Fundamentals	1.390±0.003	1.391±0.002
	Second Harmonics	1.385±0.002	1.387±0.001
	Third Harmonic high frequency lines	1.392±0.003	1.391±0.001
	Third Harmonic low frequency lines	-	1.380±0.002
Strontium Fluoride.	Fundamentals	1.392±0.002	1.395±0.001
	Second Harmonics	1.389±0.003	1.391±0.002
Barium Fluoride.	Second Harmonics	1.384±0.003	1.386±0.002

The models considered are obviously unrealistic, and do not take into account the existence of both fluorine and heavy metal ion nearest neighbours around the impurity atom site. However it would seem that the observed frequencies could be explained largely on the basis of the mass change alone. Any remaining deviations can be ascribed to different near neighbour interaction for the light impurity ion compared to that of fluorine ion. To detect such effects, an exact calculation of the effect of the mass change itself is required. Such calculations are being performed by C.T.Sennett of this laboratory and these indicate that the light ion probably has weaker near neighbour interaction than a fluorine ion.

5.2. Ratio of the Hydrogen to Deuterium Frequencies.

The frequency-mass relation given above can also be used to determine the ratio of the hydrogen to deuterium line frequencies. For independent oscillation of these light ions in the lattice, the ratio would be $\sqrt{2}$; the square root of the inverse mass ratio.

Table 10 shows the experimental values for the ratios for several of the lines measured.

If the effect of the surrounding lattice is included, the ratio becomes less than $\sqrt{2}$.

For the model of a linear chain of fluorine ions, which is approximated by barium flouride:

$$\mu_H = \frac{19}{20}$$

$$\mu_D = \frac{38}{21}$$

$$\frac{W_H}{W_D} = \sqrt{\frac{\mu_D}{\mu_H}} = 1,380$$

The model of the linear chain of alternate metal and fluorine ions, which approximately applies to the case of calcium fluoride, gives:

$$\nu_H = \frac{40}{41} \quad ; \quad \nu_D = \frac{40}{21}$$

$$\therefore \frac{W_H}{W_D} = 1,397, \text{ with values closer to } \sqrt{2}\ (1,4142) \text{ for}$$

strontium and barium fluorides.

In a more realistic model the effects of both types of neighbouring ions must be included with an appropriate weighting factor. If one assumes a relative weight proportional to the number of each kind of atom surrounding the light ion, the following results are obtained:

$\frac{W_H}{W_D}$ = 1,389 for calcium fluoride

$\frac{W_H}{W_D}$ = 1.398 for strontium fluoride

$\frac{W_H}{W_D}$ = 1.402 for barium fluoride.

A further refinement can be made for calcium fluoride case by considering the relevant force constant of the interaction of the impurity ion with its two types of neighbours. Shimanouchi, Tsuboi and Miyazawa (1961) have evaluated the Ca - F^- bond stretching force constant and the $F^- - F^-$ repulsion constant as 0,31 and 0.18 md/A° respectively using the known optical properties of calcium fluoride, namely peak reststrahlen absorption at 270cm^{-1} and Raman absorption at 321.5cm^{-1}. With the above values assumed for the Ca-H^- and $F^- - H^-$ force constants the hydrogen to deuterium frequency ratio becomes 1.385.

The above values for the ratios are in fair agreement with the values given in Table 10 calculated from the experimentally observed frequencies.

The observed impurity ion vibrational frequencies are perturbed by anharmonic effects and, for an accurate experimental value for the ratio of the hydrogen and deuterium frequencies, these shifts must be subtracted and the unperturbed or harmonic approximation, frequencies used. The magnitude of these anharmonic effects will be considered later.

An accurate calculation of the ratio requires a knowledge of the form of the two light impurity ions vibration modes. Such a calculation has been performed by Takeno, Kashiwamura and Teramoto (1963) for the localised vibrations of the U centres in the alkali halides.

5.3. Classification of the corresponding frequencies of the three fluorides.

The frequencies of corresponding lines in the three fluorides, CaF_2, SrF_2 and BaF_2 can be ordered on the basis of the empirical Mollwo-Ivey relation (Görlich (1961)):

$$Vd^n = \text{constant}$$

where V is the frequency and d the corresponding interionic radius.

For the localised vibrations frequencies observed in the alkaline earth fluorides, the value 1,43 is obtained for the exponent n. This may be compared to the average value of n of 2.3 found by Schäfer (1960) for the alkali halides for the variation of frequency with change in the anion. For the variation of frequency with change in the cation, the exponent n=1 is obtained.

The reststrahlen frequencies of the pure alkaline earth metal fluoride lattices require an exponent n of 2,7.

It should be emphasised that the value of 1.43 for the exponent probably does not have any particular significance because it depends largely on the relative masses of the two ions of the pure lattice.

This is evident from the calculation of the localised vibration frequencies above; the estimated frequencies are a function of both the reststrahlen frequencies and of the relative masses of the metal, fluorine and impurity ion. In calcium fluoride, the masses are comparable and the localised mode frequency is 3.8 times the reststrahlen frequency; in barium fluoride they are widely different and the localised mode frequency is 4.35 times restrahl.

The reststrahlen frequencies themselves are largely a function of the reduced mass of the elementary diatomic cell, modified somewhat by changes in the interatomic force constants. This can be seen from equation 27 of the paper by Shimanouchi, Tsuboi and Miyazawa (1961). This equation relates the reststrahlen frequency to the metal ion - fluorine bond stretching force constant K and to the reciprocal masses μ_M and μ_F of the metal and fluorine ion. It is:

$$\lambda = \frac{4}{3} K (\mu_F + 2\mu_M)$$

The observed variation of the reststrahlen frequencies is largely contained in the mass term. K varies only slightly through the series.

The Mollwo law exponent n of 2.7 merely relates the reststrahlen frequencies to the size of the atomic cells in a rather arbitary fashion.

For the variation of the local mode frequency one may consider the approximation of a static lattice around the impurity ion. The frequency will then be largely a measure of the force constants of the impurity's interaction with the surrounding ions. The Mollwo-Ivey exponent of 1.43 correlates this variation with the size of the atomic cell.

5.4. Frequency shift in the lines with temperature.

The frequency shift in the lines caused by the thermal expansion may be estimated from the Mollwo-Ivey formula.

If $V = C/r^n$, where C is a constant and r the interatomic spacing

then $\frac{dV}{dT} = -n\alpha V$

where α is the coefficient of linear expansion of the lattice.

For the fundamental vibration frequency of hydrogen in calcium fluoride the relevant data is, for the temperature range -192° to 17°C:

$n = 1.43$

$\alpha = 12.9 \times 10^{-6}$ averaged over the whole temperature range above; values from the Tables of Landolt - Börnstein (1923)

$\nu = 960 cm^{-1}$

and this yields for the frequency shift, $\Delta\nu$, the value $4.0 cm^{-1}$. The observed frequency shift is $7.1 cm^{-1}$. It would thus appear that the lattice contraction does not wholly explain the observed frequency shift. However, as already stated, the exponent n does not necessarily reflect the true dependence of frequency on interionic radius, and one cannot conclude from these calculations whether the lattice contraction is solely responsible for the observed frequency shift with temperature.

A more general relation is (Dawber and Elliott (1963)):-

$$\frac{\Delta w}{w} \sim \gamma \frac{\Delta r}{r}$$

where r is the interatomic spacing and γ is Grüneisen's constant. This gives an approximate frequency shift $\Delta w = -\gamma \alpha w$ where the constant γ replaces the n of the Mollwo-Ivey relation. For most substances, has a value of about 2 and this yields a frequency shift of $5.6 cm^{-1}$.

The observed linearity of the shift in peak position with temperature does not follow directly from the lattice expansion. The coefficient of linear expansion decreases by more than 50% from 17°C to -192°C and this variation is not reflected in the observed experimental behaviour of the lines.

Ganesan and Srinivasan (1962b) have carried out a theoretical study of the thermal expansion of calcium fluoride and treat the problem in some detail. They evaluate the Grüneisen constants, appropriate for lattice frequency changes with volume of the crystal, for the different branches of the dispersion curve for this substance. Using a value of 2.2 for the Grüneisen constant appropriate to an optical branch, and the thermal expansion data of Valentiner and Wallott (1915) one obtains a shift of $19 cm^{-1}$ for the temperature range 80°K to 290°K and this more than accounts for the observed frequency shift.

The effective Grüneisen constant also increases by 60% with decreasing temperature so the linearity of the observed peak positions is not necessarily inconsistent with the thermal expansion model.

A [redacted] mechanism giving rise to a peak position variation of the vibration lines with temperature is that of an anharmonic interaction of the

impurity's vibration mode with lattice modes. This is described in Section 6.6. Further discussion of the peak position variation is left to Section 7.2.

5.5. Density of the Light Impurity Ions.

The concentration of defect ions can be estimated from the Smakula formula:

$$Nf = \frac{9mc}{e^2 h} \frac{n}{(n+2)^2} E_H K$$

Where N = Concentration of defect ions/cm^3

m = mass of the defect ions

e = electronic charge

c = velocity of light

$\hbar$ = Planck's constant /2π

n = refractive index

E = photon energy

E_H= half width of the absorption band in eV

Eo = photon energy in band maximum

K = absorption constant (cm^{-1}) in the band

f = oscillator strength

This formula has been reproduced from Görlich et.al.(1961). For E=Eo it reduces to:

$$Nf = \frac{9mc}{e^2 h} \frac{n}{(n+2)^2} E_H K_{max}$$

and

$$Nf = 2.1.\ 10^{19}.E_H\ Kmax$$

where K_{max} is the absorption constant in the band maximum. This last equation uses n=1.5 and m/m_H= 1 for hydrogen.

From the formula in this reduced form, the concentration of defect ions can be evaluated from the peak optical density and halfwidth of the observed line. The main uncertainty lies in the choice of value for the oscillator strength, f. This quantity can be defined as the ratio of the number of centres concerned in an absorption process to the number actually available. In all the estimates of N given, it has been equated to unity and so the values for N are a lower limit to the correct values.

For the case of the alkali halides, Schäfer (1960) compared the integrated areas of the ultraviolet and infrared absorption bands of the U centres and found that the latter bands were about "half" the intensity of the former. This required the setting of the oscillator strength of the localised vibration absorption process to a value of about 0.5. Schäfer suggested that the whole absorption spectrum of the vibrational spectrum of the U centres may not have been observed. He states that there was definitely no nameworthy absorption on the high frequency side of the main vibrational line while lattice absorption sets in very soon on the low frequency side and it is not possible to detect any underlying defect absorption at lower frequencies.

The value of oscillator strength appropriate for the hydride ion vibrations in the alkaline earth fluorides is unknown and will require the detection, and comparison, of an electronic transition in the ultraviolet due to these centres for its determination.

The Smakula formula indicates a reason why deuterated crystals gave an absorption intensity (extinction times halfwidth) of about half that of

identically prepared hydrogenated crystals. In the formula, for a given concentration of impurity, the mass of the impurity times the absorption area is a constant so the greater mass of the deuterium gives an apparently weaker absorption. This aspect of the absorption behaviour, together with the greater width of the deuterium lines, explains why it was necessary to use a 6,9cm total thickness sample to detect the third harmonic of deuterium in calciumfluoride at 20°K while 1.8 cm thickness was sufficient for the detection of the third harmonic/hydrogen.

6. OUTLINE OF THE THEORY OF LOCALISED VIBRATION MODES.

It is now necessary to outline the general theory of lattice vibrations of crystals containing impurities before proceeding to consider the particular theory developed by C.T.Sennett of this laboratory for the special case of very light impurities in the fluorite or similar lattices.

6.1. The Perfect Lattice.

The theory of the vibrations of crystals has been treated in detail by many authors (Kittel (1956), Born and Huang (1954) Montroll (1954), Rosenstock (1955,1957) Maradadin et. al. (1958), Maradudin, Montroll and Weiss (1963) and Mitra (1963).

A crystal can be considered as a large number of atoms arranged in space in a lattice; each atom moving about its site by a small distance and coupled to its neighbours by predominantly harmonic forces. The vibrations of the atoms can be described in terms of normal modes of the crystal which are vibrations in which all the atoms vibrate at the same frequency. For a three dimensional crystal of N cells and n atoms per unit cell there are

3n independent equations of motion and the solutions of these give the normal modes. An example of the calculation is given by Kittel (1956) for the particular case of a one dimensional diatomic chain with the two types o f atoms arranged alternately. For the perfect three dimensional lattice, the normal modes have the form of plane waves; the displacement u_R of an atom at site $\underline{R}$ due to a normal mode of frequency W and wavevector $\underline{k}$ being:

$$u_R = Ae^{i(wt-\underline{k}\underline{r})}$$

The number of normal modes is equal to the number of dynamical degrees of freedom of the system and is, for the general case of a three dimensional crystal of N cells and n atoms per unit cell, 3nN. The frequencies of these normal modes all fall in a finite frequency range and, since their number 3nN is large, they form a quasicontinuous spectrum. For the diatomic lattice this spectrum consists of two bands separated by a gap. These bands form the well known optical and acoustic branches of the dispersion (w verus $\underline{k}$) curve. For a given value of wavevector $\underline{k}$ there are 3 acoustic and (3n-3) optical modes. The symmetry of the lattice determines how many of these modes are frequency degenerate.

A mathematical analysis of the dynamics of the fluorite lattice has been carried out by Cribier (1953,1958) The fluorite lattice has three atoms per unit cell so each wave vector $\underline{k}$ is associated with nine waves: three acoustic, three infrared active optical and three Raman active optical For each mode (acoustical, optical or Raman optical) one wave is nearly longitudinal and the other two nearly transverse. If $\underline{k}$ is parallel to the <100> or the <111> axes, the vibrations are purely longitudinal and transversal degenerate. Furthermore because of the

transversely degenerate. Furthermore, because of the ionic nature of the alkaline earth fluoride crystals, the infrared active vibration in these crystals splits into two and the longitudinal frequency is related to the transverse one by the Lyddane-Sach-Teller relation:

$$\frac{W_L}{W_T} = \left(\frac{\varepsilon_o}{\varepsilon_\infty}\right)^{\frac{1}{2}}$$

where ε_o is the static dielectric constant and ε_∞ is the high frequency dielectric constant. The physical significance of this formula has been discussed by Born and Huang (1954).

Cribier calculated the dispersion curves for calcium fluoride on a model of Coulomb interactions between the atoms and these curves were in agreement with the diffuse Xray scattering results for this substance only if the Lyddane-Sach-Teller relation was assumed invalid. This work was subsequently shown by Granesan and Srinivasan (1962a) to be in error in several important respects and these authors have repeated the analysis of the lattice dynamics of calcium fluoride. They give the dispersion curves for calcium fluoride for the three directions <100>, <110> and <111> calculated on a model employing both shortrange and Coulomb forces. The effects of more distant neighbours is included by a rather arbitary variation of one of the force constants across the Brillouin zone. With the latter effect included, their curves are consistent with both the specific heat data for calcium fluoride and the Lyddane-Sachs-Teller relation.

The formulae of Shimanouchi, Tsuboi and Miyazawa (1961) for the frequencies of the optically active lattice vibrations of the fluorite lattice have already been used (Section 5.3).

Raman (1962) has given a pictorial description of the various normal modes of the fluorite lattice. However Raman emphasises the atomistic

character of lattice vibrations and this viewpoint differs in important respects from the lattice wave picture of Born outlined above. These differences are critically discussed in the review article by Mitra (1963).

6.2. The optical absorption of the perfect lattice.

The frequencies for the various branches of the dispersion curve for the alkaline earth fluorides for $\underline{k}=0$ and for critical points in the zone have been recorded in Table 3 and Section 1.2.

Absorption of light by ionic crystals can occur by several processes:

(1). Absorption by direct interaction of light with infrared active lattice phonons of zero phonon wavevector. $\underline{q}$. The electric field of the light interacts directly only with transverse optical modes possessing a nonzero dipole moment. This process gives rise to the strong reststrahlen absorption observed in ionic crystals. This absorption is a single line in the harmonic approximation.

(2). Absorption by two phonon processes in which the light interacts with two lattice phonons. Conservation of momentum requires these to have zero total $\underline{q}$ vector, i.e.

$\underline{q}_1 + \underline{q}_2 = 0$ where $\underline{q}$ is positive for a created phonon and negative for a destroyed one.

The absorption is a broad envelope because of the spread in the sums of the energies of lattice phonons satisfying $\underline{q}_1 + \underline{q}_2 = 0$. The shape and intensity of the curve is determined by the density of states at the energy sum of the two lattice phonons; peaks in the density of states of the two phonon spectrum give rise to corresponding peaks in the absorption.

This absorption mechanism is responsible for the two phonon summation bands detected by Fray, Johnson and Quarrington (1963) in the absorption of calcium fluoride and referred to previously in Section 1.2.

(3). Absorption by higher order processes involving three or more phonons. These are similar to the two phonon process above; the possible phonon combinations are required to satisfy energy and momentum conservation.

(4). Raman absorption arises from a process in which the light interacts with a lattice normal mode which has a nonzero dipole moment induced by the action of the light itself (rather than induced by the lattice vibrations, as in reststrahlen absorption). In first order, the absorption consists of sharp lines, displaced by the Raman frequency from the exciting light, due to optical phonons of $\underline{q} = 0$. Raman (1962) has described the optical mode giving rise to Raman absorption in fluorite. The selection rules for direct and for Raman absorption differ (Mitra (1963)) and the respective absorptions are due to different optical phonons.

The various absorption processes just discussed will be considered in Section 8.2 in connection with the interpretation of defect induced lattice absorption bands of the alkaline earth fluorides caused by the presence of hydrogen or deuterium ions. These bands are recorded in Table 9.

6.3. The effect of defects on the lattice vibrations.

When a defect is introduced into a lattice it can alter both the nature and amplitude of the normal modes present and, under certain conditions, create new frequencies lying outside the band of normal mode frequencies. The effects will be the largest in the immediate neighbour-

-hood of the defect and become vanishingly small at large distances from it.

It was shown by Rayleigh (1877) (see also Maradudin, Montroll and Weiss (1963)) that if the mass of a single atom in a perfect lattice is reduced (or the force constant increased) all the lattice frequencies increase, but by no more than the distance to the next higher unperturbed frequencies. Similarly, for an increase in the mass (or decrease in the force constant), the frequencies cannot decrease by more than the distance to the next lower unperturbed frequencies. As the separation of the frequencies in a band is of the order of $\frac{1}{nN}$, nN being the total number of atoms in the lattice, all the frequencies are changed at most by $O(\frac{1}{nN})$, except those at the band edges. Consequently the introduction of a defect has little effect on the band of frequencies except those at the edges.

The frequencies at the band edges can be displaced by a considerable amount and may occur outside the band of normal mode frequencies. Such frequencies are not propagated by the lattice, but are attenuated in a short distance; the distance decreasing as the difference between the new frequency and the band edge increases. The associated normal mode of vibration is localised around the defect. It has an amplitude which is large at the defect and which decays exponentially away from it. These are the localised defect modes. They have been discussed by Montroll and Potts (1955) for the case of the one dimensional monoatomic lattice, by Mazur Montroll and Potts (1956) for the one dimensional diatomic lattice with an isotopic defect and by Bjork (1957) and Maradudin et.al (1958) for the general one dimensional diatomic lattice. Krumhansl (1962) has given a

non-mathematical description of the properties of localised modes.

For the case of the one dimensional diatomic lattice in which one of the masses is altered, the qualitative behaviour is:

(1) When one of the lighter masses m is replaced by a lighter isotope m' then one level jumps out of the optical band to the region above, whereas if it was replaced by a heavier isotope then one level drops from the bottom of the optical band into the gap.

(2) When one of the heavier masses M is replaced by a lighter isotope one frequency rises from the top of the acoustical band into the gap and a second band rises from the top of the optical band, while if the heavier mass M is replaced by a heavier isotope, then no frequencies emerge from the bands.

For this case of isotopic substitution in a one-dimensional diatomic lattice the frequencies of the localised modes can readily be calculated and are given by Mazur, Montroll and Potts (1956).

For three dimensions, the situation is more complicated and in particular noncentral forces have to be considered. Theoretical calculations on localised modes for this case of three dimensions usually involve the use of Green's function techniques and have been carried out by Dawber (1962), Dawber and Elliott (1963 a,b), Maradudin, Montroll and Weiss (1963) and Takeno, Kashiwamura and Teramoto (1963) among others. Wallis and Maradudin (1960) have calculated the expected infrared absorption of the U centres in the alkali halides on a three dimensional model of a diatomic lattice with nearest neighbour interaction and obtained good agreement with the

observed frequencies. This model is, however, not directly applicable to the problem of hydrogen and deuterium vibrations in the fluorite lattice.

Bjork (1957) and Krumhansl (1962) have emphasised the large effect the defect localised mode has on the motion of the defect itself and the neighbouring atoms. This result follows from the fact that the local mode has its normal components only at or near the defect and so if it is well localised, these components have a very large amplitude at the defect. The effect of the local mode is comparable to the combined effect of all the other 3nN lattice modes. While this conclusion has to be modified in light of the work of Rosenstock and Klick (1960) and of Casselman and Markham (1963) on the interaction of the lattice with the electronic wavefunctions of the defect, it can be seen that the effects of the local mode are of considerable importance in the study of properties of perturbed lattices.

Other aspects of local modes, such as their self energy and their long range clustering tendency are discussed in the treatise by Maradudin, Montroll and Weiss (1963).

6.4. The Special Case of Hydrogen and Deuterium Ions.

For the hydrogen defect the impurity atom is very light and the localised mode frequency is relatively high, between two and three times the highest frequency of the lattice vibration spectrum of any of the three alkaline earth fluorides. Consequently, the mode is strongly localised around the defect; so much so that, to a good approximation, the rest of the lattice may be considered as static. Such an approximation will be less satisfactory for deuterium. However, as the relative frequency ratio

squared, $(\frac{W_H}{W_D})^2$ equals 1,93 (for the fundamentals) while for independent oscillation of the ions it would be 2(the inverse mass ratio), the assumption of a static lattice for the deuterium impurity also is a reasonable one.

6.5. The Theory of C. T. Sennett.

C. T. Sennett of this laboratory has developed a theory of the localised vibrations of hydrogen and deuterium in alkaline earth fluorides. This uses the assumption of the rest of the lattice as static and has been applied by him to interpret some of the experimental results presented earlier. The theoretical results quoted in the following description of the theory have been obtained from Sennett's thesis which was made available to the author prior to publication.

6.6. Outline of the Theory.

The hydrogen atom vibrates in a potential well which has the symmetry of the point group of the site. This is O_h for interstitial and alkaline earth metal sites and T_d for fluorine sites.

A Hamiltonian of the following form is assumed:

$$H = \frac{1}{2m}(p^2 + mw^2r^2) + \sum A_{ijk}x_ix_jx_k + \sum B_{ijkl}x_ix_jx_kx_l$$

where the first term is the spherical harmonic oscillator Hamiltonian for a particle of mass m and momentum p vibrating with an angular frequency w, the A and B are the cubic and quartic constants of an anharmonic potential and the x's are Cartesian displacement coordinates of the particle. The Hamiltonian may be written; $H = H_0 + V_3 + V_4$

The V_3 and V_4 are anharmonic terms of the potential and are treated as perturbations on the spherical harmonic oscillator Hamiltonian, H_0. Each term is of the order $\frac{x}{a}$ smaller than the preceding one, where x is the atom

displacement and a the interionic spacing.

The number of independent constants in V_3 and V_4 depends on the symmetry of the hydrogen ion site. For T_d symmetry, group theoretical arguments allow one constant for V_3 and two for V_4 so;

$$A_{ijk}\, x_i x_j x_k = Axyz$$

$$B_{ijkl}\, x_i x_j x_k x_l = B_1 (x^4 + y^4 + z^4) + B_2 (x^2y^2 + y^2z^2 + z^2x^2)$$

For O_h symmetry there is also present the inversion operator so A = 0 in this symmetry. This fact, coupled with the experimental observation of harmonic frequencies, is the justification for assigning the observed lines to hydrogen (or deuterium) present on fluorine sites; these being the only ones with T_d symmetry. This fact also explains why no second harmonic is observed in the U centre localised vibration spectrum of the alkali halides. In this case, the halide sites also possess the full O_h Symmetry and any term cubic in the displacement, like Axyz which renders the second harmonic "visible" vanish. Third harmonics are expected in both symmetries, but these have not been reported for the alkali halides to date, presumably because of their weak intensity.

The Hamiltonian appropriate to fluorine sites in the fluorite lattice, is;

$$H = H_0 + V_3 + V_4$$

$$= H_0 + Axyz + B_1 (x^4 + y^4 + z^4) + B_2 (x^2y^2 + y^2z^2 + z^2x^2).$$

The unperturbed Hamiltonian H_0 has solutions whose wavefunctions are those of the spherical harmonic oscillator. These may be written in the form $|n_1\ n_2\ n_3>$ where n_1, n_2 and n_3 are the quantum numbers for each of the three independent linear oscillators. The following energy scheme

results:

State	Wavefunction $\lvert n_1\ n_2\ n_3\rangle$	Symmetry of the wavefunction in terms of the irreducible representations Γ_n of the group T_d.
Ground state	$\lvert 0\ 0\ 0\rangle$	Γ_1
First excited state	$\lvert 1\ 0\ 0\rangle$	Γ_4
Second excited states	$\lvert 2\ 0\ 0\rangle$ $\lvert 1\ 1\ 0\rangle$	$\Gamma_1 + \Gamma_3$ Γ_4
Third excited states	$\lvert 1\ 1\ 1\rangle$ $\lvert 2\ 1\ 0\rangle$ $\lvert 3\ 0\ 0\rangle$	Γ_1 $\Gamma_4 + \Gamma_5$ Γ_4

The anharmonic terms in the potential raise the degeneracy of the higher excited states, splitting them into components of different symmetry types appropriate to the reduced point symmetry T_d, and also mix together levels of the same symmetry Γ_n. The observable levels are those with Γ_4 symmetry; thus one sees the fundamental, a second harmonic and a third harmonic doublet.

The constants of the potential can be evaluated from the deviations/ of

the frequencies from exact multiples of the unperturbed fundamental frequency. The shifts in the levels of the harmonic oscillator produced by the anharmonic terms are calculated by perturbation theory; to second order in V_3 and to first order in V_4. The experimentally determined frequencies are sufficient to enumerate the four constants describing the potential well.

For $\bar{H}^-$ in calcium fluoride:

$$A = 4.31 \times 10^{12} \text{ ergs/cm}^3$$

$$B_1 = 2.29 \times 10^{21} \text{ ergs/cm}^4$$

$$B_2 = 1.77 \times 10^{21} \text{ ergs/cm}^4$$

w corresponds to a fundamental frequency of 952cm^{-1}.

The accuracy is only 10% because the deviations from exact harmonicity are small.

The relative intensity of the various absorption lines may also be calculated. The second and higher harmonics are made visible by the anharmonic terms and so their intensity is already fixed by the values of A, B_1 and B_2 obtained from the energy shifts.

For H^- in calcium fluoride, the results are:

$$\frac{\text{Second harmonic}}{\text{Fundamental}} \doteq \frac{1}{350}$$

$$\frac{\text{Third harmonic}}{\text{Fundamental}} \doteq 3 \times 10^{-4}$$

Ratio of third harmonic lines = 5.5.

The temperature dependence effects follow from the interaction of the localised mode with the lattice or "in-band" modes. The interaction c n be represented by additional terms in the Hamiltonian.

The width of the lines arises from the process in which lattice phonon s are scattered off the defect and suffer a momentum change while conserving energy. The appropriate term in the Hamiltonian is the product operator $b^{\dagger}b a^{\dagger}(\underline{k}')a(\underline{k})$ where $b^{\dagger}b$ and $a^{\dagger}a$ are the creation and the annihilation operators for the local and lattice modes respectively. In this term, the local mode undergoes no overall energy change while a lattice phonon changes momentum from $\underline{k}$ to $\underline{k}'$. This process gives a finite lifetime to the optically excited state and a halfwidth proportional to the transition probability fo r the scattering.

It involves two band modes which, with the assumption of a Debye distribution for these, gives a transition probability proportional to T^2 at high T and T^5 and T^7 at low T.

The diagonal term of the same perturbation represents the average number of band modes excited and gives rise to an energy shift proportional to T at high and T^3 at low T.

The residual line width observed at low temperature is due to the spontaneous decay of the local mode into band modes. Such decay processes have been discussed by Klemens (1961) for the case of two phonon decay. Subsequent to the theoretical work described here, Hanamura and Inui (1963) applied the mechanism of three phonon decay to the problem of the broadening of the infrared absorption lines of U centres in the alkali halides.

Since, for the case of H^- in the alkaline earth fluorides, the local mode frequency is more than twice the highest frequency of the lattice

continuum, the mode itself cannot split into two lattice phonons without violating energy conservation. It, however, does lie within the three phonon spectrum and decay can occur via the quartic anharmonic matrix element of form $ba^{+}(\underline{k})a^{t}(k')a^{t}(\underline{k}'')$.

The calculations yield a zero temperature halfwidth of $0.15cm^{-1}$. The contribution of this term to the temperature dependent line width is T^3 at high T, T at low T apart from the residual width, but has a negligible magnitude compared to the scattering process initially considered.

For the case of deuterium, the local mode frequency is lower and lies within the two phonon spectrum. A cubic anharmonic term is now possible of the form $ba^{+}(\underline{k})a^{+}(\underline{k}')$ and the calculations yield a zero temperature halfwidth of approximately $1cm^{-1}$. The high temperature dependence is T^2 and indistinguishable from that of the mechanism of scattering of lattice phonons off the defect treated earlier.

A further process to be considered is the interaction of the local mode with optical modes. A term of the form $b^{+}b^{+}a(\underline{k})$ mixes into the wavefunction of the second harmonic some of the reststrahlen phonon and gives enhanced second harmonic absorption. Such a process does not occur for the U centres in the alkali halides and the previous conclusion of zero intensity for the second harmonic of the U centre localised vibration is still valid.

7. DISCUSSION OF THE LOCALISED VIBRATION LINES.

7.1. The Temperature Dependence of the Width.

The theory just outlined provides a satisfactory interpretation of the temperature dependence of both the width and peak position of the lines. In the high temperature limit it predicts a T^2 dependence of the width and a linear temperature variation of the peak position. Sennett has pointed out that, due to the smoothness of the Debye integrals, this high temperature behaviour will be apparent to quite low temperatures and the T^5,T^7 width behaviour and T^3 peak position variation will both be confined to the region below $\Theta_H/50°K$. The Debye temperature Θ_H for calcium fluoride is 474°K and is lower for strontium and barium fluorides. The T^5 and T^7 line width behaviour is thus unobservable in all three systems because the lines have reached their residual width at 20°K and do not narrow on further cooling.

All the hydrogen vibrational lines studied in detail show an accurate T^2 dependence of their width in the temperature range 80°-300°K after correction for the residual widths has been applied (Table 7). Slight deviations in the results are attributed to experimental errors of measurement. The one deuterium line studied shows a deviation from T^2 behaviour, after correction, and this appears larger than can be accounted for solely on experimental error. It could arise, in part, from the additional contribution of the nonzero two phonon anharmonic decay term (present only in the deuterium impurity case) to the overall width. This term contributes a T^2 dependence width in addition to the residual width. This would tend to nullify the effect of the large zero temperature residual width itself on the slope and thus yield an apparently smaller value for the extrapolated zero temperature value (as shown in Table 7).

7.2. Variation of the Peak Position.

This aspect of the lines was discussed in some detail in Section 5.4 where the frequency vari tion of the peak position was calculated on a simple thermal expansion model. This model gave a larger shift in line position than actually observed. This can be seen from the various values for the volume Gruneisen constants $\gamma_v (= - \frac{d \log w}{d \log v})$, where w is the frequancy and v the volume. For the observed frequency variation of the fundamental vibrational line of hydrogen in calcium fluoride, this constant has the average value of 0.8 while for the various lattice frequencies of pure calcium fluoride Ganesan and Srinivasan (1962b) calculate values ranging from 2 to 3.6. Experimentally, Press (1950) found a value of 1.7 for the variation of the peak position of the Raman line of calcium fluoride. However, it is well established that Gruneisen's law is too simple to be able to explain experimental facts, and the γ_v is different for different frequencies (Viswanathan (1963)).

For a more realistic model, it is necessary to consider the direct effects of anharmonicity on the localised mode of vibration. The anharmonic scattering term (Section 6.6) yields an energy shift proportional to T at high T and so gives a variation of the peak position of the lines with temperature. Sennett shows that the anharmonic coefficients, determined earlier from the deviation of the frequencies of the harmonic lines from exact harmonicity, are of the magnitude necessary to wholly account for the observed variation in the peak position of the lines with temperature. Furthermore, the linearity

of the observed variation of the peak position with temperature (shown in Figures 15 and 16) follows directly from this anharmonic scattering process.

7.3 Variation of the Residual Widths of the Three Fluorides

The residual widths of the lines are the linewidth values at 20°K and these show a marked variation with host material and impurity ion. They are not particularly amenable to a straight-forward classification but, in general, exhibit the following relationships, with several notable exceptions.

(1) The line widths of the first and second harmonics of a given impurity in a given host are proportional to their frequencies, i.e., the proportional linewidth, $\frac{\Delta w}{w}$, is approximately constant.

(2) The deuterium linewidths are invariable larger than the corresponding hydrogen linewidths and, as the respective vibration frequencies are smaller, $\frac{\Delta w}{w}$, is larger still for the deuterium lines. It is up to six times larger than the corresponding hydrogen line value.

(3) The linewidths for a given impurity in the series CaF_2, SrF_2, BaF_2 increase with increase of the cation mass. The proportional linewidth $\frac{\Delta w}{w}$ displays an even greater variation range from 5×10^{-4} to 4×10^{-3} for the hydrogen impurity second harmonics.

The various factors that contribute to the residual or zero temperature linewidth have been discussed by Dawber (1962) and Dawber and Elliott (1963b). They are:

(a) Broadening due to the finite lifetime of the localised mode for decay into lattice modes. This effect has been already discussed

(Section 6.6) and yields, in the Debye approximation, a width of 0.15cm^{-1} for the fundamental frequency of the localised vibration of hydrogen in calcium fluoride and approximately 1 cm^{-1} for the corresponding deuterium line. Of all factors contributing to the residual width, this is the only one which predicts a larger width for the deuterium lines relative to those of hydrogen, this result immediately following from the stability of the hydrogen lines against two phonon decay. The greater width of the experimentally observed deuterium lines has already been stressed and would indicate that the mechanism of anharmonic decay of the localised modes contributes a major part of the observed linewidth.

(b) Broadening due to the random distribution of isotopes of the host lattice. Only the cations in the fluorite lattices studied have a varied isotropic composition and calculations by Sennett indicate that their contribution to the width is negligible.

(c) Broadening due to local lattice strains. It is estimated that a uniaxial stress of approximately 5 tons per square inch would be required to produce a 1 part in 1000 strain and so yield a significant contribution to the widths. Such stresses are unlikely to be present in the crystals used in view of the method of preparation. This effect must be considered as of negligible importance.

(d) Broadening due to lattice defects. This possibility is discussed later (section 8.1) in connection with the satellite structure. The contribution to the width would be small as only vibrations of ions adjacent to a defect would be affected, and these form only a small

fraction of the total.

Of all the factors enumerated above, the anharmonic broadening mechanism is the one able to explain the observed widths. It has already been used to explain the greater width of the deuterium lines.

For the variation of the linewidth of a given harmonic with host material one cannot postulate a variation of the anharmonicity as this is of similar magnitude in all three fluorides (Section 7.5). The expression for the linewidth for the three phonon decay process, calculated on the assumption of a Debye distribution of lattice modes is given by Sennett as:

$$\Gamma = \frac{2(3\pi)^5}{r_0^6}\left[\frac{B^2\hbar^2}{16M_D^3 mw}\right]\left(\frac{\hbar}{k\Theta}\right)^4 \cdot \frac{3}{2.3^9}\left(3-\frac{W}{w_m}\right)^2\left(\frac{W}{w_m}\right)^9$$

Where Γ = upper limit for the halfwidth

$2r_0$ = interionic radius

M_D = mass of the elementary cell = $(M_{metal} + 2M_F)$

m = mass of the impurity

Θ = Debye temperature

k = Boltzmann constant

W = local mode frequency

and w_m = Debye cutoff frequency of the lattice

This formula requires $W = w_1+w_2+w_3$, where w_1, w_2, w_3 are lattice frequencies all less than or equal to w_m.

For calcium fluoride the local mode frequency of the hydrogen impurity is 3.76 times the peak reststrahlen absorption frequency and

the residual width is <0.7 cm^{-1}; for strontium fluoride the local mode frequency is 4.10 times restrahl and the residual width is 1.7cm^{-1} and for barium fluoride the ratio is 4.38 and the width approximately 7 cm^{-1}. It is suggested that the increase in width with cation mass follows from the increase in the relative ratio of the local mode frequencies to the lattice frequencies. The formula above shows a ninth power dependence on the ratio $\frac{W}{w_m}$. It also involves the inverse fourth power of the Debye temperature and this yields a further contribution to the linewidth for the series, CaF_2, SrF_2 and BaF_2. However, the formula, in its present form, cannot be applied to strontium or barium fluorides as these have their local mode frequencies more than three times their Debye frequencies.

It is necessary to improve the model beyond the Debye approximation and consider the actual density of states of the two and three phonon spectra (for the deuterium and hydrogen lines respectively) at the observed frequencies of these lines. This problem of evaluating the density is insuperable at the moment due to the lack of any precise experimental knowledge of the lattice phonon spectra of the fluorite lattice; the optical data on the pure lattice given previously, in Section 1.2, only yield the two lattice phonon spectrum of zero total wavevector. One requires the results of slow neutron scattering experiments in order to calculate the complete two or three phonon spectra and such results are not yet available. Cribier, Farnoux and Jacrot (1963) have recently carried out neutron scattering experiments and their measurements are referred to by Cochran (1963). Further details of this work are not yet

known.

With the present results one can only invert the problem and take the observed linewidths as a measure of the density of the appropriate multiphonon spectrum at this frequency. Doing this, of course, implies that the contributions of all other broadening mechanisms are negligible.

It should be possible to deduce qualitatively the observed increase in residual linewidths with cationic mass from the relation of the local mode frequencies to the peaks in the density of states of the lattice frequencies. An attempt to do this is now described. The various optical branch frequencies of the three fluorides are:

	CaF_2	SrF_2	BaF_2
Longitudinal Optical frequency at $\underline{k} = 0$	463	374	326 cm^{-1}
Longitudinal Optical frequency at peak in density of states	368	325*	280* cm^{-1}
Raman frequency at $\underline{k} = 0$	321.5	-	244.0 cm^{-1}
Transverse Optical frequency at $\underline{k} = 0$	257	217	184 cm^{-1}

The asterisked frequencies have been estimated from the observed peaks of the broad satellite bands described later in Section 8.2. The local mode frequencies of the hydrogen impurity in the three fluorides are (20°K values):

CaF_2	SrF_2	BaF_2	
965	892	802	cm^{-1}

The difference in the linewidths comes from the different density of states of the three phonon spectrum at the frequencies of these lines in the respective lattices. Following Hanamura and Inui (1963) the three lattice phonons, n_1, n_2, n_3 satisfying the energy conservation relation $W = w_1+w_2+w_3$, (where W is the local mode and w_1, w_2, w_3 lattice mode frequencies) are replaced by an effective set of three equal phonons n^*_{op} with the effective frequency $w^*_{op} = \frac{1}{3} W$. The problem then reduces to an examination of the density of states of the (one phonon) lattice spectrum at a frequency equal to one third of the local mode frequency. These frequencies are:

	CaF_2	SrF_2	BaF_2	
w^*_{op}	322	297	267	cm^{-1}

These all fall wholly above the transverse optical branch and partially below the longitudinal optical branch. However, the separation of these frequencies from the respective peak in the density of states of the longitudinal branch differs in all three cases. The calcium fluoride frequency falls $46 cm^{-1}$ away, the strontium fluoride frequency $28 cm^{-1}$ and the barium fluoride frequency $13 cm^{-1}$ away. The actual density of states at these three frequencies would thus tend to increase in the order CaF_2, SrF_2, BaF_2 and the observed increase of residual width of these three substances can be qualitatively explained. The Raman frequency's peak in density of states was neglected as no satellite bands, comparable in intensity to the transverse optical and longitudinal optical ones were observed

experimentally (Section 8.2). Either the peak in density of states for this branch is small or (Section 8.2.) the transition is symmetry forbidden.

A similar analysis can be performed for the deuterium impurity lines. The width of these arises from two phonon decay processes so the density of states at half the deuterium local mode frequencies is to be considered. These are:

CaF_2	SrF_2	BaF_2	
347	320	289(estimated)	cm^{-1}

The separation of these from the adjacent longitudinal optical mode's peak m density of states is 21, 5 and -9 cm^{-1} respectively. The residual halfwidth of the lines in calcium and strontium fluorides are 2.2 and 2.5 cm^{-1} respectively, while the barium fluoride line has not been observed.

The qualitative agreement of the relative line widths with the relative separations above is not good, but it could be improved by considering the relative magnitude of the relevant peak in the density of states in the three fluorides. However, since the model is based on the approximations of a multiphonon spectrum of zero total wavevector and of local mode decay into equal lattice phonons, it is not worth attempting to refine it in such detail. As used here, the model is similar to a Debye model with Debye frequencies equal to the frequencies of a peak in the density of states of the infrared active longitudinal optical mode. It has been described to illustrate

qualitatively a reason in the lattice framework for the increase in the residual line width with cationic mass.

The increase in the residual width with mass of the cation is not nearly so pronounced in the alkali halides. Price, Smart and Wilkinson (1963) show that the 100°K linewidths do not depend upon the cation to any great extent (although there is a marked increase in linewidth with increasing mass of the anion). Hanamura and Inui (1963) have derived the residual widths at zero temperature from the results of Schäfer (1960) and confirm the small cation mass dependence of this linewidth. (The increase with anion mass was attributed to the corresponding decrease of the localised mode frequency; at a given temperature the halfwidth is largest for the crystal of a given cation with the smallest local mode frequency). The alkali halides in general thus appear to exhibit a different behaviour from the alkaline earth fluorides. However, one should only compare the alkali fluoride data with that of the alkaline earth fluorides. The data on these is, however, limited. Price, Smart and Wilkinson (1963) give the 100°K linewidths of sodium fluoride as 1.4cm^{-1} and of potassium fluoride as 2.5 cm^{-1}. They did not quote a halfwidth value for the rubidium fluoride U centre (whose frequency they measured). It is not possible to say, without further information, whether there is a systematic increase in the residual widths with the cation mass or whether there is any similarity in residual width behaviour between these fluorides and those of the alkaline earth fluorides.

7.4 The Exceptions to the Residual Linewidth Variation Pattern

There are several exceptions to the general variation of the residual linewidth outlined above. These are:

(a) The second harmonic of deuterium in strontium fluoride has a smaller residual width than would be expected from the value for the fundamental and from the residual widths of the corresponding lines in calcium and barium fluorides. This width has been confirmed by H. Macdonald.

It is suggested that this particular anomaly arises from a pronounced variation in the density of states of the two phonon spectrum in the neighbourhood of the local mode frequency. Examination of the approximate model above shows that while the fundamental frequency is 5 cm^{-1} lower than the relevant longitudinal optical mode frequency, half the second harmonic frequency is 7 cm^{-1} lower.

This, together with the sharp peaking in the density of states about the maximum (implied in the sixth power dependence of the width on $\frac{W}{W_m}$ shown by the formula given by Sennett for the two phonon decay process on the Debye model) could qualitatively explain the anomalously small width of the second harmonic line.

(b) The fundamental of hydrogen in barium fluoride has an anomalously large residual width in relation to the second harmonic line. The shape of this line is, however, not symmetric and the line appears to be made up of two partially resolved lines. This line shape was obtained repeatedly in different crystals.

The relation of the linewidths of the fundamental and second

harmonic is ascribed to the steep variation in the peak of density of states near the fundamental local mode frequency. This explanation is the same as the one given above for the deuterated strontium fluoride lines.

(c) The third harmonic lines for hydrogen and deuterium in calcium fluoride do not fit any obvious pattern. While one of the two third harmonic lines in both cases has $1\frac{1}{2}$ times the second harmonic width, it is the opposite member of the third harmonic doublet in the two cases. The other lines have a larger width, bearing no simple relation to the first line's width. No simple particular explanation can be offered for the behaviour of these lines.

7.5 Variation of the Room Temperature Linewidths of the Three Fluorides

The room temperature linewidths display the following relationships:-

(1) For the various harmonics of a given impurity in a given lattice the width is approximately proportional to the frequency of the harmonic, i.e., $\frac{\Delta w}{w} \sim$ constant.

(2) The hydrogen lines are a factor of around 1.6 times wider than the corresponding deuterium lines. This can be attributed to the greater anharmonicity of the hydrogen localised vibration which, in turn, arises from the larger amplitude of oscillation of the lighter impurity ion. This larger anharmonicity results in a bigger contribution of the lattice scattering process (section 6.6) to the width at all temperatures; at low temperatures the "anharmonic decay" term dominates and causes the relative inversion of the hydrogen and deuterium linewidths.

(3) The linewidths are approximately constant for a given harmonic of a given impurity and for variation of the host material. This indicates that the anharmonicity of the localised vibration of a given impurity ion is similar in all three fluorides. The conclusion is confirmed by the constancy of the frequency ratio of the second harmonic to the fundamental in the three fluorides.

From this fact one can predict that the spacing of the third harmonic doublets will be similar in all three fluorides. Thus one would expect the third harmonic doublets in strontium fluoride and barium fluoride, which were not detected in this work, to have spacings of approximately 85 cm^{-1} in the hydrogen case and 45 cm^{-1} in the deuterium case. The first conclusion is confirmed by the recent measurements of Price, Smart and Wilkinson (1963).

7.6 The Harmonic Ratios

Comparison of the observed and calculated harmonic ratios reveals a large discrepancy. The different harmonics are much more intense relative to the fundamental than the anharmonic coefficients, determined from the frequency deviations off exact harmonicity, would allow. The enhanced intensity is attributed to the interaction of the defect with the optical modes (described in section 6.6.); a process in which the harmonics "borrow" intensity from the reststrahl phonon.

The ratio of 5.5. calculated for the lines of the third harmonic doublet is in good agreement with observation.

7.7 Variation of the Intensity of the Vibrational Lines with Temperature

This is shown in Figure 17 for some of the observed lines. Part of the decrease in intensity above 200°K can be attributed to two causes:

(a) the thermal excitation of the hydride or deuteride ions.

This process has been discussed by Schäfer (1960) for the case of the alkali halides. The local mode frequency of hydrogen in calcium fluoride is 960 cm^{-1} and corresponds to a temperature of 1370°K. At room temperature, therefore, a few of the hydride ions are excited and, assuming a Bose-Einstein distribution, there is a decrease of 1% in the occupation number of the ground level at 290°K compared to 20°K. The transition probability is proportional to the product of the number of sites occupied in the ground state and free in the excited state so the absorption at 290°K is 98% of the low temperature value.

This process does not account for more than a small fraction of the observed decrease of the absorption above 200°K of hydrogen or deuterium in calcium fluoride.

(b) the partaking of the impurity ions in the absorption of the satellite bands.

These bands are discussed in detail in Section 8.?. It is sufficient here to state that they arise from the process in which the incident light interacts with, and creates or destroys, a lattice phonon to create an impurity vibrational mode phonon. The absorption of the low frequency bands decreases at low temperatures as $\exp[-\hbar\omega/kT]$

where $\hbar\omega$ is the lattice phonon energy and T is the temperature. The high frequency bands have an absorption largely independent of temperature at low temperature.

For hydrogen in calcium fluoride, there are prominent satellite bands 150cm^{-1} lower and higher in frequency than the main vibrational line. The energy of the required lattice phonon of this frequency of 150 cm^{-1} is comparable to the thermal energy kT at room temperature and so the more general formulae for the absorption dependence on temperature, given in Section 8.2 must be used. The absorption of the low frequency satellite band is calculated to have the following variation pattern:

290°K	200°K	100°K	20°K
100%	54.5%	14.4%	0.2%

where the absorption has been expressed as a percentage of the room temperature value. The effect of this variation on that of the main absorption line requires a knowledge of the intensity ratio of the low frequency satellite band to this line. The 150cm^{-1} lower frequency satellite band has only been observed about the second harmonic for hydrogen in calcium fluoride and the room temperature ratio of intensities is 22. The expected absorption variation of the main line thus is:

290°K	200°K	100°K	20°K
95.8%	97.6%	99.5%	100%

The high frequency sideband shows a less steep absorption

variation, viz:

290°K	200°K	100°K	20°K
100%	78.5%	59.5%	52.6%

Its ratio to the main vibrational line is 12 hence the variation of the absorption of the main line due to this particular contribution is:

290°K	200°K	100°K	20°K
96.4%	98.1%	99.7%	100%

The combined effect of both satellite bands yiels an overall absorption variation for the main vibrational line of:

290°K	200°K	100°K	20°K
92.3%	95.7%	99.1%	100%

The contribution of these satellite bands is smaller than that necessary to fully explain the observed absorption decrease of the second harmonic of hydrogen in calcium fluoride. As for the remaining 3% observed decrease in the absorption of this line at high temperature, one is inclined to attribute it to errors in determination of the integral absorption. The main factor of uncertainty, which can be considerable at high temperature, lies in the fixing of the line of complete transmission. The resulting absorption values could be in error to the extent of 10% at high temperatures.

Of all the lines studied in detail, the fundamental and second harmonic lines of hydrogen in calcium fluoride are the only ones possessing an almost constant absorption intensity above 100°K and for which the slight high temperature decrease can be reasonably accounted for. All the other lines studied in detail show a considerable decrease (up to

50%) in absorption from low temperature to room temperature.

The process, discussed above, of the transfer of intensity to the satellite bands by the localised vibrations will be more important in strontium and barium fluorides, because their satellite bands are closer to the main vibrational lines (the relevant lattice phonons being of smaller energy). The intensity variation will be larger and will extend to lower frequencies. However, even in these cases, it is unable to account for more than a small fraction of the decrease of absorption intensity observed.

Of the other lines, which were measured only at three temperatures (290, 77 and 20°K), the second harmonic line of deuterium in strontium fluoride has approximately the same absorption intensity at all three temperatures, while the second harmonic of hydrogen in strontium fluoride shows a 25% decrease in intensity from 77°K to 290°K. The second harmonic line of deuterium in barium fluoride shows a 50% decrease in absorption at room temperature from low temperature and so is similar in behaviour to the second harmonic of hydrogen in barium fluoride shown in Figure 17.

Similar large absorption decreases were observed in the alkali halides by Schäfer (1960). No completely satisfactory explanation was offered for this phenomenon.

Apart from the "electrical anharmonicity" effect mentioned by Raman (1947) in his discussion of lattice vibrations of crystals, no suggestion can be made for the observed absorption decrease of the lines with temperature.

The fundamental and second harmonic lines of hydrogen in calcium fluoride show an apparent decrease in integral absorption at temperatures below 80°K, while all the other lines examined (with the possible exception of the second harmonic of hydrogen in strontium fluoride) maintain, or increase in, intensity from 80°K to lower temperatures (20°K). This particular decrease is related, in part, to the narrow width (<1 cm^{-1}) of the lines at low temperatures. For these linewidths, the effects of finite instrumental resolution are significant and can account for up to 10% of the observed decrease (Brügel (1962)). The remaining actual decrease in absorption is difficult to estimate accurately, but amounts to some 25% for both lines. There is no corresponding decrease in the third harmonic line of hydrogen in calcium fluoride. No explanation can be offered for this decrease.

8. DISCUSSION OF THE SATELLITE STRUCTURE

The structure about the main vibrational line consists of two kinds of lines distinguishable in their temperature dependent behaviour. These will be discussed separately.

8.1 The Strongly temperature dependent lines

These lines occur in the vicinity of the main line. The research work on these lines is by no means completed and no one model can be postulated to explain all the lines observed. At this stage of research one can only advance tentative explanations for their appearance.

The lines are of small intensity relative to the main vibrational

line and must arise from anomalies of one kind or another which affect the symmetry of nature of the site of the light ion impurity and thus perturb the vibrational frequencies. The displaced lines will retain the dependence of width on temperature, characteristic of the undisturbed vibrational line.

Possible reasons for the observed lines include the following:

(a) the occurrence of adjacent light impurity ions.

The problem of two defects in a lattice has been investigated by Montroll and Potts (1955). They show that the frequency of an isolated defect is split into two as two isolated defects are brought together. A shift in the mean frequency is also produced and the two frequencies are not symmetrical about the single unperturbed frequency.

An order of magnitude calculation using equation 5.16 of Montroll and Potts yields a 1 part in 150 splitting for the hydride ion with a five times greater frequency shift of the doublet to lower frequencies, i.e., the perturbed hydride frequencies are given by the relation:

$$W_{perturb} = W_{unperturb}\left(1 \mp \frac{1}{150} - \frac{1}{30}\right)$$

For the fluorite lattice, this can only be an approximation. However, one would expect doublets on the low frequency side displaced by a frequency of the order of five times the doublet spacing.

Such low frequency doublets are evident in the structure around the fundamentals of hydrogen in both calcium and strontium fluorides. The calcium fluoride sample has a doublet at 943.5 and 947 cm^{-1} displaced by 19.5 cm^{-1} from the main line at 965 cm^{-1}, which gives a displacement to splitting ratio of 5.6; while the strontium fluoride sample has a doublet at 886.5 and 884.5cm^{-1} displaced by 7.5cm^{-1} from the main line at 893cm^{-1}, which yields

displacement to splitting ratio of 3.7.

The results for the fundamental of hydrogen in barium fluoride are inconclusive because of the large linewidth of the main vibrational line. The anomalous behaviour of this line has been discussed already in Section 7.4.

A verification of this particular interpretation would be the existence of similar doublets in the deuterated crystals occurring at the same relative distance from the unperturbed frequency, but having twice the relative splitting. This could not be verified as the presence of strong lattice reststrahlen absorption prevents the examination of crystals of the thickness necessary to show the deuteride satellite structure.

For the next nearest neighbour impurity ions, the splitting and displacement of the vibrational frequency is very small (1 part in 1200 displacement and a much smaller splitting) and the effects of more distant impurity ions must be considered negligible.

The model of adjacent hydride (or deuteride) ions would be expected to be strongly concentration dependent since the probability of a random juxtaposition of impurity ions decreases rapidly with reduction in the concentration of defects. However, there may be a tendency for the defects to cluster and this could modify the concentration dependent behaviour.

The model in its present form seems only capable of interpreting a few of the observed lines. It cannot explain the simple structure around the second harmonic line in hydrogenated barium fluoride (Fig. 23)

without a large reduction in the magnitude of the frequency displacement term given in the analysis of Montroll and Potts (1955). It is quite possible that the agreement of the observed doublets with predictions of the theory purely fortuitous; particularly since adjacent similar lines have been neglected. An example is in the analysis of the satellite structure around the fundamental of hydrogen in strontium fluoride (Fig. 21); where the doublet at 886.5 and 884.5 cm^{-1} is interpreted by this model while the 905.4 cm^{-1} line is ignored.

(b) The presence of vacancies

The effect of a nearby vacancy is to distort the field around the impurity and raise the threefold degeneracy of the localised vibration. In general, one would expect line triplets around the unperturbed frequency. The overall spacing of these lines would decrease with increasing separation of the vacancy and the impurity ion. For the magnitude of this spacing one can refer to the calculation of Fritz (1962) for the same effect for the case of interstitial hydride ions in the alkali halides. With due consideration for the differences in the fluorite and alkali halide lattices and for the different sites of the impurity, one can estimate an order of magnitude splitting of up to one fifth of the unperturbed frequency for the particular case of immediately adjacent anion vacancy and impurity ion. For the fundamental of hydrogen in calcium fluoride this model thus gives lines up to 200 cm^{-1} away from the unperturbed frequency. The satellite line spectra should consist of recognisable groups of two or three lines centred about the main vibrational line.

Further aspects of this model will be discussed in conjunction with the third model now to be considered.

(c) The presence of interstitial hydride ion lines

In the alkali halides, the interstitial hydride ions have their vibrational frequencies at about twice that of the substitutional ions (Fritz (1962)) and this can be qualitatively understood by the smaller dimensioned cell available to an interstitial ion in this lattice. In the fluorite lattice, there are vacant interstitial sites in every unit cell comparable in size to the fluorine site cell and a large frequency shift of the interstitial hydride ion vibrations from those of the substitutional ions would not be expected to occur. The actual resultant frequency for these interstitial ion vibrations is difficult to estimate with any degree of certainty, but is most likely to be 10-20% higher than that of the substitutional ion vibrations.

The alkali halides also differ in that interstitial hydrogen atoms are only stable to 108°K (Delbecq, Smaller and Yuster (1956)) in this lattice, while they are readily observable at room temperature in the alkaline earth fluorides and only anneal rapidly at temperatures above 350°K. The hydrogen atoms must therefore be much less mobile in the fluorite lattice and be unable to diffuse to form molecules or recombine with vacancies without a high activation energy being supplied.

Because of this, the existence of interstitial hydride ions stable at room temperature should be possible in the fluorite lattice even

though these centres have completely annealed by room temperature in the alkali halides. It can therefore be postulated that some of the observed satellite lines arise from the presence of such interstial ions possibly modified by the occurrence of nearby vacancies.

Discussion of the last two models

The method of preparation is a simultaneous colouration of the pure alkaline earth fluorides with aluminium metal and decolourisation by hydrogen or deuterium gas. It depends on the relative efficiencies of these two reactions whether there are vacancies present in the final crystal. The incompletely decolourised crystals certainly possess negative ion vacancies associated with electrons (F centres) and it would thus seem possible for the colourless crystals to have negative ion vacancies alone despite the charge compensation requirements of the colouring reaction.

The lines around the fundamental can only be explained by the presence of nearby lattice defects such as vacancies, since the alternative model of adjacent impurity ions has already proved unable to account for more than two of the lines. The large number of satellite lines observed necessitates the hypothesis that different lines come from variations in the separation between the impurity ion and the lattice defects.

The interstitial hydride ion model would yield vibrational lines centred about another frequency. A vacancy may also be present as the interstitial ion may have initially migrated from a substitutional site leaving a vacancy behind. At room temperature, only the

interstitial ions fairly remote from the vacancy are expected to be stable and these would give a close group of lines clustered around the unperturbed interstitial impurity frequency.

(d) The presence of impurities

One other possibility to be considered is the presence of impurities, such as oxygen, either present originally in the pure alkaline earth fluoride crystals or introduced during the preparation of the doped crystals. The original alkaline earth fluoride crystals had been scavenged of oxygen during their growth by the addition of lead fluoride to the melt. The aluminium was in the form of powder and turnings supplied by B.D.H. Ltd., Both the calcium fluoride and aluminium were well outgassed in a vacuum system to less than 10^{-3}mm pressure before heating was commenced. The hydrogen gas used was of commercial quality. During the entire heating of the crystal, a liquid nitrogen trap was connected to the system so impurities such as water vapour and carbon dioxide were condensed out. The possibility of impurities such as oxygen being present is, therefore, not very great but it cannot be discounted because only a very small amount of impurity could easily give rise to absorption lines of the magnitude observed for the satellite lines.

It is not possible to carry out more than a very tentative application of the first three models to the observed satellite spectra Several experiments that could help resolve some of the obvious questions about these models are being carried out by H. Macdonald of this

laboratory. A description of these is in Appendix 1.

The most promising experimental technique for determining which satellite lines arise from impurity ions in substitutional fluorine sites is the Stark splitting experiment described in Section 4.6. A first order splitting or shift can only occur for ions in the substitutional fluorine sites as these are the only ones not possessing inversion symmetry. Unfortunately, present equipment limitations coupled with the smallness of the effect have prevented its observation in even the main substitutional hydride line.

Discussion of the various satellite line spectra

(a) For the satellite structure around the fundamental of hydrogen in calcium fluoride, the spectrum given in Figure 18 is obtained repeatedly for several samples of heavily doped crystals. In a lighter doped crystal two of the more distant satellite lines only are present and at greatly enhanced intensity relative to the main vibrational line. (Figure 19). These particular satellite lines have, therefore, a different origin to the others and in view of their large relative intensity are probably due to interstitial hydride ions. They bear a very different intensity ratio to each other in the heavily doped crystals so are not directly related.

The whole group of lines in the 1050 cm^{-1} region shown in Figure 18 is tentatively assigned to interstitial hydride ions. Each line is unrelated in intensity to the others so corresponds to a difference in the site from the others. The group is some 100 cm^{-1} higher in frequency than the main substitutional line and so is at about the

expected frequency for an interstitial hydride ion vibration.

The remaining lines in Figure 18 are clustered about the fundamental and so appear to be due to hydride ions in substitutional sites, slightly perturbed (up to 15 cm^{-1} shift in 960 cm^{-1}) by lattice defects such as vacancies. The 943.5 cm^{-1} and 947 cm^{-1} doublet has already been tentatively ascribed to the effect of a neighbouring hydride ion.

The origin of the 848 cm^{-1} line is obscure. It, however, is related to the hydrogen impurity in some way and is not due to, for example, surface contamination because it displays the strong temperature dependence of width characteristic of the main vibrational line.

(b) The satellite structure around the fundamental of hydrogen in strontium fluoride is given in Figure 20 for a heavily doped crystal and in Figure 21 for a lightly doped one. The corresponding spectra for barium fluoride are in Figure 22. The satellite structure about the second harmonic of hydrogen in barium fluoride is given in Figure 23.

The satellite structure shown by the weakly doped crystals is relatively simple (Figures 21 and 23) but no quantitative explanation can be offered for it in either case.

For the heavily doped crystals there is structure around the main vibrational line and this, as in the case of calcium fluoride, above, is ascribed to substitutional hydride ions perturbed slightly by lattice defects. There are also strong lines at 846 cm^{-1} in strontium fluoride (Figure 20) and 730 cm^{-1} in barium fluoride (H.Macdonald, Private communication). These are very tentatively assigned to interstitial

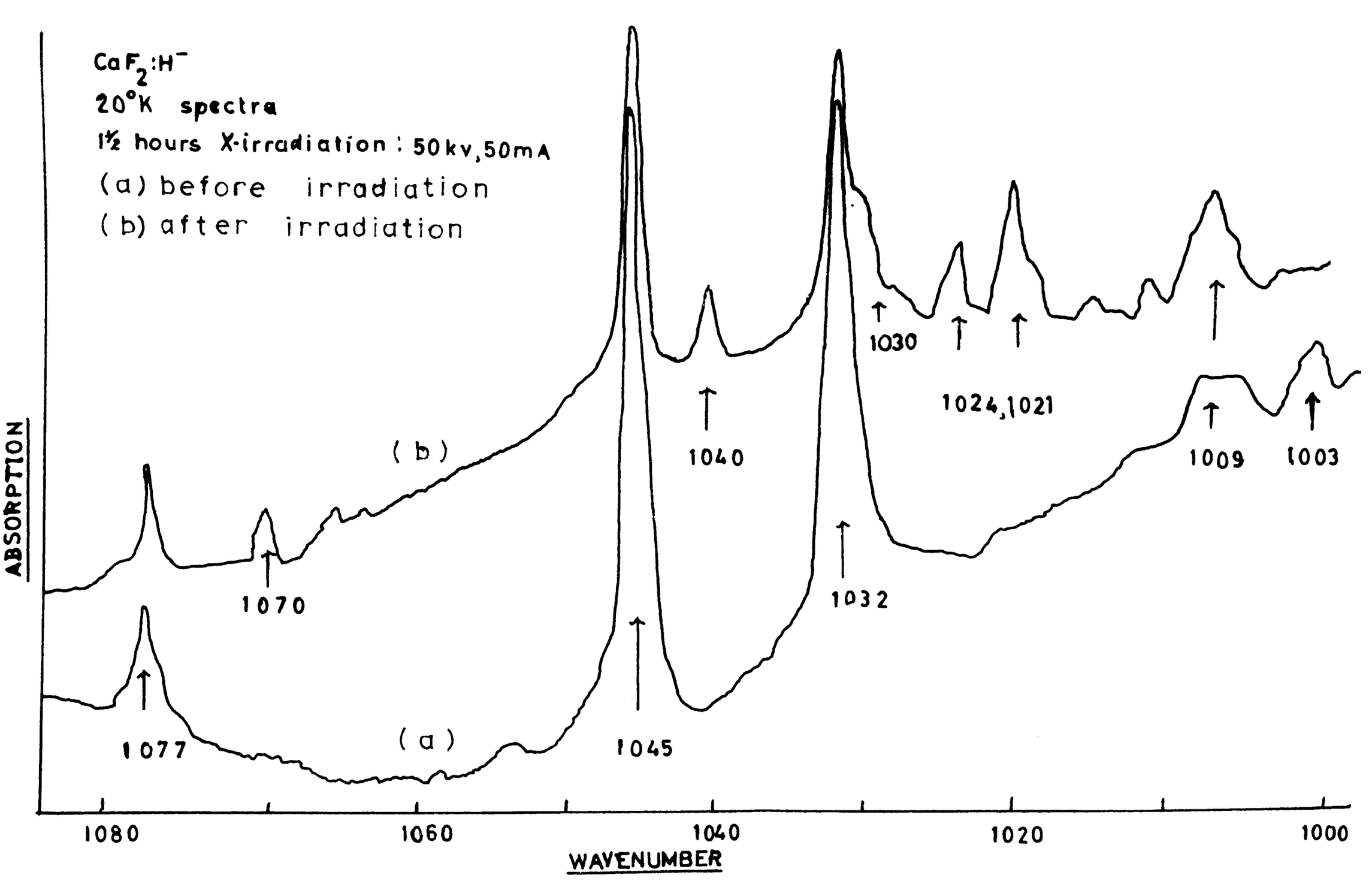

FIGURE 26 Effect of room temperature X irradiation on the $CaF_2:H^-$ satellite lines.

hydride ions. They bear the same ratio to the 1040 cm^{-1} group in calcium fluoride as the respective lattice reststrahlen absorption frequencies bear to the restrahlen frequency for calcium fluoride.(i.e., (The three frequencies have a Mollwo exponent of 2.7 relating them). This is consistent with the interstitial hydride ion model as this has only fluorine ion nearest neighbours about the hydride ion and so the vibrational frequencies would follow the respective lattice frequencies (Section 5.1)

The Effects of X Irradiation of the Satellite Structure

Figure 26 shows the effect of room temperature X irradiation on the satellite structure of hydrogen in calcium fluoride.

These additional lines were approximately correlated with the presence of interstitial hydrogen atoms in these crystals (section 4.3) but their intensity is quite large for the absorption of neutral atoms. The results of an accurate correlated infrared absorption and electron spin resonance thermal annealing experiment (section 4.3) are required before anything definite can be said about this model for the origin of the lines.

The lines themselves bear a simple relation to the prominent lines present before irradiation in the 1050 cm^{-1} region. They are some 8cm^{-1} lower in frequency and, in addition, there is a line at 1020 cm^{-1}. It would seem that they are closely related to the prominent lines and differ only slightly in origin from these. The difference could be due to the formation of an adjacent colour centre (e.g. F centre), which perturbs the original lines slightly. This model is supported by the

decrease in intensity of the prominent lines on irradiation and their restoration to original intensity by thermal annealing of the irradiation lines (by heating of the crystal to 220°C for 10 minutes)

Further speculation as to the origin of the observed satellite lines is obviously unprofitable at this stage of the research.

8.2 The broad bands of largely temperature independent width

8.2.1 Frequencies of the Satellite Bands and their assignment

These broad satellite bands which do not sharpen more than slightly on cooling are assigned as combination bands whose frequencies are the sum and difference of those of the localised mode and the various lattice mades. These bands thus reflect the variation of the density of states of the local ± lattice spectra. Table 9 enumerates the frequencies of the various bands observed, their frequency separation from the local mode frequenoy and their assignment as a combination of the local mode frequency and a particular lattice mode frequency.

In regard to this assignment it should be pointed out that Lax and Burstein (1954) in their analysis of the absorption of homopolar lattices of atoms with inversion symmetry at each site showed that, although there is no one phonon absorption, two phonons can simultaneously interact with the light and produce absorption. These two phonons must have equal and opposite wavevector and also must come from distinct branches of the vibration spectrum. Later Kleinman and Spitzer (1960) stated that the latter restriction does not apply in ionic crystals.

Birman (1963) has derived selection rules for these multiphonon combination bands, but his analysis does not directly cover the fluorite lattice case. In the assignment of the observed bands to be made here, any combination of local and lattice phonons has been considered possible, and the absence of any band corresponding to a particular combination ascribed either to a low peak density of states of the corresponding phonon spectrum or to infrared inactivity of this phonon combination. The latter hypothesis is open to verification by a study of the selection rules appropriate for the fluorite lattice.

The broad bands are of the continuous type, but singularities in the phonon frequency distribution give rise to absorption peaks. These singularities occur at critical points in the Brillouin zone where the frequency as a function of wavevector is flat. Such points tend to occur at the origin or near the edge of the zone.

The observed absorption peaks of the bands are thus associated with phonons near the origin or the edge of the Brillouin zone. For this reason, the lattice phonon energy data of Fray, Johnson and Quarrington (1963) for calcium fluoride is used as it is evaluated from the frequencies of observed two phonon summation bands and so is appropriate for the same critical regions near the zone origin and boundary.

Exact agreement is not achieved and is not expected as the local mode frequency itself is evaluated for $\underline{k} = 0$ only and may differ in other parts of the zone. However, any variation of the local mode frequency across the Brillouin zone will be small because, in the

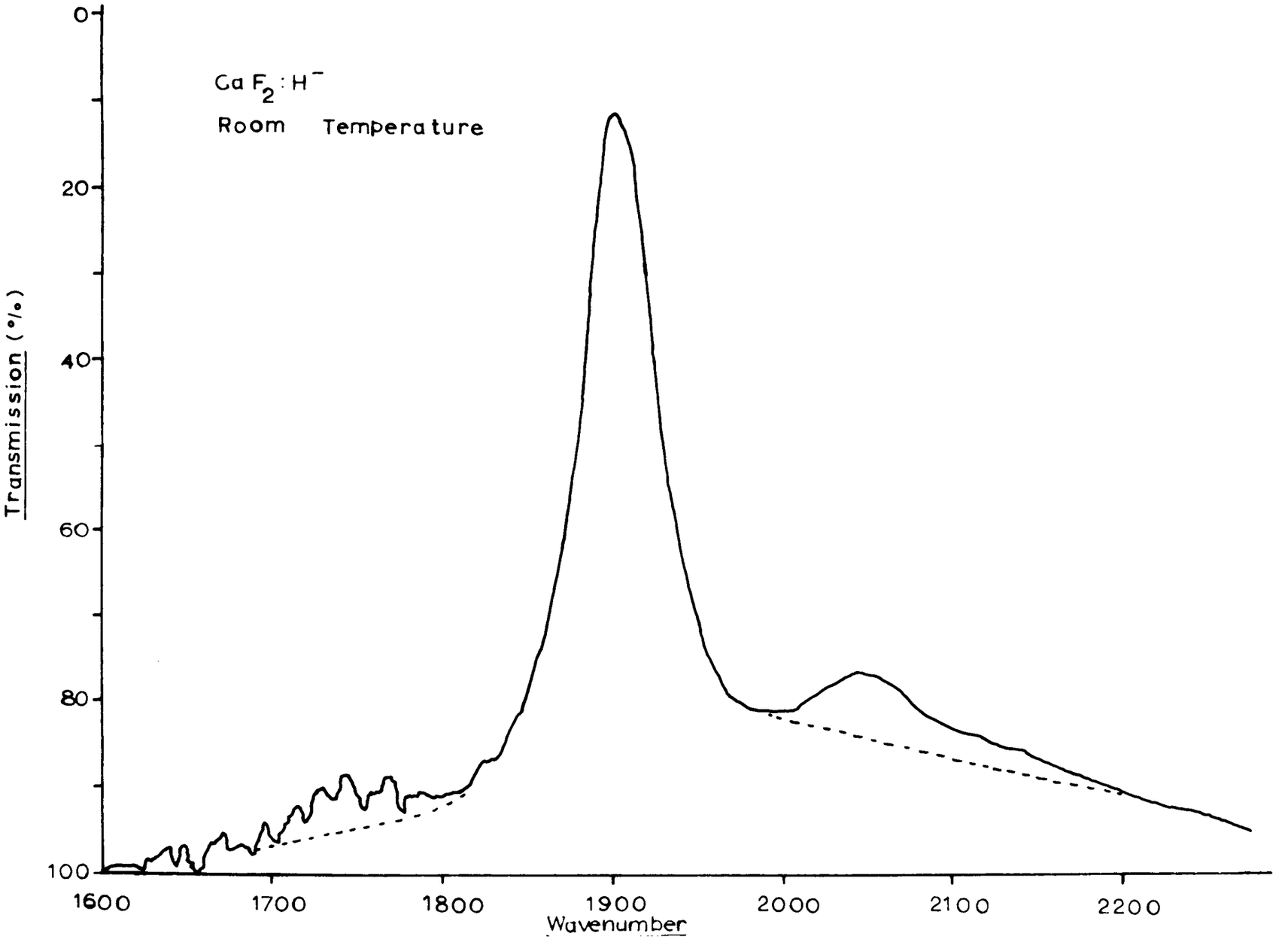

FIGURE 25 Satellite bands around the second harmonic line of the localised vibration of hydrogen in calcium fluoride as recorded on a Perkin-Elmer model 21 spectrometer.

approximation of a static lattice about the impurity ion, the latter is virtually "free" and may be likened to an Einstein oscillator, which is characterised by constant w with varying $\underline{k}$.

For strontium fluoride and barium fluorides no data is available on the lattice mode frequencies away from $\underline{k} = 0$. The optical mode frequencies will be smaller at the zone boundary critical points and a crude estimate of their value can be made by comparison with the variation of the calcium fluoride lattice frequencies across the zone. The acoustic mode frequencies are evaluated from the elementary formula for these waves given for the model of a one dimensional diatomic chain by Mitra (1963). Their values agree well with the values obtained from the observed satellite band frequencies. The various results are in Tables 9 and 11.

In calcium fluoride, the low frequency sideband of the hydrogen fundamental line has not been observed due to the rapid onset of lattice reststrahlen absorption. It has only been observed at room temperature on the low frequency side of the second harmonic and is shown in Figure 25. Its intensity relative to the main second harmonic line is $\frac{1}{22}$, and relative to the corresponding high frequency satellite band $\frac{1}{1.8}$. The latter value is in good agreement with the ratio of $\frac{1}{2.16}$ given by the temperature dependence formulae of Section 8.2.2. It was unfortunately not possible to record the low temperature behaviour of this sideband. The high frequency sidebands can be observed about both the fundamental and the second harmonic lines. The agreement between the two sets of frequencies obtained confirms the assignment of the

Table 9. The Broad Satellite Bands

(a) Bands around the fundamental of hydrogen in calcium fluoride

Observed Frequency ($\pm$ 5cm^{-1})	Separation from Main Line	Assignment	Lattice mode frequencies. (Fray et.al.(1963))
(1) Room Temperature			
1115	155	Local + TA	149
1195	235	Local + TO_1	262
1325	365	Local + LO_1	368
(2) Liquid Nitrogen Temperature			
1122	147	Local + TA	149

(b) Bands around the second harmonic of hydrogen in Calcium Fluoride

Observed Frequency ($\pm$ 5cm^{-1})	Separation from Main Line	Assignment	Lattice mode frequencies (Fray et.al. (1963))
(1) Room Temperature			
1745	-155	Local - TA	149
2050	150	Local + TA	149
2150	250	Local + TO_1	262
(2) Liquid Nitrogen Temperature			
2070	150	Local + TA	149

broad bands to combination bands of the localised mode with lattice modes. The alternative model, which was used to interpret the satellite lines (section 8.1), that the bands are due to lattice anomalies cannot be valid as the two sets of bands would have to bear a harmonic ratio to each other as well as possess the strong temperature dependence width characteristic of the main vibrational lines.

The non-observation of more than one low frequency satellite band is explained by the temperature dependent effects (discussed in detail in the next section). The more distant bands have very small intensity on the low frequency side because there are only very few lattice phonons of the required energy available to give rise to this absorption even at room temperature.

Strontium fluoride and barium fluoride are characterised by both smaller acoustic and optical branch frequencies and by reduced reststrahlen absorption. The former is due to the higher masses of the metal ion and the latter is due to a greater ratio of the local mode frequency to the peak reststrahlen absorption frequency (Section 7.3). These two factors enable the low frequency satellite bands to be observed around the fundamental in these lattices and these are listed in Table 9. For the more distant high frequency bands a knowledge of the optical frequencies of the pure lattices at the critical points of the dispersion curve is required for a definite assignment of the bands observed to be made. As this data is not known for either strontium or barium fluoride, the problem has been inverted, and the observed band frequencies have been used to estimate the frequencies

Table 9. The Broad Satellite Bands

(c) Bands around the fundamental of hydrogen in strontium fluoride

Observed Frequency (± 5 cm^{-1})	Separation from Main Line	Assignment	Estimated Lattice Mode Frequency
(1) Room Temperature			
785	-100	Local - TA	100
985	100	Local + TA	100
1065	180	Local + LA	180$_t$
1110	225	Local + TO_1	225^t
1210	325	Local + LO_1	325
(2) Liquid Hydrogen Temperature *			
995	105	Local + TA	100
1065	175	Local + LA	180

t - Infrared active TO_1 mode at k=0 is 217 cm^{-1} (Table 3)
* - Additional more distant lines have been subsequently observed by H. Macdonald.

(d) Bands around the fundamental of hydrogen in barium fluoride

Observed frequency ($\pm$ cm^{-1})	Separation from Main Line	Assignment	Estimated Lattice Mode Frequency
(1) Room Temperature			
715	-85	Local - TA	80
875	75	Local + TA	80
930 (weak)	130	Local + LA	135$_t$
985	185	Local + TO_1	185^t
1075	275	Local + LO_1	275
(2) Liquid Hydrogen Temperature*			
880	80	Local + TA	80
935	135	Local + LA	135

t - Infrared active TO_1 mode at k=0 is 184 cm^{-1} (Table 3)
* - Additional more distant lines have been subsequently observed by H. Macdonald.

of the pure lattices at the critical points. This data has already been used earlier (Section 7.3). The correctness of the assignment is open to verification by data for the pure lattice when this becomes available. Table 11 shows the estimated values for the frequencies of the various branches at the critical points of the dispersion curves of these two fluorides. The calcium fluoride data of Fray, Johnson and Quarrington (1963) is shown for comparison and the values for strontium and barium fluoride listed are consistent with it.

The width and intensity of the observed combination bands is an approximate indication of the sharpness of the peaks in the density of states. The structure of the bands also gives some information about the critical points of the dispersion curve. Subsidiary peaks occur in the contour of the several of the observed bands and these are shown, for the particular case of the high frequency "transverse acoustic" satellite band of the fundamental of hydrogen in calcium fluoride, in Figure 27. They probably arise from lattice phonons of energies corresponding to critical points in particular symmetry directions of the crystal.

8.2.2 Temperature Dependence of the Satellite Bands

The high frequency sidebands are local plus lattice phonon modes of vibration and are formed by a process in which the incident light creates both a local and a lattice phonon. The absorption of these bands would not be expected to show much variation with temperature as the lattice can always accept a phonon.

The low frequency sidebands are local minus lattice modes of

Table 11 Critical point lattice frequencies for the alkaline earth fluorides as determined from the frequencies of the hydrogen induced lattice band absorption

	CaF_2 (Fray et.al.(1963))	SrF_2	BaF_2
Transverse acoustic	149	100	80
Longitudinal acoustic	-	180	135
Transverse optical	262	225	185
Longitudinal optical	368	325	275

vibration and result from a process in which the incident light interacts with and destroys a lattice phonon present in the lattice to give a local mode phonon. The probability for this process is strongly dependent on the number of lattice phonons available and will vary as exp $(-\hbar w/kT)$, where $\hbar w$ is the lattice phonon energy.

Such temperature dependent intensity behaviour has been reported by Fritz (1963) for the two sidebands in the alkali halide U centre spectra (Section 1.4)

A general analysis of the temperature dependence of the intensity of combination bands has been given by Johnson (1959) and is as follows:

(1) For the summation band, two phonons are created. If v_1 and v_2 are their "wavenumbers" their number, n_1, n_2 is given by the expression:

$$n = \left[\exp\left(\frac{hcv}{kT}\right) - 1\right]^{-1}$$

evaluated for v_1 and v_2 respectively. This term is responsible for the temperature dependence of the absorption .

The net absorption of the summation band is the difference between the probability of phonon absorption less the probability of induced emission and so equals:

$$(1 + n_1)(1 + n_2) - n_1 n_2$$

(2) For the difference band one phonon is created (v_2) and one destroyed (v_2) and the net absorption is now:

$$n_1(1 + n_2) - n_2(1 + n_1)$$

The value of n is approximately unity when $\frac{hcv}{kT} \simeq 0.6$ and decreases exponentially with decreasing temperature. Hence only the

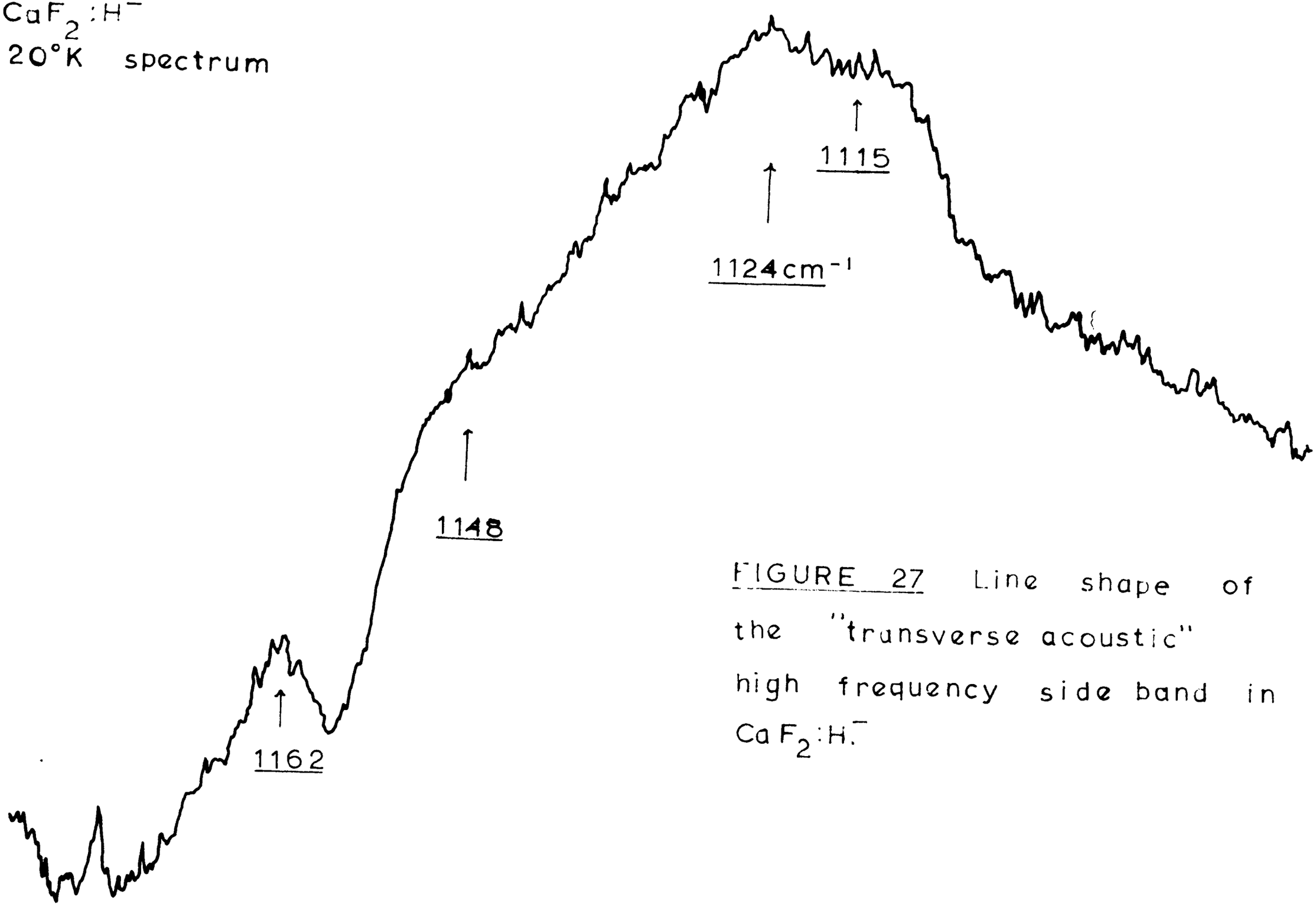

FIGURE 27 Line shape of the "transverse acoustic" high frequency side band in $CaF_2:H^-$

summation band will be observable at low temperature. It has an absorption largely independent of temperature until the thermal energy (kT) becomes comparable with the energy of one of the created phonons and will increase at higher temperature.

For the combination bands observed, the local mode has a higher frequency than any of the lattice modes and so the latter dominate the low temperature behaviour. The previously described low temperature dependence is thus valid.

A detailed study of the temperature dependence of the various combination bands observed is being carried out by H. Macdonald. His results for the temperature dependence of the "transverse acoustic" satellite bands of hydrogenated barium fluoride show good agreement with the formulae given above.

9. SUMMARY

A description has been given of an investigation of the localised vibrations of hydrogen and deuterium present as substitutional impurities in crystals of the alkaline earth fluorides. These vibrations were detected as lines in the infrared absorption spectrum of the doped fluorides. From the occurrence of harmonic lines, the light impurity ions were shown to be on fluorine sites.

The deviation of the frequencies of the lines off exact harmonicity, the shift of the peak position of the lines with temperature and the strong temperature dependence of the linewidths were all ascribed to anharmonic effects. The experimental data is sufficient to determine the constants of the potential well, in which the impurity ions vibrate,

to terms quartic in the displacement. Deuteration of the fluorides enabled the mass dependence of the anharmonic forces to be examined.

The satellite line structure around the main vibration lines reflects the actual site symmetry around the light ion impurity. The latter could, therefore, be used as a probe for investigating the nature of the various other defects present in the lattice.

The satellite broad bands arise from the interaction of the lattice modes with the impurity vibration modes. These impurity induced lattice bands occur in a frequency region well above that of strong lattice reststrahlen absorption and so are much more readily accessible than the pure lattice combination bands to experimental study. From the positions of these impurity induced bands the frequencies of various lattice modes were determined.

APPENDIX 1

Several experimental lines of investigation that could help resolve some of the uncertainties about the assignment of the satellite line structure to the models described in section 8.1 are described here. They include:

(a) a study of the method of sample preparation

An alternative method of preparation that may yield useful results is the colouration of the calcium fluoride crystals with calcium metal alone followed by a heat treatment of the crystals in an atmosphere of hydrogen gas. This would check whether the satellite lines are unique to the method of preparation used up to now and so arise from the presence of vacancies due to the incomplete action of the hydrogen gas. This experiment would also show whether the preparation itself requires the simultaneous presence of both constituents and consequently depends on the formation of an intermediate metal hydride compound (e.g. aluminium hydride) which decomposes at high temperatures, yielding atomic hydrogen which diffuses into the crystal. Heating of the pure crystals in hydrogen gas alone had no effect on the crystals.

The suggested experiment was tried with aluminium metal and was inconclusive due to the complete clouding of the fluoride crystals in the colouring stage.

(b) A study of the thermal annealing properties of the various lines

Any lines due to interstitial ions would be expected to anneal at lower temperatures than those due to substitutional lines. The exact temperature at which either centre anneals will also depend on its

separation from a vacancy. A high temperature annealing experiment would thus serve to distinguish between lines of different activation energies due to these differences

(c) A study of the effects of ultraviolet irradiation on the lines

It has already been suggested that interstitial hydride lines could be present in the room temperature spectra and these lines would arise from interstitial hydride ions fairly remote from a vacancy.

Analogous to the alkali halide case, a low temperature ultraviolet irradiation into the electronic absorption band of the substitutional ions should cause the formation of interstitial hydride ions at all distances from their associated vacancies. Interstitial hydrogen atoms would also be produced, but the absorption due to these would be relatively weak. Interstitial hydride ions close to the vacancy would give lines of large spacing and these would anneal by room temperature. In general, an annealing behaviour similar to that reported by Fritz (1962) for the alkali halides is expected.

The main experimental problem is in the attaining of the preferential bleaching of the substitutional ion centres. Their electronic absorption band is not yet accurately known, but appears to peak in the vacuum ultraviolet. One would need to use a lamp with high output in this region together with a suitable filter or, alternatively, an arc lamp having a strong emission line of the required wavelength. It will be important to avoid irradiation into any interstitial hydride ion band as this would promote the back reaction.

Preliminary X irradiation experiments of a similar type have been

tried and the results were discussed in Section 8.1.

(d). A study of the effect of oxygen impurity

As pointed out in Section 8.1 some of the satellite lines could be due to the presence of oxygen or similar impurity. An experiment to check this hypothesis would be a study of the absorption spectrum of a hydrogenated crystal before and after heating treatment in an oxygen atmosphere. Lines due to adjacent oxygen defects should be greatly enhanced. As the introduction of oxygen into the fluorite lattice will probably create additional lattice defects and, with high concentration of oxygen, precipitated particles of calcium oxide, the interpretation of the results will not be straightforward. It may be necessary to resort to isotropic substitution of O^{16} by O^{18} to definitely correlate any altered satellite lines to the presence of adjacent oxygen impurity. The effect of such substitution would be small and difficult to detect.

REFERENCES.

Birman, J.L., 1963, Phys. Rev., 131, 1489.

Bjork, R.L., 1957, Phys. Rev., 105, 456.

Bontinck, W., 1958, Physica, 24, 650.

Born, M., and Huang, K., 1954, (Dynamical Theory of Crystal Lattices) (Oxford; University Press).

Brügel, W., 1962, (An Introduction to Infrared Spectroscopy (London;Methuen).

Casselman, T.N., and Markham, J.J., 1963, J. Phys. Chem. Solids, 24, 669.

Cochran, W., 1963, Rep. Prog. Phys. 26, 1.

Crandall, R. S., 1963, J. Chem. Phys., 38, 1036.

Cribier, D., 1953, Acta Cryst., 6, 293.

Cribier, D., 1958, Rev. Mod. Phys., 30, 228.

Cribier, D., Farnoux, B., and Jacrot, B., 1963, (Proc. Symposium on Inelastic Scattering of Neutrons in Solids and Liquids, Vienna)(Vienna; International Atomic Energy Agency).

Dawber, P.G., 1962. Thesis, Oxford.

Dawber, P.G., and Elliott R.J., 1963a, Proc.Roy.Soc., A 273, 222.

Dawber, P,G, and Elliott, R.J., 1963b, Proc. Phys. Soc., 81, 453.

Delbecq, C.J., Smaller, B., and Yuster, P.H., 1956, Phys. Rev., 104, 599.

Delbecq, C.J. and Yuster, P.H., 1956, Phys. Rev., 104, 605.

Fray, S.J. Johnson, F.A., and Quarrington, J.E., 1963, Proc. Int. Conf. on Lattice Dynamics, Copenhagen.

Freytag, E., 1960, Optics and Spectroscopy of all Wavelengths Meeting, Jena.

Fritz, B., 1962, J. Phys. Chem. Solids, 23, 275.

Fritz B., 1963, Proc. Int. Conference on Lattice Dynamics, Copenhagen.

Ganesan, S., and Srinivasan, R., 1962a, Canad. J. Phys., 40, 74.

Ganesan, S., and Srinivasan, R., 1962b, Canad. J. Phys., 40, 91.

Görlich, P., Karras, H., and Lehmann, R., 1961, Physica Status Solidi, L, 390.

Görlich, P., Karras, H., Lehmann, R., and Meisel, E., 1963, Physica status solidi, 3, k220.

Hall, J.L., and Schumacher, R.T., 1962, Phys.Rev., 127, 1892.

Hanamura, E., and Innui, T., 1963, J. Phys.Soc.Japan,18, 690.

International Union of Pure and Applied Chemistry, 1961 (tables of Wavenumbers for the Calibration of Infrared Spectrometers) (London Butterworths).

Johnson, F.A., 1959, Proc. Phys. Soc., 72, 265.

Kaiser, W., Spitzer, W.G., Kaiser, R.H., and Howarth, L.E., 1962, Phys. Rev., 127, 150.

Kittel, C., 1953, Introduction to Solid State Physics, (New York; Wiley)

Kleinman, D.A., and Spitzer, W.G., 1960, Phys. Rev. 118, 110.

Klemens, P.G., 1961, Phys. Rev., 122, 443.

Krishan, R.S., and Narayanan, P.S., 1963, Ind. J. Pure Applied Physics,1,196.

Krumhansl, J.A., 1962, J. Appl. Phys., 33, 307.

Lax, M., and Burstein, E., 1955, Phys. Rev. 97, 39.

Landolt-Börnstein, 1923, Physikalisch-Chemische Tabellen (Berlin: Julius Sphinger).

Maradudin, A.A., Mazur, P.,Montroll, E.W., and Weiss, G.H.,1958, Rev.Mod. Physics, 30, 175.

Maradudin, A.A., Montroll, E.W., and Weiss, G.H., 1963. Theory of Lattice Dynamics in the Harmonic Approximation (New York: Academic Press).

Mazur, P., Montroll, E.W., and Potts, R.B., 1956, J.Wash. Acad.Sci.,46, 2.

Mitra, S.S., 1962, Solid State Physics, Vol.13 (New York: Academic Press).

Mitsuishi, A., Yamada, Y., and Yoshinaga, H., 1962, J.Opt.Soc.Am., 52, 14.

Mitsuishi, A., and Yoshinaga, H., 1963, J. Phys. Soc. Japan, 18, 321.

Mitsuishi, A., and Yoshinaga, H., Prog. Theor. Phys., Suppl. 23, 243.

Montroll, E.W., 1954, Proc. Berk. Symp.Math.Statistics and Prob. 3, 209.

Montroll, E.W., and Potts, R.B., 1955, Phys.Rev.,100, 525.

Morton, G.A., Schultz, M.L., and Harty, W.E., 1959, R.C.A. Review, 20, 599.

Mott, N.F., and Gurney, R.W., 1950, Electronic Processes in Ionic Crystals (Oxford: Clarendon).

Press, D.C., 1950, Proc.Ind.Acad.Sci., A31, 56.

Price, W.C., Smart, C., and Wilkinson, G.R., 1963 (The Vibrational Spectra of H^- and D^- in alkali Halides (U Centres)), to be published.

Raman C.V., 1947, Proc.Ind.Acad.Sci.,A26, 339.

Raman C.V., 1960, Proc. Ind.Acad.Sci., A56, 291.

Rassetti, F., 1931, Nature, 127, 627.

Lord Rayleigh, 1877, Theory of Sound (New York: Dover reprint, 1945).

Roberts, V., 1953, The Leiss Double Monochromator, T.R.E.Memorandum No.708.

Roverts, V., 1954, J.Sci.Instrum.,31, 251.

Roberts, V., 1955, J.Sci.Instrum.,32, 294.

Roberts, V., 1959, J. Sci. Instrum., 36, 99.

Rollin, B.V., and Russell, J.P., 1963, Proc.Phys.Soc.,81, 578.

Rosenstock, H.B., 1955, J. Chem. Phys., 23, 2415.

Rosenstock, H.B., 1957, J. Chem. Phys., 27, 1194.

Rosenstock, H.B., and Klick, C.C., 1960, Phys.Rev.,119,1198.

Schäfer, G., 1960, J.Phys. Chem. Solids, 12, 233.

Seitz, F., 1953, Rev. Mod. Phys., 26, 7.

Shimanouchi, T., Tsuboi, M., and Miyazawa, T., 1961, J.Chem.Phys., 35, 1597.

Sierro, J., 1962, Resonance Paramagnetique Electronique de Gd^{3+} dans CaF_2, SrF_2 et BaF_2 (Genève: private print).

Smakula, A., 1962, Optica, Acta, 9, 205.

Takeno, S., Kashiwamura, S., and Teramoto, E., 1963, Proc.Theor.Phys. Suppl. 23, 124.

Valentiner, S., and Wallott, J., 1915., Ann Physik (LPZ), 46, 837.

Viswanathan, K. S., 1963, Canad. J. Physics, 41, 423.

Wickersheim, K.A., and Hanking, B.M., 1959, Physica, 25, 569.

CHAPTER TWO

OPTICAL ABSORPTION OF NICKEL AND COBALT IN LITHIUM FLUORIDE

1. Introduction

In this chapter a description is given of an experimental study of:

(a) the optical absorption of lithium fluoride crystals containing nickel and cobalt;

(b) the effect of these impurities on the formation of intrinsic lattice defects in lithium fluoride;

(c) the X-irradiation properties of sodium fluoride and a comparison of the effect of impurities on the formation of intrinsic lattice defects in this substance with that of lithium fluoride.

2. Experimental Techniques

A Unicam SP700 automatic recording spectrophotometer was used to record the optical absorption of the crystals over the range 4000 cm^{-1} to 50,000 cm^{-1}. The spectra were measured at room, liquid nitrogen, liquid hydrogen and liquid helium temperature and for the low temperature measurements a dewar similar to the designs of Duerig and Mador (1952) and Geiger (1955) was employed. Cooling of the crystal is through thermal contact between the crystal and a copper block, the latter being in contact with the liquid refrigerant. Good contact was achieved by clamping the crystal to the block with an additional copper plate and

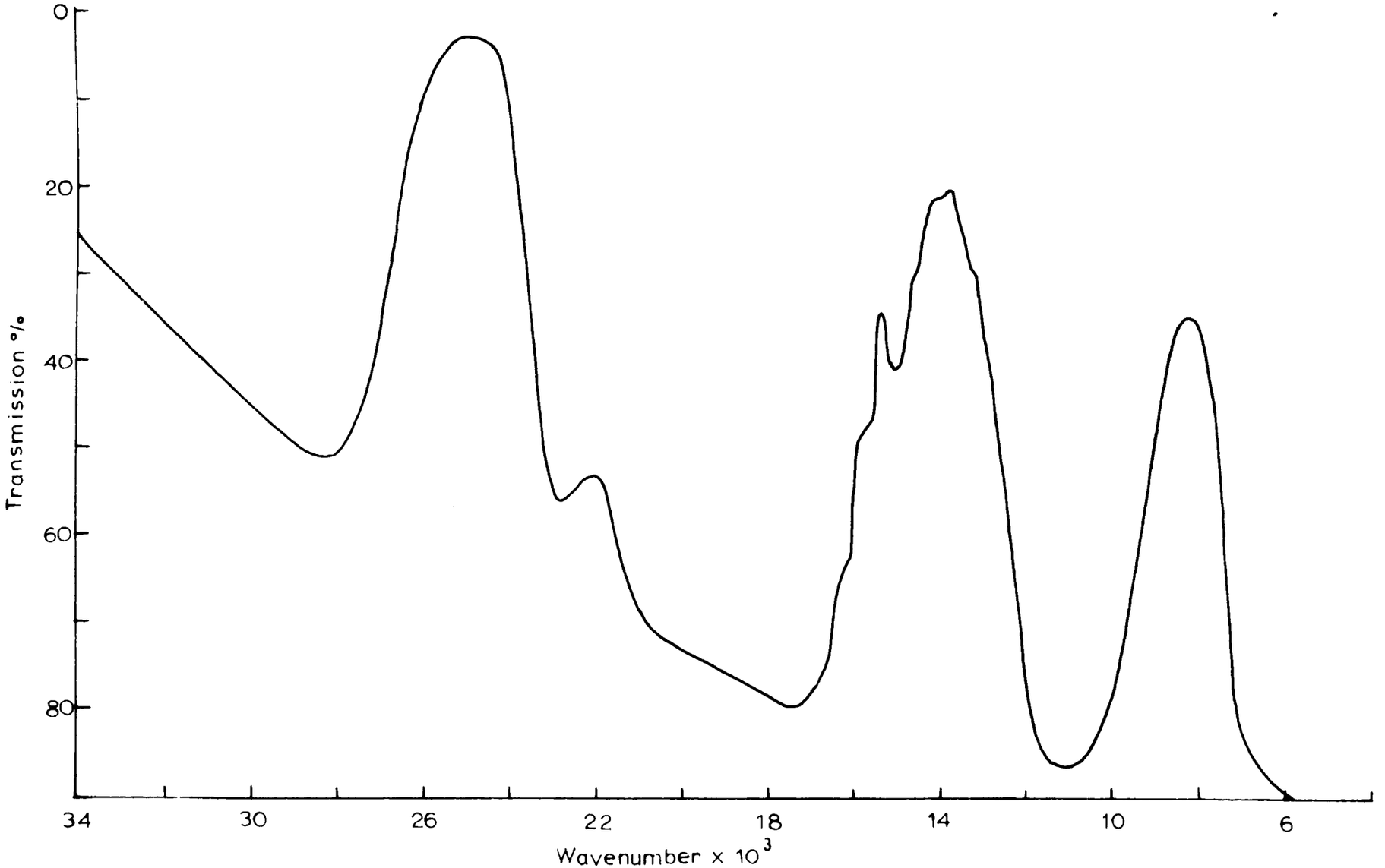

FIGURE A1 Optical absorption at liquid nitrogen temperature of a crystal of lithium fluoride containing 0·7% molar concentration of nickel
Crystal thickness : 5·7mm.

by lightly smearing the edges of the crystal with silicone grease. The crystal temperature was monitored with a gold + 2.11% cobalt alloy verus copper thermocouple and was within 10°K of the temperature of the refrigerant.

The dewar was fitted with four windows, two of quartz and two of thin aluminium foil. The former were used in the optical absorption measurements while the latter were used for low temperature X-irradiation of the crystals. The different windows could be brought into use during an experiment by rotating the tail of the dewar through 90°.

In the study of the thermal bleaching properties of various low temperature irradiation induced bands, a slow warmup of the crystal from low temperature was required and the thermal inertia of the copper block and crystal holder part of the dewar was raised substantially by partially filling the dewar with lead shot. A heater, wound around the copper block, enabled the rate of temperature rise to be adjusted as desired.

The crystal samples used in this work were grown by Dr. R. W. H. Stevenson, of Aberdeen University, using the Stockbarger (1949) technique. Impurities were incorporated in the growing stage. For the optical measurements small pieces of crystal were cleaved to shape and polished on paper laps using successive grades (45, 8, 3 and ¼ micron) of "Hyprez" diamond compound. The final crystal sizes averaged 10 x 6 x 1mm.

TABLE A1. Ni^{2+} band positions in LiF

Transition	Calculated band positions cm^{-1}	Observed band positions at liquid nitrogen temperature cm^{-1}
$3\Gamma_5(^3F) - 3\Gamma_3(^3F)$	8019	8200
$- 3\Gamma_4(^3F)$	8106	
$- 3\Gamma_5(^3F)$	8370	
$- 3\Gamma_2(^3F)$	8482	
$- 3\Gamma_1(^3F)$	13150	13300
$- 3\Gamma_4(^3F)$	13490	13680
$- 3\Gamma_3(^3F)$	13778	14050
$- 3\Gamma_5(^3F)$	14057	14480
$- 3\Gamma_3(^1D)$	15097	15300 15710 16310
$- 1\Gamma_5(^1D)$	22332	21900
$- 1\Gamma_1(^1G)$	23736	
$- 3\Gamma_3(^3P)$	24761	24900
$- 3\Gamma_5(^3P)$	24939	
$- 3\Gamma_4(^3P)$	25082	
$- 3\Gamma_1(^3P)$	25241	
$- 1\Gamma_4(^1G)$	27274	-
$- 1\Gamma_3(^1G)$	33268	-
$- 1\Gamma_5(^1G)$	33706	-
$- 1\Gamma_1(^1S)$	59724	-

3. Experimental Observations

(a) Optical measurements on pure and doped lithium fluoride crystals.

Pure lithium fluoride exhibits no absorption in the frequency range studied (50,000 to 4,000 cm^{-1}), apart from a slight absorption rise (to 90% transmission at 50,000 cm^{-1}) in the far ultraviolet.

The optical absorption of Ni^{2+} ions present in lithium fluoride at 0.2% molar concentration (measured by spectrochemical analysis) and 0.7% molar concentration was measured at room, liquid nitrogen and liquid hydrogen temperature. The observed spectrum at liquid nitrogen temperature is shown in Figure A.1. The frequencies of the bands and their level assignments are given in Table A.1.

The optical absorption of Co^{2+} ions present at 0.1% molar concentration in lithium fluoride was measured at the same three temperatures and the band frequencies with their level assignment are listed in Table A.2. The spectrum is characterised by two absorption bands of which the band at 19600 cm^{-1} has structure visible at room temperature, [redacted] but better resolved at low temperatures, while the infrared band at 8000 cm^{-1} shows no structure.

(b) Irradiation effects on the optical absorption of pure and doped lithium fluoride crystals.

(i) The pure crystals

Room temperature irradiation of pure lithium fluoride crystals causes the growth of several absorption bands of which the F band at

TABLE A2. Co^{2+} Band Positions in Lithium Fluoride.

Transition	Calculated band positions (cm^{-1})	Observed band positions at liquid hydrogen temperature (cm^{-1})
$^4T_1(^4F) \rightarrow {}^4T_2(^4F)$	7967	8000 ± 50
$^2E\ (^2G)$	8736	-
$^2T_1(^2G)$	16007	-
$^2T_2(^2G)$	16414	-
$^4A_2(^4F)$	17067	16800±200
		18300±200
		19000±200
$^4T_1(^4F)$	19960	20000±200
$^2T_1(^2D,H)$	20655 (30% triplet character)	21200±100 21600±100
$^2A_1(^2G)$	22867	-

40,000 cm^{-1} and the M band at 22,400 cm^{-1} are the most well established. (Delbecq and Pringsheim (1953)). These absorption bands, together with additional bands produced at low temperature, have been the subject of much experimental work in recent years. A summary of the various bands observed and their assignment to colour centre models has recently been given by Kaufman and Clark (1963) and by Gorlich, Karras and Kotitz (1963).

The experimental investigations on irradiation effects carried out here were directed to the specific effects of transition metal ion impurities on the formation of the F and M bands. The experimental results obtained for the spectrum of lithium fluoride will, therefore, only be described in so far as necessary to interpret these effects.

Room temperature irradiation of pure lithium fluoride gives rise to the already mentioned F and M bands and an additional weaker band at 15700 cm^{-1} and the crystal has a greenish-yellow colour. Within one day the latter band disappears and the crystal becomes yellow. Little change is observed in either the F or M band in the same period.

Liquid nitrogen temperature irradiation of pure lithium fluoride gives a spectrum which does not show the M band and only possesses the F band and an additional band at 28700 cm^{-1}. This latter band imparts a yellow colour to the crystal. It anneals on warming the crystal above 140°K and has been shown by Delbecq, Hayes and Yuster to be due to the presence of a V centre of the F_2^- molecular ion type. This particular band is discussed in Chapter 3.

FIGURE A2.

Optical absorption at room temperature of (a) undoped LiF, (b) LiF:Ni^{2+} and (c) LiF:Co^{2+} after 8 minutes X-irradiation at room temperature. Crystal thicknesses: 0.4mm.

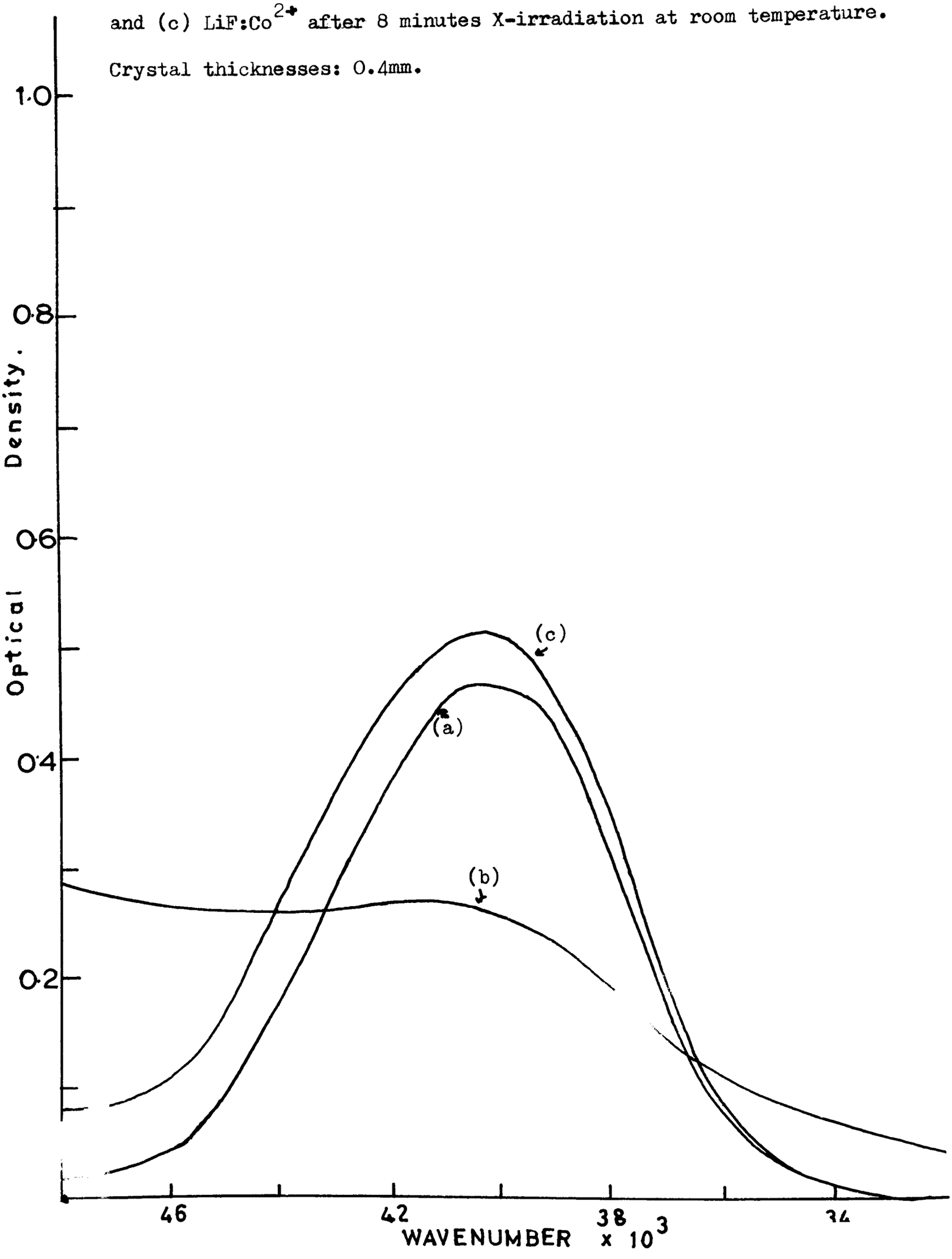

If the initial irradiation of lithium fluoride crystals at low temperature is sufficiently long (approximately 10 hours with 50kv, 50mA X rays), the crystals show, when warmed up to room temperature, a weak M band. The intensity of this band increases slowly (at room temperature) over a period of days, but does not come sufficiently intense to noticeable colour the crystal, and is still much weaker than the M band created in a similarly irradiated lithium fluoride crystal maintained at room temperature.

(ii) The nickel doped crystals

Examination of the room temperature X irradiation spectrum of nickel doped lithium crystals showed that nickel ions greatly suppress the formation of both F and M bands.

The F centre formation for small irradiation doses is shown in Figure A.2. It was not possible to investigate the effect of large irradiation doses because an intense background absorption is produced in the nickel doped crystals.

The room temperature M centre formation is shown in Figure A.3. and it can be seen that the nickel impurity has a pronounced effect on the intensity of this band. For low temperature irradiations, the M band is only formed weakly in pure lithium fluoride crystals that have been subsequently warmed to room temperature, but does not form in nickel doped crystals treated in a similar manner.

It is difficult to determine whether the 15,700 cm^{-1} (620mμ) band is also suppressed by the presence of the nickel impurity, because

FIGURE A3

OPTICAL ABSORPTION AT ROOM TEMPERATURE OF (a) undoped LiF, (b) LiF:Ni^{2+} and (c) LiF:Co^{2+} after 30 minutes X-irradiation at room temperature.

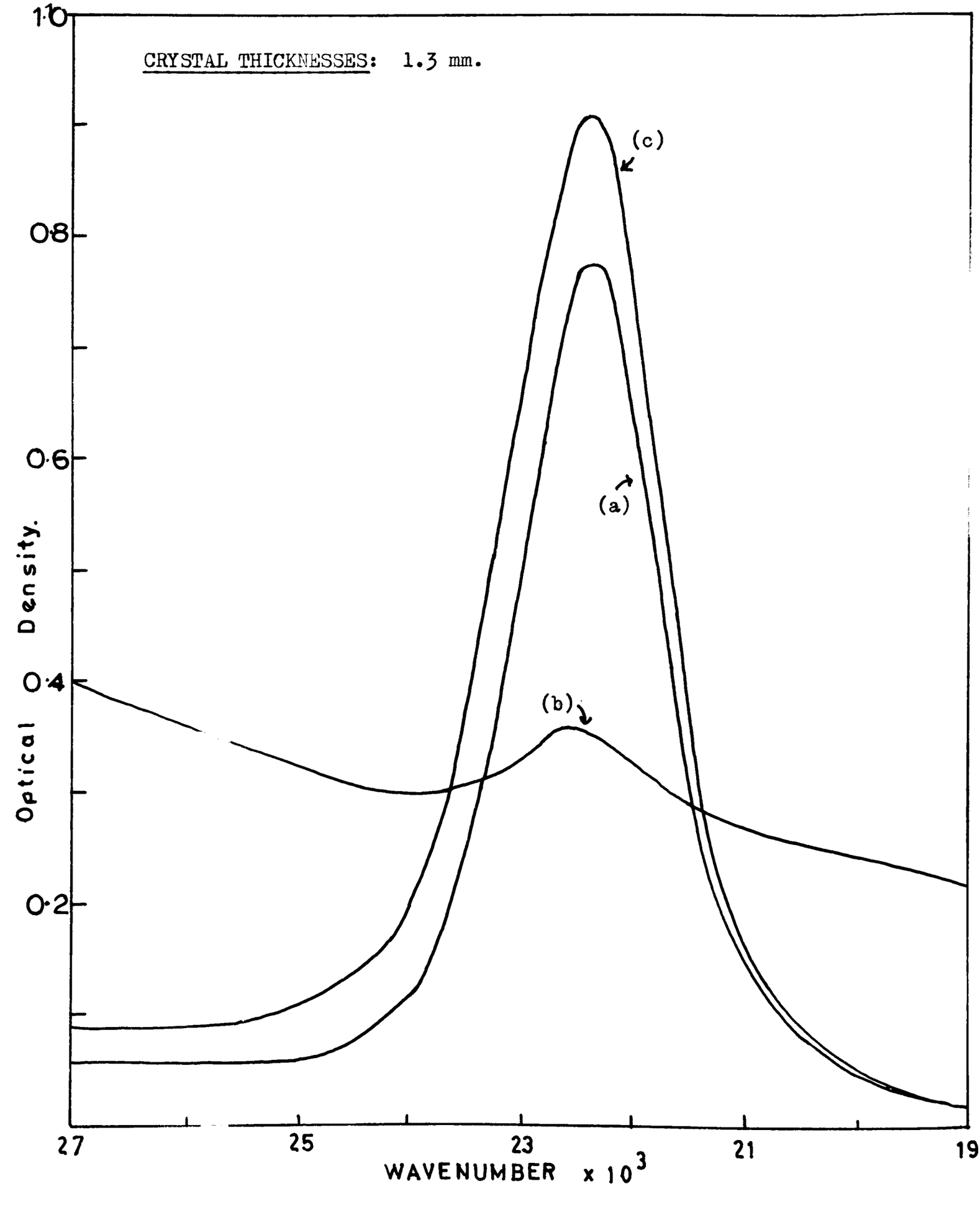

of the absorption due to Ni^{2+} ions themselves in this region. However, the result of a careful subtraction of this particular absorption from the irradiated crystal's spectrum indicates that the 15700 cm^{-1} band is also suppressed in nickel doped crystals.

(iii) The cobalt doped crystals

That the large reduction in the rate of formation of intrinsic lattice defects is due to the nickel impurity itself and not to the suppression of negative ion vacancies around the divalent impurity ion is shown by the irradiation results for cobalt doped lithium fluoride crystals. As shown in Figures A.2 and A.3, the presence of cobalt ions does not greatly affect the rate of formation of either the F or M bands. The 15,700 cm^{-1} band is also present in the irradiation spectrum of this substance.

The irradiation spectrum of cobalt doped lithium fluoride is somewhat complex in several respects as shown by the work of Huml and Bohun (1963) on heavily cobalt doped samples of lithium fluoride. In particular, they find evidence for the formation of cobalt complexes and clusters. This tendency for Co^{2+} ions to aggregate has been previously pointed out by Hayes (1962). However, the effect of the cobalt impurity on the growth of the F and M bands is relatively small and it is concluded that the suppression of these bands by nickel is connected with specific properties of this ion.

A discussion of these irradiation results is given in Section 4.

(c) Irradiation effects on the optical absorption of pure and nickel doped sodium fluoride crystals.

(i). The optical absorption of room and low temperature irradiated sodium fluoride crystals has not received much attention in the past. Onaka and Fujita (1960) have investigated the spectra in the vacuum ultraviolet.

Room temperature irradiation of pure sodium fluoride crystals yields two main bands at 29200 cm^{-1} and 19700 cm^{-1} of width 4600 and 1370 cm^{-1} respectively. These bands are in good agreement with the bands reported by Blum (1962) at 342 mμ (29200 cm^{-1}) and 510 mμ (19700 cm^{-1}) and assigned by him as F and M bands on the basis of the Mollwo law relationship of their frequencies to the F and M bands of potassium chloride. There is also a small shoulder at approximately 35000 cm^{-1} on the first band.

Irradiation of sodium fluoride crystals at liquid nitrogen temperature produces the F band at 30,000 cm^{-1}, a band on the side of this band at 27,300 cm^{-1}, and three bands at 43,000, 37,000 and 34,900cm^{-1}. Pulse annealing experiments, in which the crystal is quickly warmed up to successively higher temperatures in 10°K steps and cooled to liquid nitrogen temperature between each step and the spectrum recorded, were carried out to elucidate the thermal behaviour of these bands. The band at 27,300 cm^{-1} anneals at approximately 175°K and is assigned to V centres of the F_2^- molecular ion type. It is the subject of Chapter 3. The three bands at higher frequencies than the F band are analogous to

the V bands observed in potassium chloride (Seitz (1953)). They anneal just below 0°C and at room temperature only a small shoulder at approx. 35,000 cm^{-1} due to the 34,900 cm^{-1} band is evident on the F band peak. No M band is produced either during the low temperature irradiation or during the subsequent warmup to room temperature, and the crystals are colourless. They therefore differ from room temperature irradiated crystals which are reddish in colour and possess a strong M band absorption.

(ii) Nickel doped crystals

Sodium fluoride is not a good solvent for nickel and the crystals used were almost colourless and an absorption spectrum due to Ni^{2+} could not be detected. The presence of Ni^{2+} in these crystals at a molar concentration of 0.01% was inferred from electron spin resonance measurements. (Hayes, [redacted] and Wilkens (1963)).

It was found that after an hour's exposure to X rays at room temperature that the intensity of the M band was greater in the doped crystals than in pure sodium fluoride. However, after exposure of the crystals to room light for several days the intensity of the M band in pure sodium fluoride increased to the value found in the nickel doped crystals while the intensity of the M band in these doped crystals was unaffected. The intensity of the F band in the pure crystals decreased markedly in the same time.

The initial large intensity of the M band in the doped crystals may be due to fluorescence in the F band during irradiation; the doped crystals showed a blue fluorescence under irradiation whereas the

undoped crystals showed an orange fluorescence.

Because of these effects of fluorescence and because of the low concentration of nickel impurity present in the crystals, it does not appear to be feasible to make a direct comparison between the rates of formation of F and M centres in the nickel doped and the undoped crystals.

4. Discussion of the Results

(a) Optical absorption of nickel and cobalt in lithium fluoride

The optical absorption spectra of both octahedrally co-ordinated nickel and cobalt divalent ions are well understood. (Low (1958a,b)).

The d^8 configuration energy level scheme applies to nickel and Liehr and Ballhausen (1959) have extended the crystal field theory of Tanabe and Sugano (1953) to include the effects of spin orbit coupling. The three parameters used by Tanabe and Sugano are the cubic field Dq, and the Racah parameters B and C, and these are regarded as empirical parameters to be determined from the experimental data. The spin orbit coupling constant λ is determined from the measured g value of Ni^{2+} in lithium fluoride through the relation $g = 2 - \frac{8\lambda}{10Dq}$. For lithium fluoride, Hayes, [redacted] and Wilkens (1963) give the value of g as 2.22 and this yields $\lambda = -225\ cm^{-1}$. A computer diagonalisation of the matrices of Liehr and Ballhausen with the parameter values $Dq = 820\ cm^{-1}$, $B = 950\ cm^{-1}$, $C = 4100\ cm^{-1}$ and $\lambda = -225\ cm^{-1}$ yields the energy level values listed in Table B.1. The value of B is 8% less than the free ion value of $1030\ cm^{-1}$, C is 15% less than the free ion

value of 4850 cm^{-1} and the ratio C/B equals 4.3, which is reasonable compared to the free ion value of 4.7.

The splitting of the red band at 13880 cm^{-1} into four transitions at liquid nitrogen temperature may be due to resolution of transitions to the electronic levels $\Gamma_1(^3F)$, $\Gamma_4(^3F)$ and $\Gamma_5(^3F)$ and $\Gamma_3(^3F)$. The weak transitions observed at 15710 cm^{-1} and 16310 cm^{-1} cannot be fitted into the Liehr-Ballhausen scheme, and their origin is obscure. Their intensities relative to the other bands are the same in the 0.2% and 0.7% samples so they do not arise from pairs of Ni^{2+} ions. The relatively high intensities of the spin forbidden transitions to the $\Gamma_3(^1D)$ level at 15310 cm^{-1} and the $\Gamma_5(^1D)$ level at 21900 cm^{-1} is due to a 17% admixture of triplet character into the former and 8% into the latter.

The d^7 configuration applies to cobalt. Tanabe and Sugano (1954) give the crystal field theory matrices for this configuration and these have been extended by Eisenstein (1961) and Runciman and Schroeder (1961) to include spin orbit coupling effects. The spin orbit coupling constant is - 180 cm^{-1} for the free ion, and, as generally, a reduction of 20% with respect to the free ion value is found for first row divalent transition elements in octahedral co-ordination (Owen (1955)), a value of $\lambda = -150$ cm^{-1} is assumed for the solid. This value together with Dq = 910 cm^{-1}, B = 875 cm^{-1} and C = 3800 cm^{-1} have been used in a computer diagonalisation of the matrices of Eisenstein (1961). The energy levels obtained are listed in Table A.2. The value of B is 10% less than the free ion value of 971 cm^{-1} while the C value is

15% less than the free ion value of 4500 cm^{-1}, and $\frac{C}{B}$ equals 4.3.

Although there are three spin allowed quartet-quartet transitions possible in the $3d^7$ configuration, only two strong absorption bands (at 8000 and 20,000 cm^{-1}) are observed. These are assigned to the transitions $^4T_1(^4F) \rightarrow {}^4T_2(^4F)$ and $^4T_1(^4F) \rightarrow {}^4T_1(^4P)$ transitions respectively. The third quartet-quartet transition $^4T_1(^4F) \rightarrow {}^4T_1(^4F) \rightarrow {}^4A_2(^4F)$ then falls at 17000 cm^{-1} and there is only a weak absorption band at this frequency. The relative weakness of this transition can be explained as follows. The $^4A_2$ state comes from the strong field configuration $d\varepsilon^3 d\gamma^4$. Here $d\varepsilon$ and $d\gamma$ are the t_{2g} and e_g one electron wavefunctions for a d electron in a cubic field. $d\varepsilon$ corresponds to the triplet of levels $\frac{1}{\sqrt{2}}(|2\rangle - |-2\rangle)$, $|+1\rangle$ and $|-1\rangle$ while $d\gamma$ corresponds to the doublet $|0\rangle$ and $\frac{1}{\sqrt{2}}(|2\rangle + |-2\rangle)$, where $|m_s\rangle$ is the wavefunction of an $\ell = 2$ electron corresponding to an angular momentum component of m_s (Moffitt and Ballhausen (1956)). The ground $^4T_1$ state is principally $d\varepsilon^5 d\gamma^2$ with a small admixture of the $d\varepsilon^4 d\gamma^3$ configuration coming from the ^4P level of the free ion. A transition involving the change of two d orbitals will be weak, and the absorption to the $^4A_2$ level occurs through the component of the ^4P level in the ground state. For the values of Dq and B above, the ground state has the wavefunction:

$$0.96\,{}^4T_1(^4F) \quad - \quad 0.27\,{}^4T_1(^4P)$$

and hence the $^4T_1(^4F) \rightarrow {}^4A_2(^4F)$ transition is 0.07 times as

strong as the other two quartet-quartet transitions.

(b) Irradiation effects on the optical absorption of pure and doped lithium fluoride crystals

(i) The pure crystals

In both lithium and sodium fluoride crystals the M band is present at much weaker intensity in the room temperature spectrum of a low temperature irradiated crystal than in that of a room temperature irradiated crystal, while the F band intensity is similar in both spectra.

Van Doorn (1957, 1960, 1962) and Faraday, Rabin and Compton (1961) have shown that the intensity of the M band produced at room temperature is proportional to the square of the F band intensity and this supports the model of the M centre as a pair of F centres. The weak intensity of the M band in a crystal irradiated at low temperature suggests that a motion of F centres is necessary in M centre formation. Riegand and Smoluchowski (1959) have reported that measurements on a very heavily low temperature irradiated lithium fluoride crystal failed to reveal any increase in the M band between 90° and 165°K, while between 165°K and 300°K the M band increased by at least a factor of 45. This is in agreement with the hypothesis of the motion of F centres being necessary to form M centres.

These various observations are consistent with the results obtained here for the low temperature irradiation properties of lithium and sodium fluoride, in particular, no M band after low temperature irradiation but the subsequent appearance of a weak M band after warming the crystal to room temperature.

(ii) The doped crystals

The almost complete suppression of the F and M bands in lithium fluoride by nickel impurity ions is attributed to the strong electron trapping properties of these ions.

Wilkens (1961) and Hayes and Wilkens (1961) have given a detailed description of the electron spin resonance spectra of monovalent nickel in lithium fluoride. These ions are obtained by room and low temperature irradiation of the nickel doped crystals. Their results show that the divalent nickel ions initially present are efficient electron traps and readily capture electrons to form the monovalent ions.

Room temperature irradiation of the cobalt doped lithium fluoride crystals does not produce an electron spin resonance of Co^{+} ions and it is concluded that Co^{2+} ions are not effective electron traps in lithium fluoride. The failure to observe Co^{+} ions is not due to experimental difficulties of detecting the electron spin resonance of these ions, because these monovalent ions are readily observed in cobalt doped sodium fluoride crystals irradiated in a similar manner.

The concentration of Ni^{+} ions produced by irradiation of the 0.2% nickel sample is estimated as 0.001% from the electron spin resonance measurements so the optical absorption of these ions is undetectable. The decrease in intensity of the Ni^{2+} absorption is approximately 1% and is also too small for detection.

The suppression of the F and M bands occurs through the preferential

trapping of electrons, produced by the irradiation, by the Ni^{2+} ions. Furthermore, F centres moving at room temperature are trapped by the Ni^{2+} ions to form monovalent nickel ions associated with a negative ion vacancy. By these mechanisms the F band absorption is strongly suppressed while M centre formation is suppressed through the trapping of the F centres by Ni^{2+} ions before they can combine to form M centres.

There are eight different types of monovalent nickel centres detectable by electron spin resonance and these are distinguishable in their symmetry and annealing behaviour. Of these centres, two show the presence of a negative ion vacancy. They are produced by room temperature irradiation and always occur at the ratio 2:1 at 80°K. Their concentration is estimated as approximately $10^{16}/cm^3$ while the amount of M band absorption "suppressed" is also estimated, from the Smakula formula (Gorlich (1961)) assuming an oscillator strength of 0.4 (Faraday, Rabin and Compton (1961)), as approximately $10^{16}/cm^3$. There thus appears to be an approximate correlation between the formation of these particular monovalent nickel ion centres and the suppression of the M band.

These nickel centres also appear weakly in a crystal which has been irradiated at low temperature and subsequently warmed to room temperature. They increase in intensity on storing at room temperature for several weeks. This behaviour of the centres, together with their ready production by room temperature irradiation, follows closely the qualitative behaviour of the M band in the undoped crystals and is

consistent with the hypothesis of the F centres being preferentially trapped by Ni^{2+} ions to form these Ni^{+} centres rather than combining with each other to form M centres.

The effect of the Co^{2+} ion impurity is to increase slightly the F and M band formation. This slight increase could be attributed, as suggested by Crawford and Nelson (1960), to the generation of additional negative ion vacancies by the divalent ion. This mechanism has been discussed by Hayes (1962).

The behaviour of the nickel doped sodium fluoride crystals has been described in Section 3 (c). Due to the unavailability of strongly nickel doped crystals and to the apparent effects of fluorescence under irradiation it is not possible to draw any conclusions about the effect of nickel impurity ions on the rate of formation of F and M bands in this substance.

REFERENCES

Blum, H., 1962, Phys. Rev., 128, 627

Crawford, J. H., and Nelson, C. M., 1960, Phys. Rev. Letters, 5, 314

Delbecq, C. J., and Pringsheim, P., 1953, J.Chem.Phys., 21, 794

Delbecq, C. J., Hayes, W., and Yuster, P.H., 1961, Phys.Rev. 121, 1043

Duerig, W. H., and Mador, I. L., 1952, Rev. Sci. Instrum., 23, 421

Eisenstein, J. C., 1961, J. Chem. Phys., 34, 1628

Faraday, B. J., Rabin, H., and Compton, W. D., 1961, Phys. Rev. Letters, 7, 57

Geiger, F. E., 1955, Rev. Sci. Instrum., 26, 383

Gorlich, P., Karras, H., and Lehmann, E., 1961, Physica Status, Solidi, 1, 390

Gorlich, P., Karras, H., and Kotitz, G., 1963, Physica Status Solidi, 3, 1629

Hall, T. P. P., Hayes, W., Stevenson, R. W. H., and Wilkens, J., 1963 J. Chem. Phys., 39, 35.

Hayes, W., 1962, J. Appl. Physics. Suppl. 33, 329

Hayes, W., and Wilkens, J., 1963, to be published

Huml, K., and Bohun, A., 1963, Physica Status Solidi, 3, 250

Kaufman, J. V. R., and Clark, C. D., 1963, J.Chem.Phys., 38, 1388

Low, W., 1958a, Phys.Rev., 109, 247

Low, W., 1958b, Phys.Rev., 109, 256

Liehr, A. D., and Ballhausen, C. J., 1959, Annals. of Physics, 6, 134

Moffitt, W., and Ballhausen, C. J., 1956, Annual Review of Physical Chemistry, 7, 107

Onaka, R., and Fujita, I., 1960, Phys. Rev., 119, 1597

Owen, J., 1955, Proc. Roy. Soc. A227, 183

Runciman, W. A., and Schroeder, K. A., 1962, Proc.Roy.Soc. A 265, 489

Seitz, F., 1953, Rev. Mod. Physics, 26, 7.

Stockbarger, D. C., 1949, J. Opt. Soc. Am., 39, 731

Tanabe, Y., and Sugano, S., 1954, J. Phys. Soc. Japan, 9, 753, 766

Van Doorn, C. Z., 1957, Philips Res. Reports, 12, 309

Van Doorn, C. Z., 1960, Phys. Rev. Letters, 4, 236

Van Doorn, C. Z., 1962, Philips Res. Repts. Suppl. No.4

Wiegand, D. A., and Smoluchowski, R., 1959, Phys. Rev., 116, 1069

Wilkens, J., 1961, Thesis, Clarendon Laboratory, Oxford.

CHAPTER THREE

OPTICAL ABSORPTION BY THE F_2^- CENTRE IN SODIUM FLUORIDE

1. Introduction

X-irradiation at liquid nitrogen temperature of pure sodium fluoride crystals produces, in addition to the other bands already described in chapter 2, section 3(b), an absorption band at 27,300cm^{-1}. This band is ascribed to a V centre of the X_2^- molecular ion type described by Delbecq, Smaller and Yuster (1958). The structure of this centre was elucidated by Känzig et. al. (1957, 1958) by electron spin methods. It consists of a hole located on two neighbouring fluorine ions and is oriented along <110> directions of the crystal. Delbecq, Hayes and Yuster (1961) have investigated these centres for several alkali halides by both electron spin resonance and optical methods. The F_2^- centre, observed here in sodium fluoride, was studied in lithium fluoride by these workers.

The electron spin resonance spectrum of the F_2^- centre in sodium fluoride has been reported by Wilkens (1961).

In sodium fluoride the F_2^- absorption band occurs on the side of the F centre absorption band at 29,000 cm^{-1} (chapter 2, section 3) and is partially swamped by it, but it is readily detected through its disappearance on warming the crystal from 77°K to room temperature. The temperature of maximum decay rate was determined to be $\sim$ 175°K and this is in agreement with the value of $\sim$ 160°K obtained by Wilkens

(1961) for the maximum rate of disappearance of the electron spin resonance. It is also in agreement with the [redacted] value of 180°K obtained by Heckelsberg and Daniels (1957) for the first glow peak in the thermoluminescence spectrum of sodium fluoride.

Polarised bleaching experiments of the type described by Delbecq, Smaller and Yuster (1958) were performed on this absorption band to verify its assignment to F_2^- centres. This technique consists of bleaching the absorption band of the irradiated crystal by polarised light incident along one of the face diagonals of the crystal and observing the effect on the optical absorption. If the centres responsible for the band have orientations along these specific crystal directions, a realignment of them into the unbleached directions will occur and the resulting optical absorption will be anisotropic.

2. Experimental Arrangement for Polarised Bleaching

In the bleaching of the sodium fluoride crystals, light from an Osram 200 watt high pressure mercury lamp passed through a 360 mμ (28,000 cm^{-1}) narrow band Corning filter and then through a Glan-Thompson prism before impinging upon the crystal mounted in the dewar. The axis of the polarising prism was oriented parallel to one of the cubic axes of the crystal and the prism rotated about this axis so that the electric vector of the light lay along a face diagonal (<110> direction). The absorption spectra were recorded for both directions of polarisation, viz., parallel and perpendicular to the bleached direction. The polariser used for these measurements was Polaroid

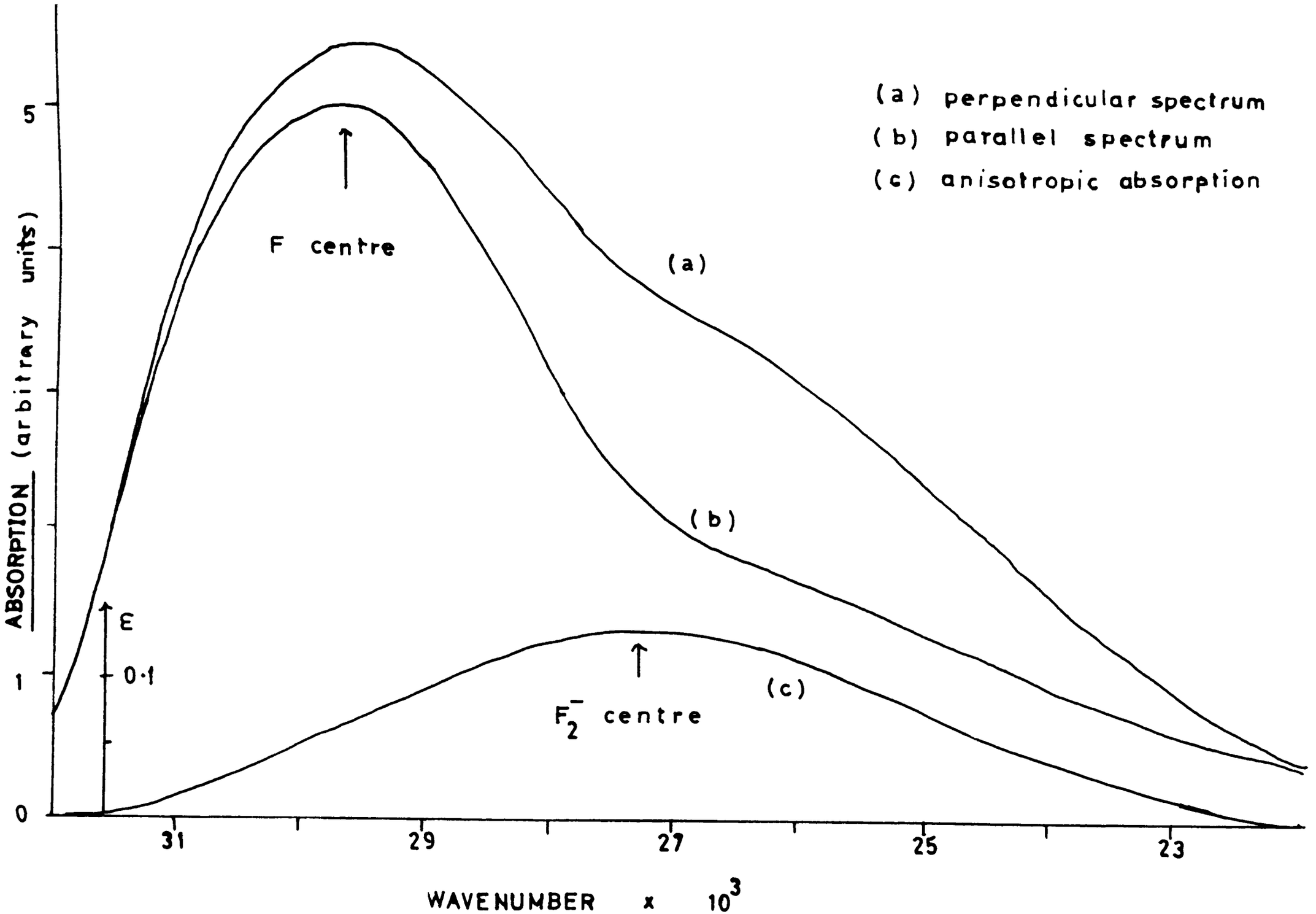

FIGURE BI. POLARISED ABSORPTION OF F_2^- CENTRES IN SODIUM FLUORIDE

type "HN" and this was placed in the spectrophotometer immediately before the beam splitter so that its own absorption was automatically compensated for.

3. Experimental Results

Figure B.1 shows the optical absorption of a sodium fluoride crystal after a 10 hour irradiation, for both perpendicular and parallel polarisations with respect to the bleaching direction. The difference between the two absorption curves is defined as the anisotropic absorption and a curve of this is also shown in the figure. This subtraction eliminates all absorptions that do not show anisotropy. Hence the F centre absorption also present is subtracted out and the resulting absorption curve is solely due to the F_2^- centres.

The temperature at which the F_2^- molecular ions lose their preferential orientation is defined as the disorientation temperature. It is somewhat lower and more sharply defined that the decay temperature, at which the centres disappear, because disorientation may be achieved by a movement of the centre through one lattice spacing whereas, on the average, many lattice spacings are covered before the centre meets an electron and is destroyed. The disorientation temperature was determined here for the F_2^- centre in sodium fluoride by monitoring the dichroism of the absorption band as the crystal was warmed up from low temperature. Its value was measured as 155°K.

Similar experiments on lithium fluoride yielded the value of 114°K and this is in good agreement with the value of -160°C (113°K)

reported by Delbecq, Hayes and Yuster (1961).

The F_2^- absorption bands in sodium and lithium fluoride also possess other differences and these are listed in Table B.1. The results obtained here for lithium fluoride are in agreement with those of Delbecq, Hayes and Yuster (1961). The decay temperatures agree with the thermoluminescence data of Heckelsberg and Daniels (1957).

	Peak absorption frequency	Halfwidth, ev	Disorientation Temperature	Decay Temperature
NaF	27300 cm^{-1}	0.66	155°K	175°K
LiF	28700 cm^{-1}	1.35	114°K	138°K

Table B.1

Experiments to detect the presence of the additional 750mμ (13,500 cm^{-1}) absorption band in both lithium and sodium fluoride were unsuccessful. The method consists of orienting the centres by a 360mμ irradiation and then exposing them to unpolarised light of other wavelengths. If the anisotropy is destroyed with a particular wavelength an additional absorption band of the centres must occur in this wavelength region. The peak of this band is determined by the rate of disappearance of the anisotropy of the main band as a function of the wavelength of the bleaching light.

The failure to observe any decrease in the anisotropy of the F_2^- centres in lithium fluoride by unpolarised 750 mμ light, and the consequent inability to confirm the presence of the weak 750 mμ absorption band due to these centres in lithium fluoride, reported by

Delbecq, Hayes and Yuster (1961), was attributed to the use of an insufficiently powerful lamp.

4. Discussion of the Results

The absorption data has been presented in Table B.1.

One significant difference is the relative linewidths of the bands. This could be a consequence of the greater localisation of the centre in sodium fluoride than lithium fluoride, which was shown by the electron spin resonance measurements of Wilkens (1961). The sodium fluoride linewidth obtained is similar to the linewidths reported for other alkalis halide X_2^- centres by Delbecq, Hayes and Yuster (1961).

A much greater rate of formation of F_2^- centres in lithium fluoride compared to X_2^- formation in other alkali halides was observed by these workers. It was found here that the rate of formation of F_2^- centres in lithium fluoride was much greater than in sodium fluoride and this supports the above workers' hypothesis of an additional mechanism for trapping electrons which is only operative in lithium fluoride. The anomalous behaviour of lithium fluoride in relation to that of the other alkali halides has already been pointed out by Kaufmann and Clark (1963) and by Gorlich, Karras and Kotitz (1963) in connection with their unsuccessful experiments to additively colour lithium fluoride.

The variation of the disorientation and decay temperatures could be explained in a qualitative way by the effect of the lattice dimensions on the energy levels of the F_2^- ion. Hayes, Delbecq and

Yuster (1958) have examined the effect of environment for the Cl_2^- ion centre in the series LiCl, NaCl, KCl, RbCl. They observed an increase in the disorientation and decay temperatures along the series and attributed this to the increase in lattice spacing of the host substances.

5. Summary

The F_2^- centre's main absorption band in sodium fluoride has been detected at 27300 cm^{-1}, and compared to that of the same centre in lithium fluoride.

REFERENCES

Delbecq, C. J., Hayes, W., and Yuster, P. H., 1961, Phys. Rev. 121, 1043

Delbecq, C. J., Smaller, B., and Yuster, P. H., 1958, Phys. Rev. 111, 1235

Gorlich, P., Karras, H., and Kotitz, G., 1963, Physica Status Solidi, 3, 1629

Hayes, W., Delbecq, C. J., and Yuster, P. H., 1958, Bull. Am. Phy. Soc. Ser.II 3, 325

Heckelsberg, L. F., and Daniels, F., 1957, J.Phy.Chem., 61, 414

Kanzig, W., and Castner, T. G., 1957, J.Phys.Chem.Solids, 3, 178

Kanzig, W., and Woodruff, T. D., 1958, J.Phys.Chem.Solids, 5, 268

Kaufman, J. V. R., and Clark, C. D., 1963, J.Chem.Phys., 38, 1388

Wilkens, J., 1961, Thesis, Clarendon Laboratory, Oxford

CHAPTER FOUR

ANTIFERROMAGNETIC ORDERING EFFECTS IN SOME TRANSITION METAL FLUORIDES

1. Introduction

The occurrence of antiferromagnetic ordering in various transition metal compounds is well known (Kanamori (1958), Hirakawa Hirakawa and Hashimoto (1960)). The transition to the antiferromagnetic ordered state by the metal ions occurs at the Néel temperature and this temperature can be determined in several ways. These include the measurement of the magnetic susceptibility of the substance as a function of temperature (de Haas, Schultz and Koolhaas (1940)), the determination of the temperature where peaks in the specific heat, the molar heat capacity (Millar (1928)) and the thermal expansion coefficients (Foex (1948)) occur, the study of neutron diffraction spectra (Erickson (1953)) and the observation of the temperature of disappearance of the magnetic resonance of the transition metal ion nuclei. (Baker, Lourens and Stevenson (1961)).

The exchange interaction which gives rise to antiferromagnetic effects may substantially modify the energy levels of the transition metal ion and so affect the optical absorption. It is thus possible to observe the onset of antiferromagnetic ordering by the shift of absorption lines near the Néel temperature, and to study the antiferromagnetic ordered states spectroscopically. There is no great change in the principal features of the absorption spectra because the

FIGURE C1 Optical absorption band of MnF_2 corresponding to the $^6A_{1g}(^6S) \rightarrow {}^4T_{2g}(^4D)$ transition.

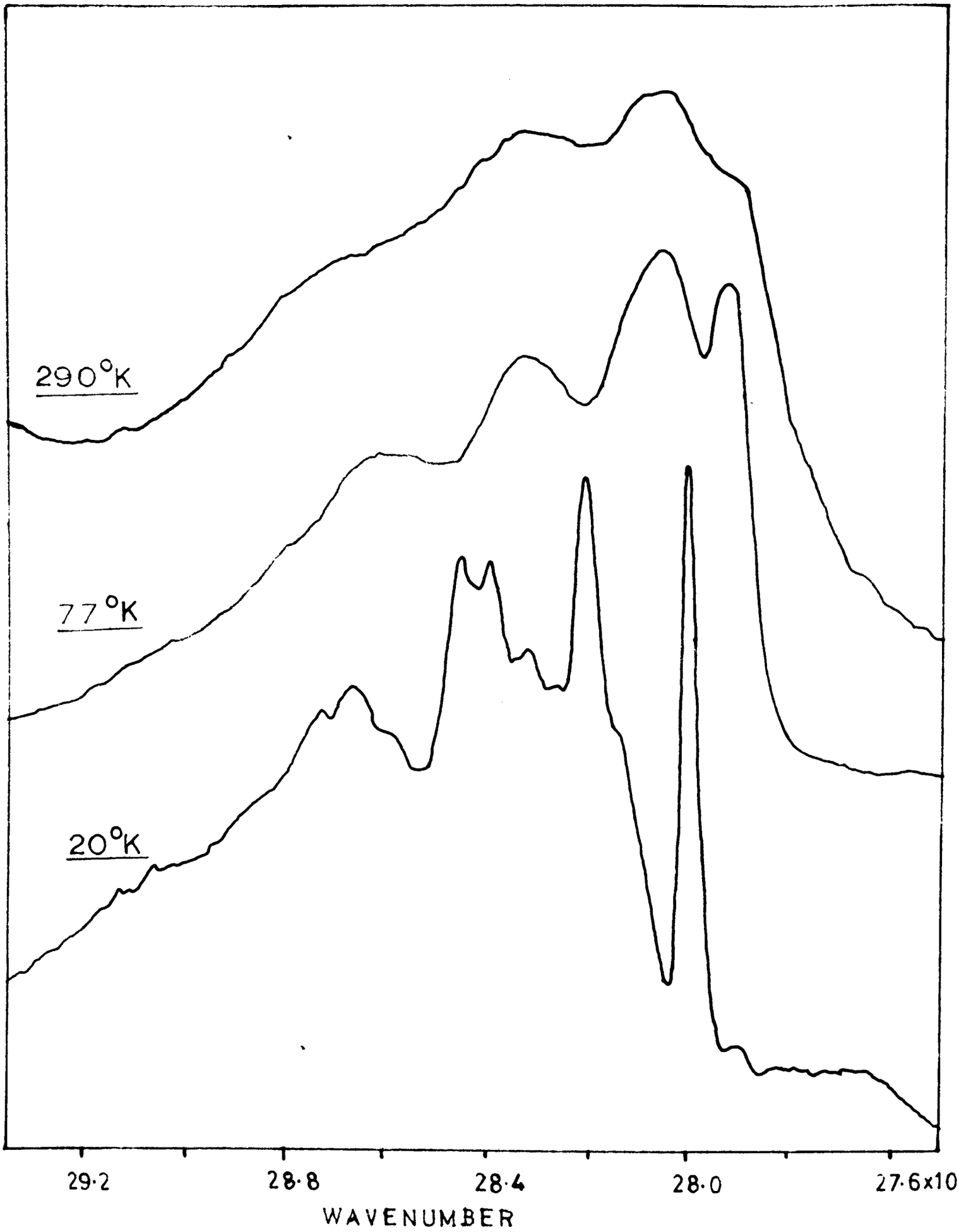

energy of magnetic interaction is of the order of 100cm^{-1} whereas optical transitions in the visible region correspond to energies of 10 - 30,000 cm^{-1}. The frequency shifts are quite small and can only be observed in narrow absorption lines.

Experimental studies of magnetic ordering effects on optical spectra have been carried out by Pratt and Coelho (1959) for CoO and MnO, by Newman and Chrenko (1959 a,b,c) for NiO and CoF_2, by Tsujikawa (1958) and Tsujikawa and Kanda (1959) for $MnCl_2 \cdot 4H_2O$ and $MnBr_2 \cdot 4H_2O$, by Stout (1959) and Finlayson, Robertson, Smith and Stevenson (1960) for MnF_2 and, subsequent to the completion of the experimental work given here, by Knox, Schulman and Sugano (1963) for $KNiF_3$.

The experimental investigations carried out here were:

(a) a detailed study of the narrow optical absorption lines at 25250cm^{-1} and 25150 cm^{-1} in MnF_2. The frequency shift of these lines on cooling the crystal through its Néel temperature (68°K) was investigated to determine how the line frequency varies in the neighbourhood of this temperature. In the earlier work by Stout (1959) on MnF_2 the line frequencies were only determined at 20°K, 64°K, 77°K and the frequency difference between the 20°K and 77°K values attributed to antiferromagnetic ordering effects at 68°K. It was not demonstrated that the shift observed did occur in the vicinity of this temperature. The later measurements of Finlayson, Robertson, Smith and Stevenson (1960) only extended down to 62°K and did not fully cover the antiferromagnetic transition.

(b) A study of the temperature variation of one of the narrow optical

FIGURE C2

$^6A_{1g}(^6S) \rightarrow {}^4A_{1g}(^4G), {}^4E_g(^4G)$ for MnF_2

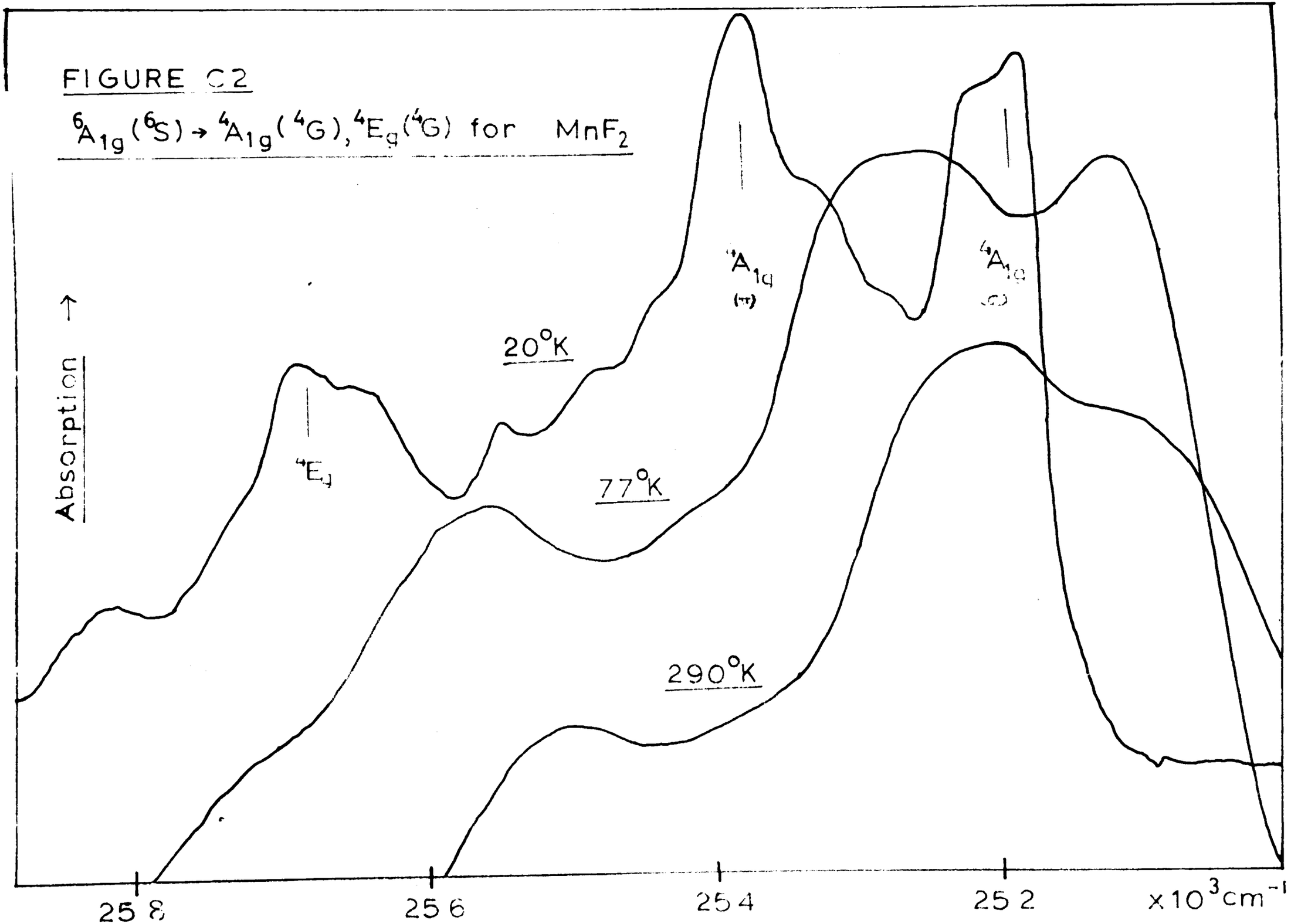

lines near 25,200cm^{-1} in $KMnF_3$. The Néel temperature of this substance is 88°K (Beckman and Knox (1961)).

(c) An analysis of the optical absorption spectra of $KNiF_3$ and of nickel doped $KMgF_3$ crystals together with a study of the effects of antiferromagnetic ordering on the spectrum of the $KNiF_3$ crystal. This substance has a relatively high Néel temperature (275°K)(Okazaki, Suemune and Fuchikami (1959)) and the effects of magnetic ordering on the optical absorption are quite large. The nickel containing $KMgF_3$ crystal had 2% molar concentration of nickel present. It was also investigated to determine the temperature behaviour of Ni^{2+} ions in the absence of magnetic exchange effects. The similarity of the lattice dimensions of $KNiF_3$ (4.01A°) and $KMgF_3$ (4.00A°) shows that the Ni^{2+} ion has an almost identical environment in both lattices and a comparison of the two spectra should readily display the specific effects of antiferromagnetic ordering.

2. Experimental Details

The crystals of manganese fluoride, potassium manganese fluoride ($KMnF_3$), potassium nickel fluoride ($KNiF_3$) and nickel doped potassium magnesium fluoride ($KMgF_3:Ni^{2+}$) were grown in graphite crucibles by the Stockbarger method by Dr. R. W. H. Stevenson of Aberdeen University. Evaporation from the melt was reduced by maintaining a pressure of 20-30lb./in^2 of oxygen free nitrogen in the furnace during the growth period.

The manganese fluoride starting material was obtained by repeated recrystallisations of selected commercial material. The

FIGURE C3 Effect of antiferromagnetic ordering on the transition $^6A_{1g}(^6S) \rightarrow {}^4A_{1g}(^4G)$ of MnF_2.

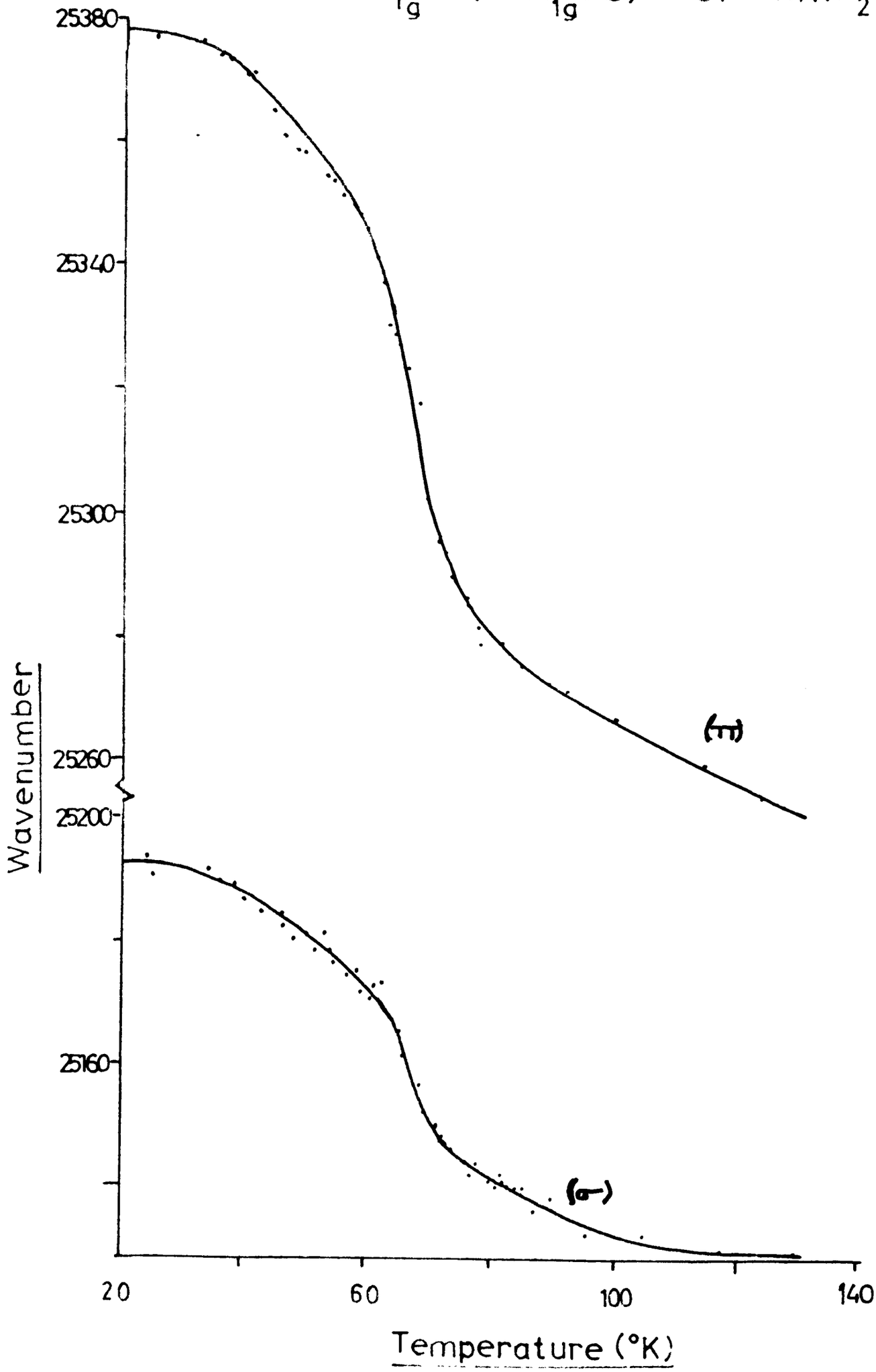

crystals of $KMnF_3$, $KNiF_3$ and $KMgF_3$; Ni^{2+} were grown using a stoichiometric mixture of KF and the transition metal fluoride.

Neither MnF_2 or the double fluorides cleave well so suitably sized plates were sawn from the crystal and the surfaces polished. The absorption of the $KNiF_3$ crystals is high in the wavenumber regions where the spin allowed transition of nickel occurs and it was necessary to grind the crystals to $\frac{1}{4}$mm thickness to observe the top of these bands. In MnF_2 and $KMnF_3$ all transitions are spin-forbidden and in $KMgF_3$;Ni^{2+} the nickel concentration is relatively low so these crystals were examined in thicknesses ranging from 1 to 4mm.

The Unicam SP700 spectrophotometer and the cryostat described in Chapter 2 were used for the optical measurements.

3. Experimental Observations and Discussion for MnF_2

The optical absorption spectrum was observed for MnF_2 for the four temperatures: room, 77°K, 20°K and 4°K. It agrees well with that reported by Stout (1959) and Finlayson, Robertson, Smith and Stevenson (1960).

The spectrum observed is characterised by the presence of broad bands and narrow lines. The lines occur at 25150 cm^{-1}, 25250 cm^{-1} 25,500 cm^{-1} and 30,200 cm^{-1} (room temperature values) and are attributed to transitions from the sextet ground state ($^6A_{1g}(^6S)$) to the quartet levels $^4A_{1g}^{\sigma}(^4G)$, $^4A_{1g}^{\pi}(^4G)$, $^4E_g(^4G)$ and $^4E_g(^4D)$ respectively. These levels arise from the same strong field configuration $d\varepsilon^5 d\gamma$ as the ground state so are largely independent of the

FIGURE C4 Optical absorption band of $KMnF_3$ corresponding to the $^6A_{1g}(^6S) \rightarrow {}^4T_{2g}(^4D)$ transition.

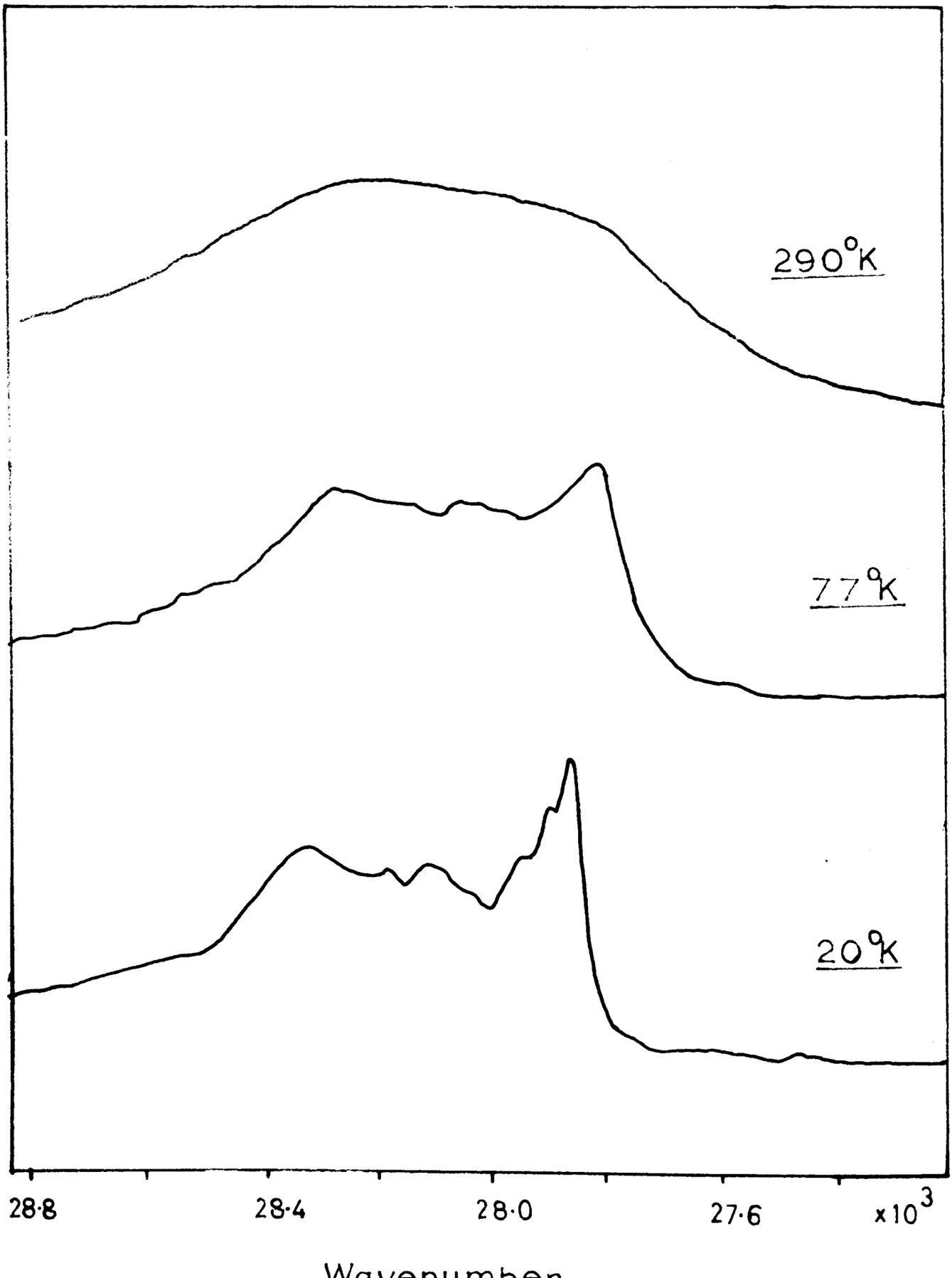

crystal field. The broad bands at 19500cm^{-1}, 23500cm^{-1}, 28100cm^{-1} 33050cm^{-1}, 39000cm^{-1} and 41400cm^{-1} (room temperature values) come from transitions to energy levels arising from different strong field configurations. The fitting of the observed absorptions to the various energy levels of the $3d^5$ configuration, with the assumption of a cubic crystal field, has been performed by both Stout (1959) and Finlayson et.al.(1960) and so need not be elaborated here. Satisfactory agreement between the observed data and the calculated energy levels was obtained in both the previous investigations.

As for the explanation of the structure of the various absorptions little quantitative work has been done. Manganese fluoride crystals have the rutile structure which shows macroscopic tetragonal symmetry. There are two manganese ions in the unit cell, each with only orthorhombic symmetry whose axes differ by a 90° rotation about the c axis. There is, therefore, present a low symmetry crystal field and the cubic field approximation is inadequate. This is shown by the strong polarisation properties displayed by several of the bands (reported in the works above and confirmed here).

Furthermore, the optical transitions all occur between electronic states of even parity and so are parity forbidden. They must, therefore, be accompanied by the excitation of odd vibrations and these are also responsible for some of the structure. As an example of the importance of vibrational effects Figure C.1 shows the spectrum of the broad absorption band at 28,100cm^{-1}, which arises from the transition $^6A_{1g}(^6S) \rightarrow$

FIGURE C5

$KMnF_3$

$^6A_{1g}(^6S) \rightarrow {}^4A_{1g}(^4G), {}^4E_g(^4G)$

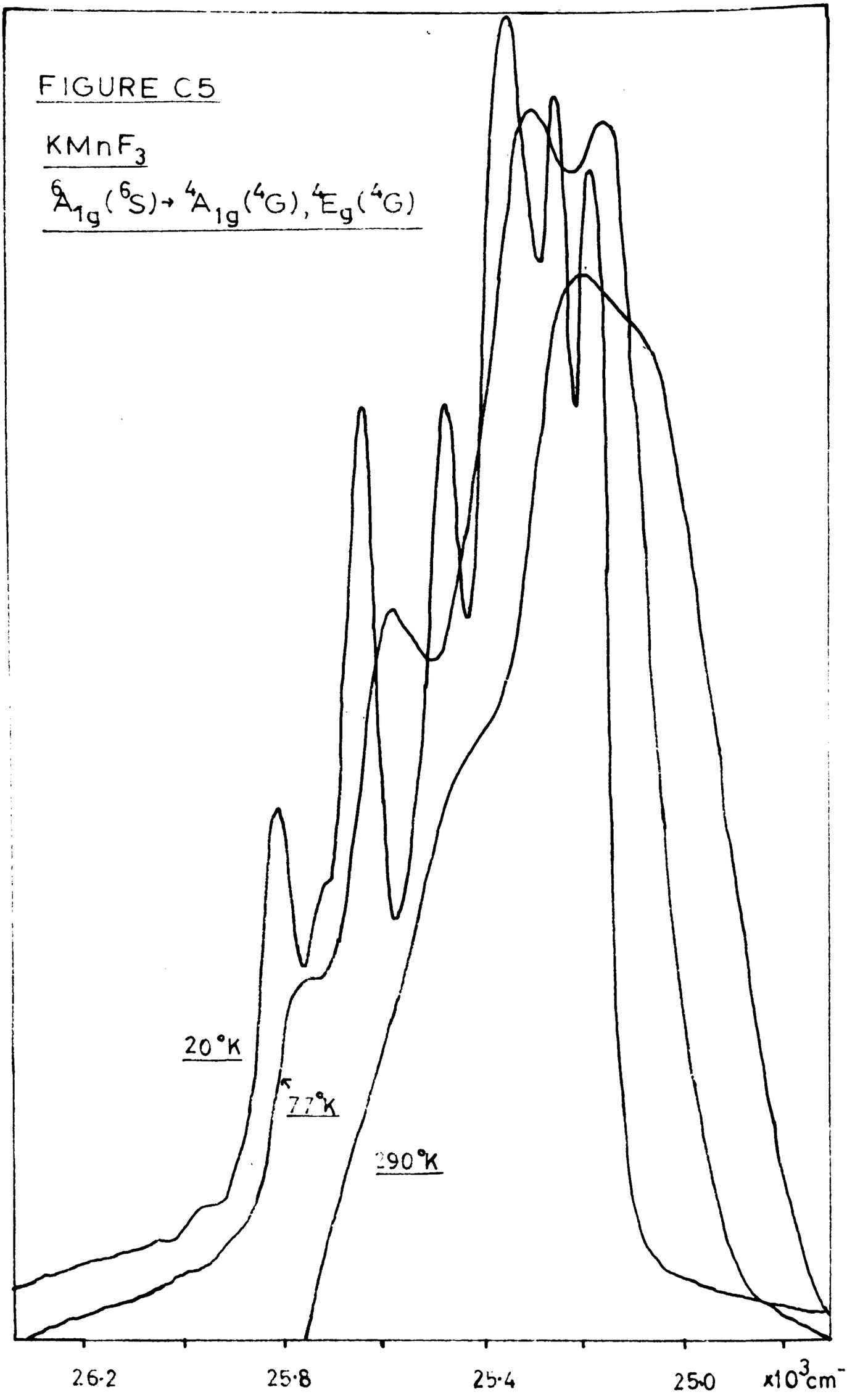

$^4T_{2g}(^4D)$, for various temperatures. This particular absorption band was given by Finlayson, Robertson, Smith and Stevenson (1960) in Figure 2 of their paper, but as their measurements extend down to 62°K only, the vibrational structure is not fully revealed.

The problem of explaining the structure of the absorption bands of MnF_2 is clearly a complicated one. For a satisfactory interpretation a knowledge of the vibrational frequencies of MnF_2 is required.

The sharp line transitions $^6A_{1g}(^6S) \rightarrow {}^4A_{1g}(^4G)$, $^4E_g(^4G)$ and $^4E_g(^4D)$ have quite narrow widths so can be used to determine the effects of magnetic exchange interactions. The last two transitions' lines are wider than the others and so were neglected and attention directed to the temperature dependence of the two 25200cm^{-1} lines. Figure C.2 shows the spectrum of MnF_2 in this region for the three temperatures, 20°K, 77°K and room temperature. Several weak subsidiary lines are also evident in the low temperature spectra.

The peak position of these lines was determined at approximately 5°K intervals in the temperature range 20°K to 150°K by repeatedly scanning this spectrum of the two lines while slowly warming the crystal up from low temperature. The variation in the peak position of the lines is shown in Figure C.3. There is an approximately linear shift in the peak position with temperature which is of the type usually observed in optical spectra of paramagnetic materials and is caused by thermal contraction effects, and superposed on this a pronounced frequency shift in the lines near 70°K. This frequency shift has maximum value at 72°K and this is in good agreement with the

FIGURE C6 Effect of antiferromagnetic ordering on the frequency of the optical transition $^6A_{1g}(^6S) \rightarrow {}^4A_{1g}(^4G)$ of $KMnF_3$.

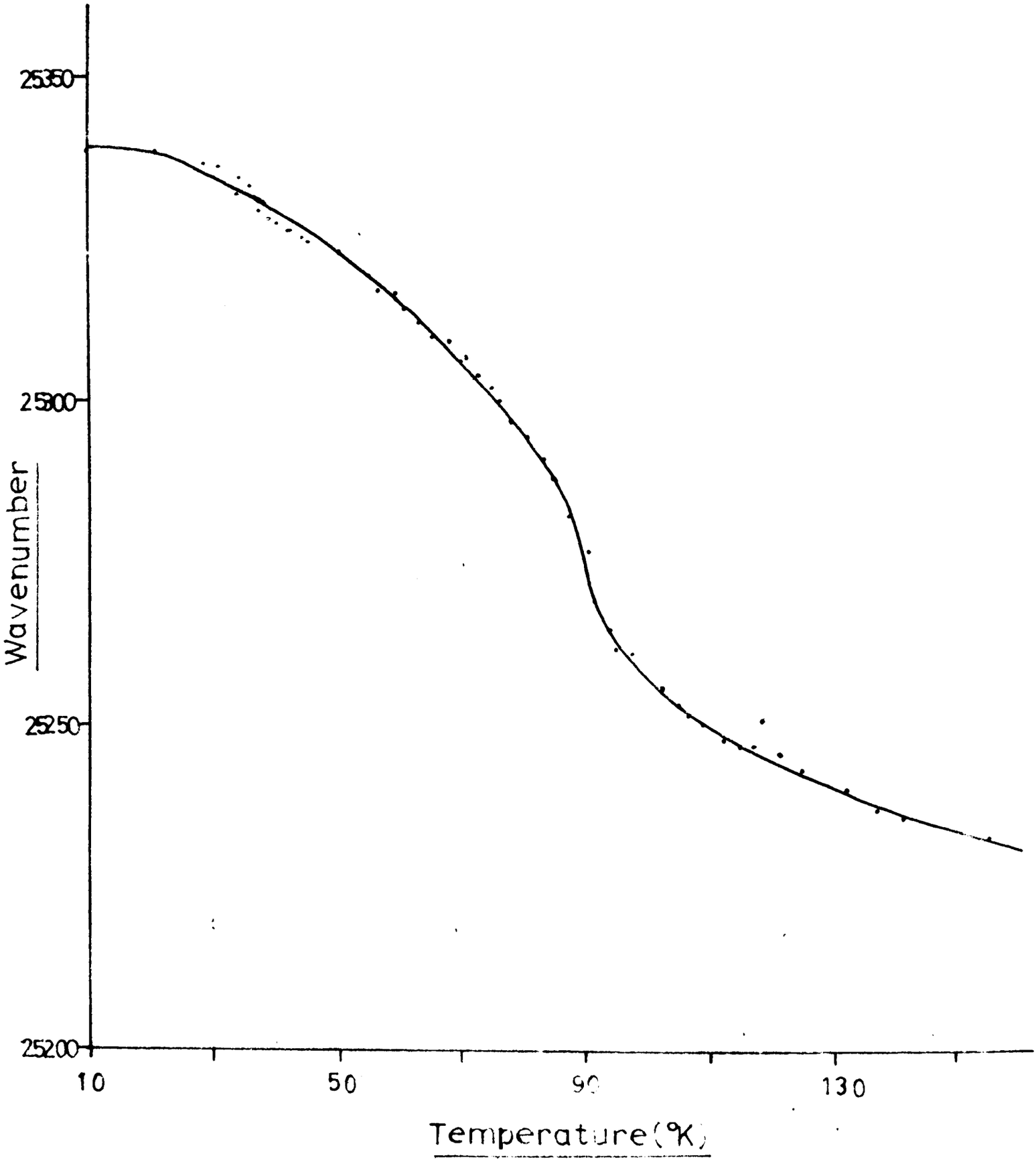

Néel temperature of 68°K for manganese fluoride. The large shift in frequency occurs in the temperature range 80°K to 40°K. The gradualness of this transition presumably represents the onset of short range ordering above the Néel temperature, while complete long range ordering is not reached till below 40°K.

The problem of explaining the magnitude of the line shift is a difficult one. Sugano and Tanabe (1963) have discussed this problem in some detail. The simplest model that can be applied is that of the molecular field. In this it is assumed that the single atom is exposed to an effective magnetic field in addition to the crystal field. Sugano and Tanabe give the simple formula for the stabilisation of the ground level, E, by this field, as:

$$E = \frac{3kT_N}{(S + 1)}$$

where k is the Boltzmann constant

T_N is the Néel temperature

and S is the effective spin

For MnF_2 this yields $E = 47cm^{-1}$. When antiferromagnetic ordering sets in the optical transition will come from the lower of these split levels and the absorption line will appear to shift $47cm^{-1}$ to higher frequencies. This shift is in order of the magnitude agreement with the observed splittings of $80cm^{-1}$ and $40cm^{-1}$ for the π and σ polarised lines respectively.

Stout (1959), following a suggestion of Kanamori (1959),

Table C.1 Ni^{2+} band positions in $KNiF_3$ and $KMgF_3:Ni^{2+}$

Transition	Calculated band positions (cm^{-1})	Observed band positions for $KNiF_3$ at room temperature (cm^{-1})	Observed band position for $KMgF_3:Ni^{2+}$ at room temperature (cm^{-1})
${}^3\Gamma_5({}^3F) \rightarrow {}^3\Gamma_3({}^3F)$	7098		
$\rightarrow {}^3\Gamma_4({}^3F)$	7200	7400	7450
$\rightarrow {}^3\Gamma_5({}^3F)$	7506		
$\rightarrow {}^3\Gamma_2({}^3F)$	7627		
$\rightarrow {}^3\Gamma_1({}^3F)$	11732		
$\rightarrow {}^3\Gamma_4({}^3F)$	12121	12650	12800
$\rightarrow {}^3\Gamma_3({}^3F)$	12695		
$\rightarrow {}^3\Gamma_5({}^3F)$	12780		
$\rightarrow {}^1\Gamma_3({}^1D)$	15561	15350	15420
$\rightarrow {}^1\Gamma_5({}^1D)$	21913	21220	21360
$\rightarrow {}^3\Gamma_3({}^3P)$	23710		
$\rightarrow {}^3\Gamma_5({}^3P)$	24013	23650	24050
$\rightarrow {}^3\Gamma_4({}^3P)$	24092		
$\rightarrow {}^1\Gamma_1({}^1G)$	24149		
$\rightarrow {}^3\Gamma_1({}^3P)$	24392		
$\rightarrow {}^1\Gamma_4({}^1G)$	27194		
$\rightarrow {}^1\Gamma_3({}^1G)$	32320		
$\rightarrow {}^1\Gamma_5({}^1G)$	32798		
$\rightarrow {}^1\Gamma_1({}^1S)$	60643		

developed a calculation of the frequency shift from the model of antiferromagnetic coupling through a superexchange interaction of the $d\delta$ orbitals of the Mn^{2+} ions with the fluorine orbitals. The effect of magnetic ordering on both the ground and excited states was determined and good agreement obtained with experiment.

The measurements here were performed to confirm the identification of the large frequency shift with antiferromagnetic ordering processes by showing that such shift occurs in the same temperature region as does the ordering process itself.

4. Experimental Results and Discussion for $KMnF_3$

The optical absorption of this substance was recorded at 4°K, 20°K and 77°K and room temperature. In agreement with the results of Hrostowski and Kaiser (1959) the absorption bands and lines occur in almost identical frequency positions to those of MnF_2. However, the structure on the bands is different and as an example, the $^6A_{1g}(^6S) \rightarrow {}^4T_{2g}(^4D)$ and $^6A_{1g}(^6S) \rightarrow {}^4A_{1g}, {}^4E_g(^4G)$ absorptions are recorded in Figures C.4 and C.5 and may be compared to those of MnF_2 in Figures C.1 and C.2 respectively.

$KMnF_3$ crystallises in the cubic perovskite structure (Beckman and Knox (1961)) at room temperature, but distorts below 184°K to an orthorhombic phase and below 81.5°K a further distortion occurs. This distortion of magnetic compounds near and below the magnetic transition temperature is discussed by Kanamori (1960). Its occurrence in $KMnF_3$ greatly complicates an analysis of the structure of the optical absorption bands.

FIGURE C7 $^3A_2(^3F) \rightarrow {}^3T_2(^3F)$ optical absorption band in $KMgF_3:Ni^{2+}$.

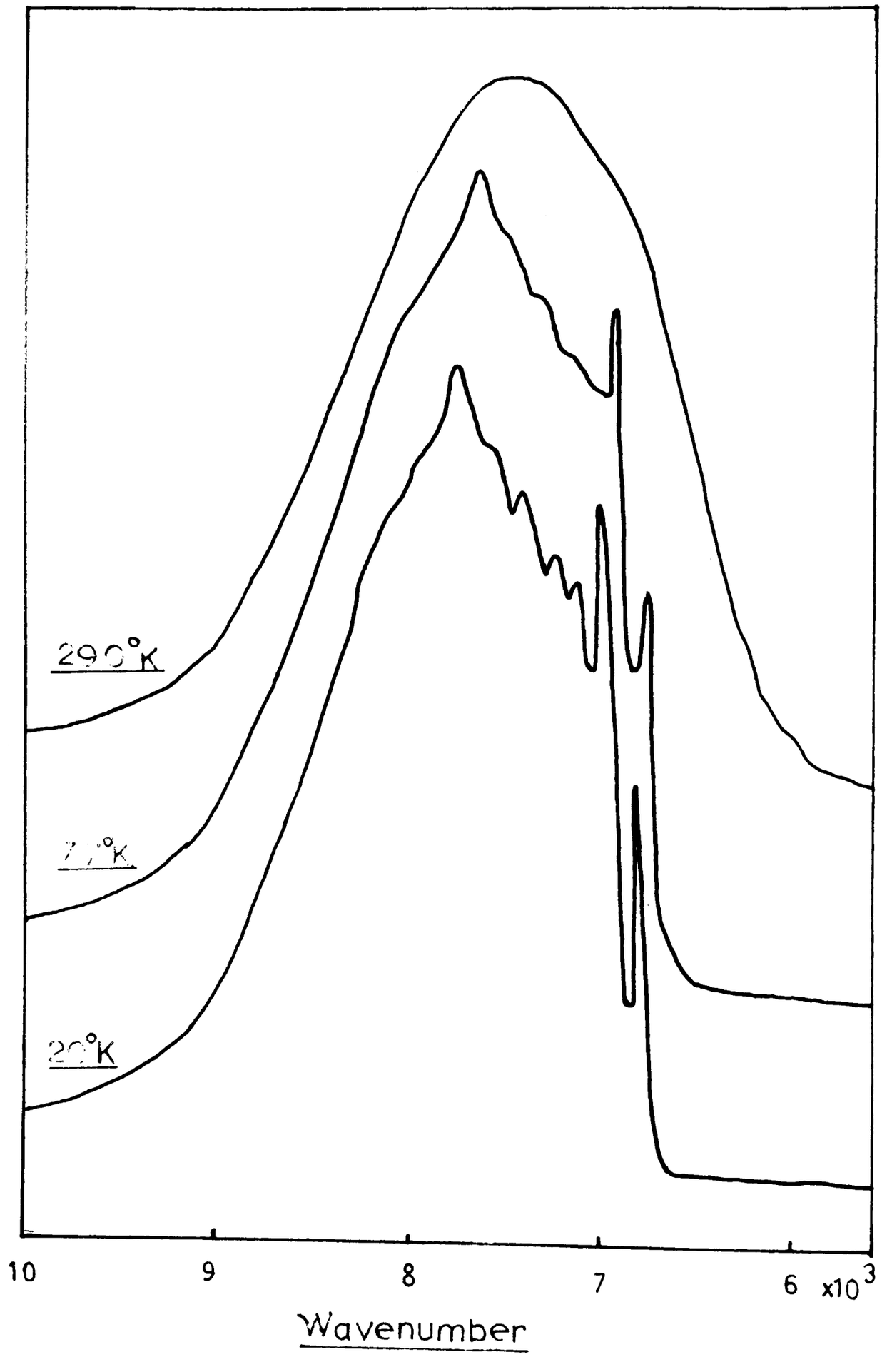

The shift of the one main line at 25250cm^{-1} is shown in Figure C.6. There is a slight inflection in the frequency verus temperature plot near 90°K, which is close to the temperature of the main antiferromagnetic ordering transition, (88.3°K). However, the line shift below this temperature is quite large and, in view of the complexity of the magnetic behaviour of this substance (Heeger, Beckman and Portis (1961)), this cannot be simply explained.

5. Experimental Observations and Discussion for $KMgF_3:Ni^{2+}$ and $KNiF_3$

The optical absorption spectra of these substances were recorded at 20°K, 77°K and room temperature. The room temperature results are given in Table C.1. together with the energy level assignment. This data was chosen for fitting to the energy level scheme of the $3d^8$ configuration (discussed in Chapter 2) because it is, in the case of $KNiF_3$, the only data unperturbed by antiferromagnetic ordering. The two sets of data, one for $KNiF_3$ and the other for $KMgF_3:Ni^{2+}$, are sufficiently close for the same values of B, C, and λ to be used. Hall, Hayes, Stevenson and Wilkens (1963) report a g value of 2.28 for nickel in $KMgF_3$ and this yields $\lambda = -250cm^{-1}$ The values, obtained by fitting the $3d^8$ energy levels to the experimental data, for Dq, B and C are -730cm^{-1}, 950 and 4200cm^{-1} respectively and $\frac{C}{B} = 4.4$ B here is 8% less than free ion value while C is 13% less than free ion value.

The bands show considerable vibrational structure and this is

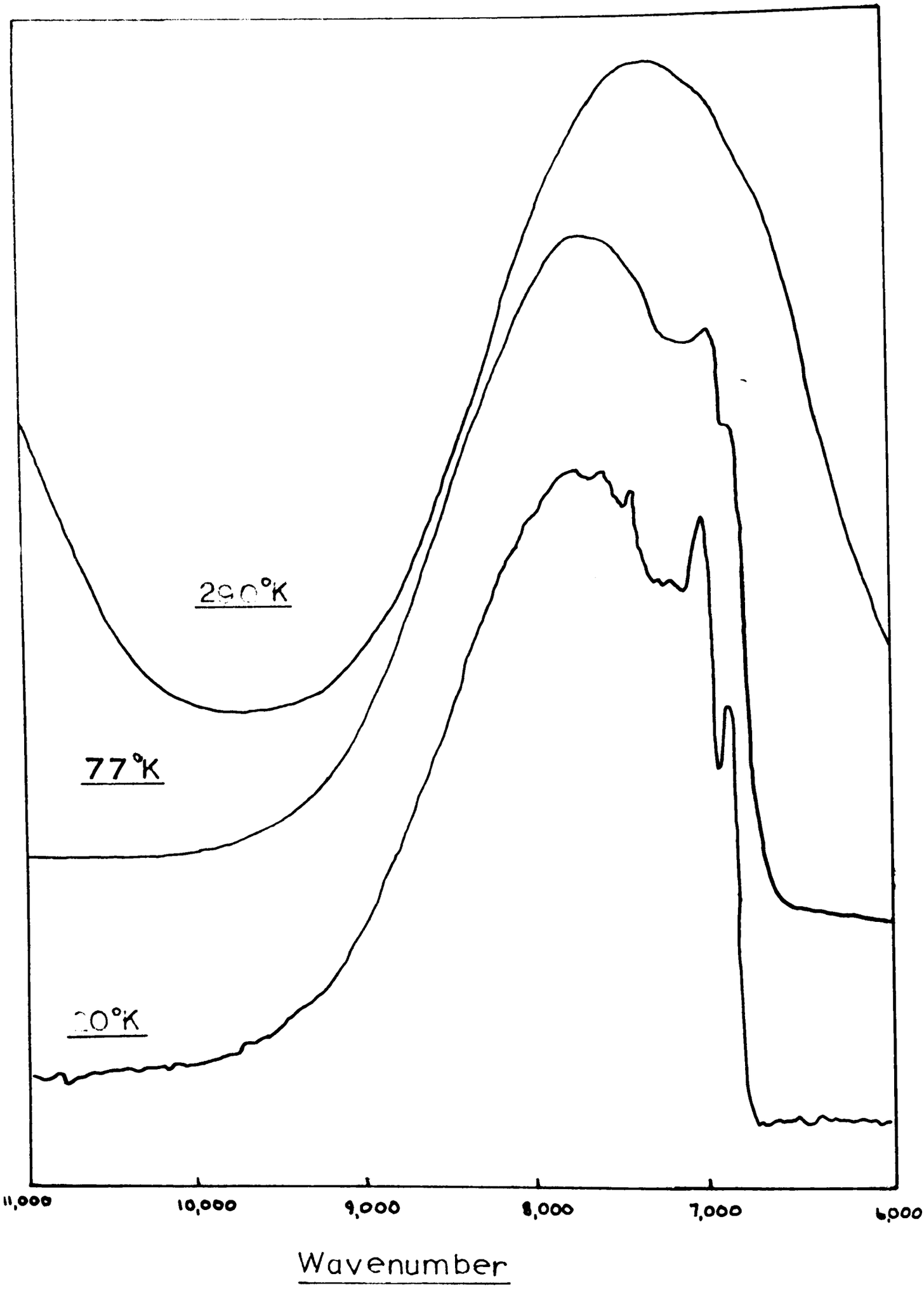

FIGURE 28 $^3A_2(^3F \rightarrow {}^3T_1(^3F)$ transition of $KNiF_3$

Illustrated by Figures C.7 and C.8 which show the absorption band corresponding to the first spin allowed transition $^3A_2(^3F) \rightarrow {}^3T_2(^3F)$ for $KMgF_3:Ni^{2+}$ and $KNiF_3$ respectively. As in the case of MnF_2, a knowledge of the vibrational frequencies of these substances is required before this vibrational structure could be satisfactorily interpreted.

The $KNiF_3$ spectrum also displays additional absorption bands beyond 28000 cm^{-1}, and extending to 50000 cm^{-1}, which are of weaker intensity than the absorption bands listed above in Table C.1. These bands cannot be fitted to the $3d^8$ configuration and appear to be $3d^8 \rightarrow 3d^7 4s$ transitions of the weak intensity type discussed by Jorgensen (1955). No quantitative explanation is offered for their frequencies or intensities.

Of the absorption bands which are well understood and arise from the $3d^8$ configuration the $^1E(^1D)$ level has the same parent strong field configuration ($d\varepsilon^6 d\gamma^2$) as the ground state $^3A_2(^3F)$ and thus the optical absorption band corresponding to the transition to this level is sharp. Figure C.9 shows this line for both $KNiF_3$ and $KMgF_3:Ni^{2+}$ for the three temperatures 20°K, 77°K and 290°K. The room temperature $KNiF_3$ line becomes at 77°K a doublet whose mean frequency is displaced 420cm^{-1} to higher wavenumbers while the room temperature $KMgF_3:Ni^{2+}$ line also splits to become a doublet, but is only displaced 80 cm^{-1} to higher wavenumbers. The pattern of the temperature dependence of these frequency shifts is shown in Figure C.10. The $KNiF_3$ line clearly undergoes a large frequency shift below the Néel

FIGURE C9 Optical absorption line corresponding to the transition $^3A_2(^3F) \rightarrow {}^1E(^1D)$ of Ni^{2+} for (a) $KNiF_3$ and (b) $KMgF_3:Ni^{2+}$.

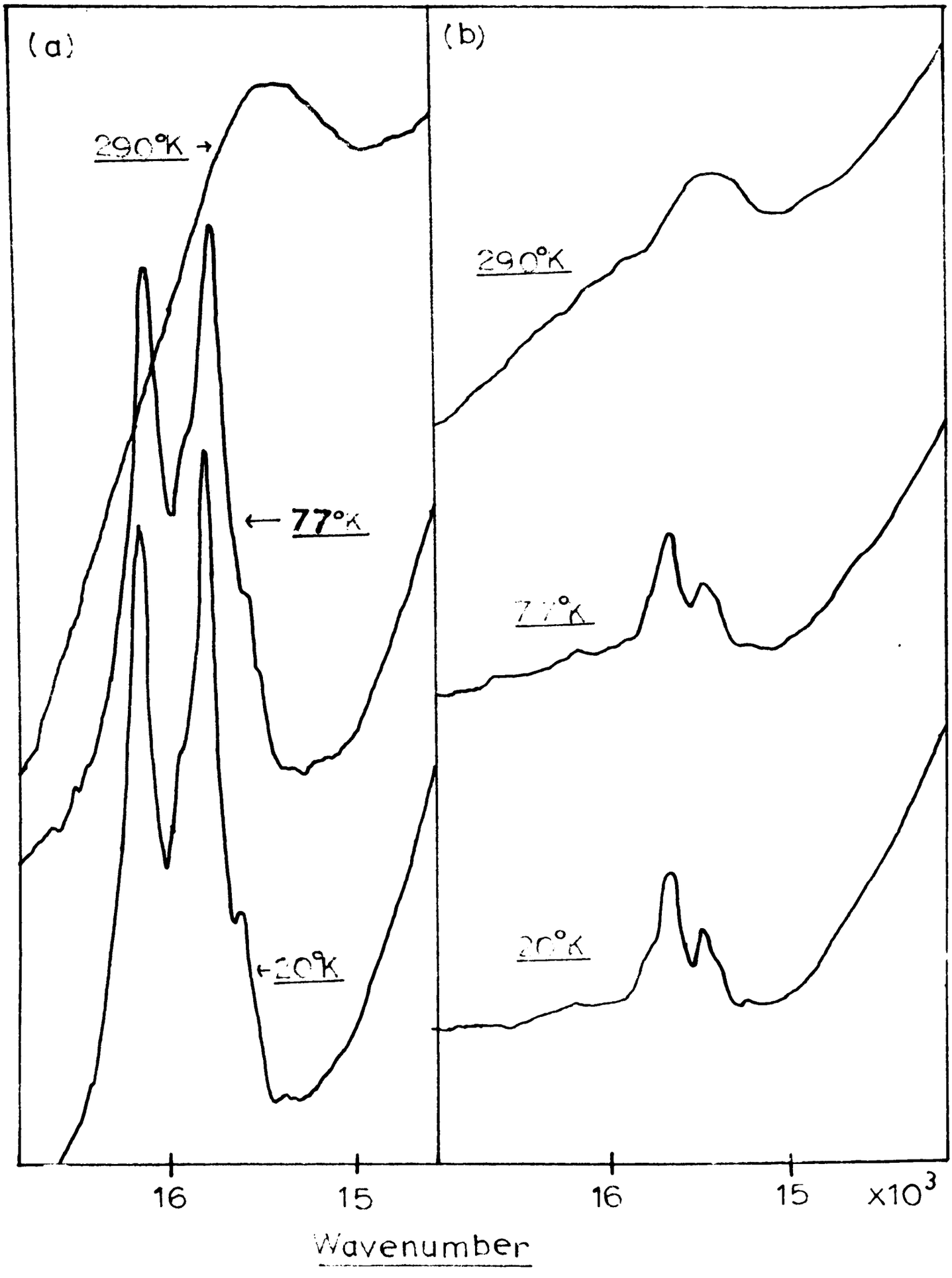

temperature (275°K) and the doublet is formed by the appearance of a satellite line below this temperature. The $KMgF_3:Ni^{2+}$ line is, at room temperature, a poorly resolved doublet which, on cooling, becomes clearly resolved and very little frequency shift of either line occurs from 300°K to 20°K.

The slight displacement of the $KMgF_3:Ni^{2+}$ lines is attributed to thermal contraction of the lattice and subtracting this shift from the $KNiF_3$ frequency shift leaves a frequency shift of 340 cm^{-1} due to antiferromagnetic ordering processes in the latter crystal.

Using the previously described formula of Sugano and Tanabe (1963) for the stabilisation of the ground state, the frequency shift, E, is calculated to be:

$$E = \frac{3kT_N}{S + 1}$$

and with S = 1, E = 290 cm^{-1} which is in good agreement with the observed shift.

Since the completion of the experimental work on $KNiF_3$ described here, a report on the same substance was published by Knox, Schulman and Sugano (1963) and the results obtained by them are in good agreement with those given here. As in their work, no explanation can be offered for the occurrence of the additional satellite line appearing on $KNiF_3$ below the Néel temperature. It has been discussed by Sugano and Tanabe (1963), but no conclusive explanation was offered by them.

The results of Knox, Schulman and Sugano (1963) also agree in the frequency shift of the $KNiF_3$ line being largest at about 240°K (see

FIGURE C10 Effect of antiferromagnetic ordering on the $^3T_2 \rightarrow {}^1E$ transition of Ni^{2+}.

(a) $KNiF_3$ ——

(b) $KMgF_3:Ni^{2+}$ - - - -

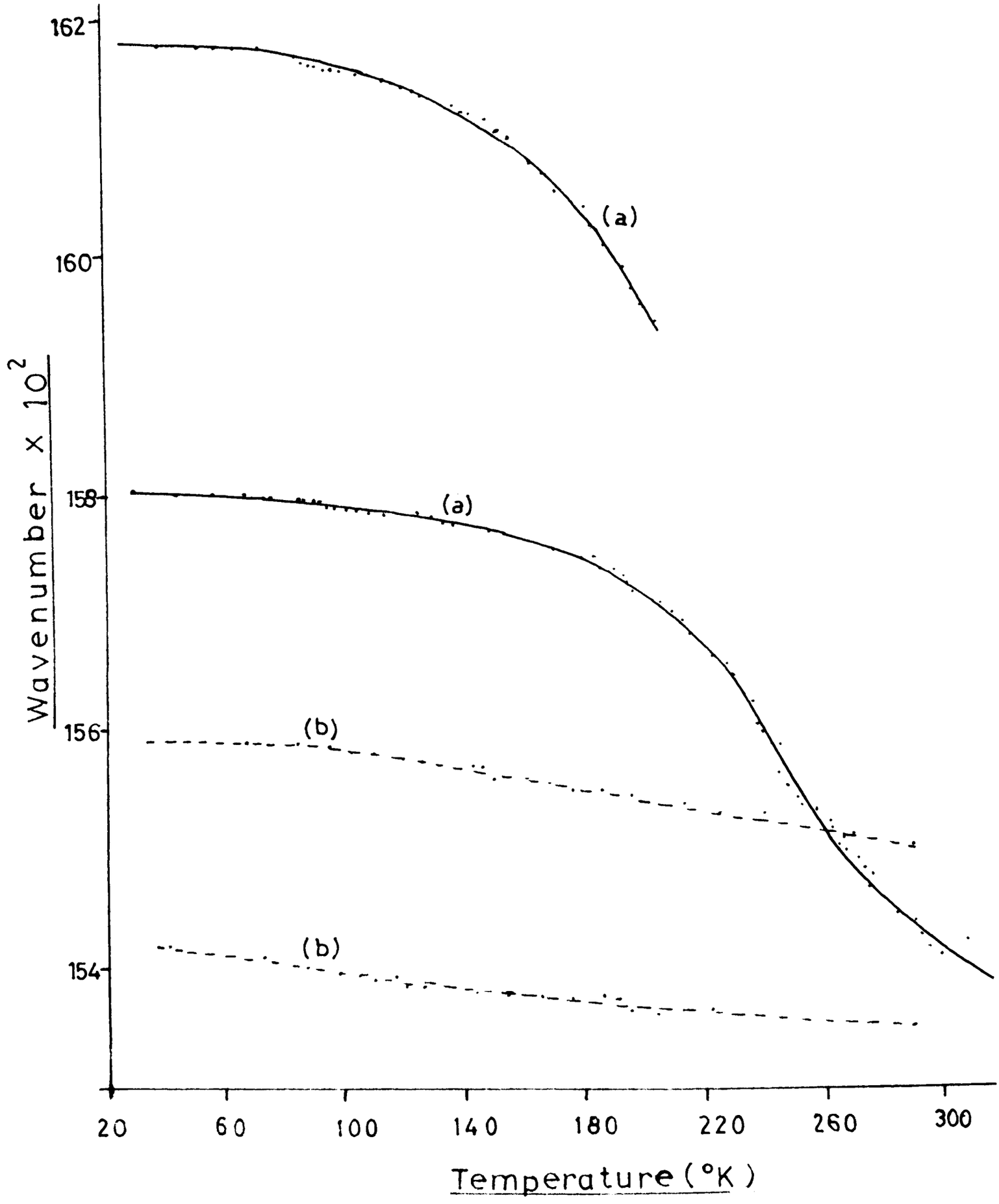

their Figure 4) and not at the Néel temperature (275°K). This behaviour of $KNiF_3$ is in marked contrast to that of MnF_2 and $KMnF_3$ where the largest shift occurred just above the Néel temperature. It would appear that the onset of magnetic ordering differs in the two cases and this is reflected in the frequency shifts.

6. Additional Magnetic Materials

Several other substances that show antiferromagnetic ordering phenomena were investigated in this research work. They were, with their Néel temperatures in brackets, FeF_2 (90°K), $KFeF_3$ (113°K), $FeCl_2$ (24°K) and $CoCl_2$ (25°K). However, in all cases, there was no pronounced frequency shift that could be attributed to antiferromagnetic ordering. The detection of such shift was hampered by the greater width of the optical lines in these substances, but the negative result for $CoCl_2$ is in agreement with the subsequent work on this substance by Ferguson, Wood and Knox (1963).

Recently, Belyaeva and Eremenko (Soviet Physics JETP 17, 319, 1963) reported a strong temperature dependence of the optical absorption bandwidth for MnF_2 crystals in the temperature range below the Néel point. The bandwidth in the paramagnetic region depended weakly on the temperature. They suggest that the width in the antiferromagnetic crystals is governed by interactions with oscillations of the ionic magnetic moments. In the work done here on FeF_2 a similar behaviour was observed (Figure C11) and it is suggested that a similar linewidth mechanism is operative in this substance.

FIGURE C11

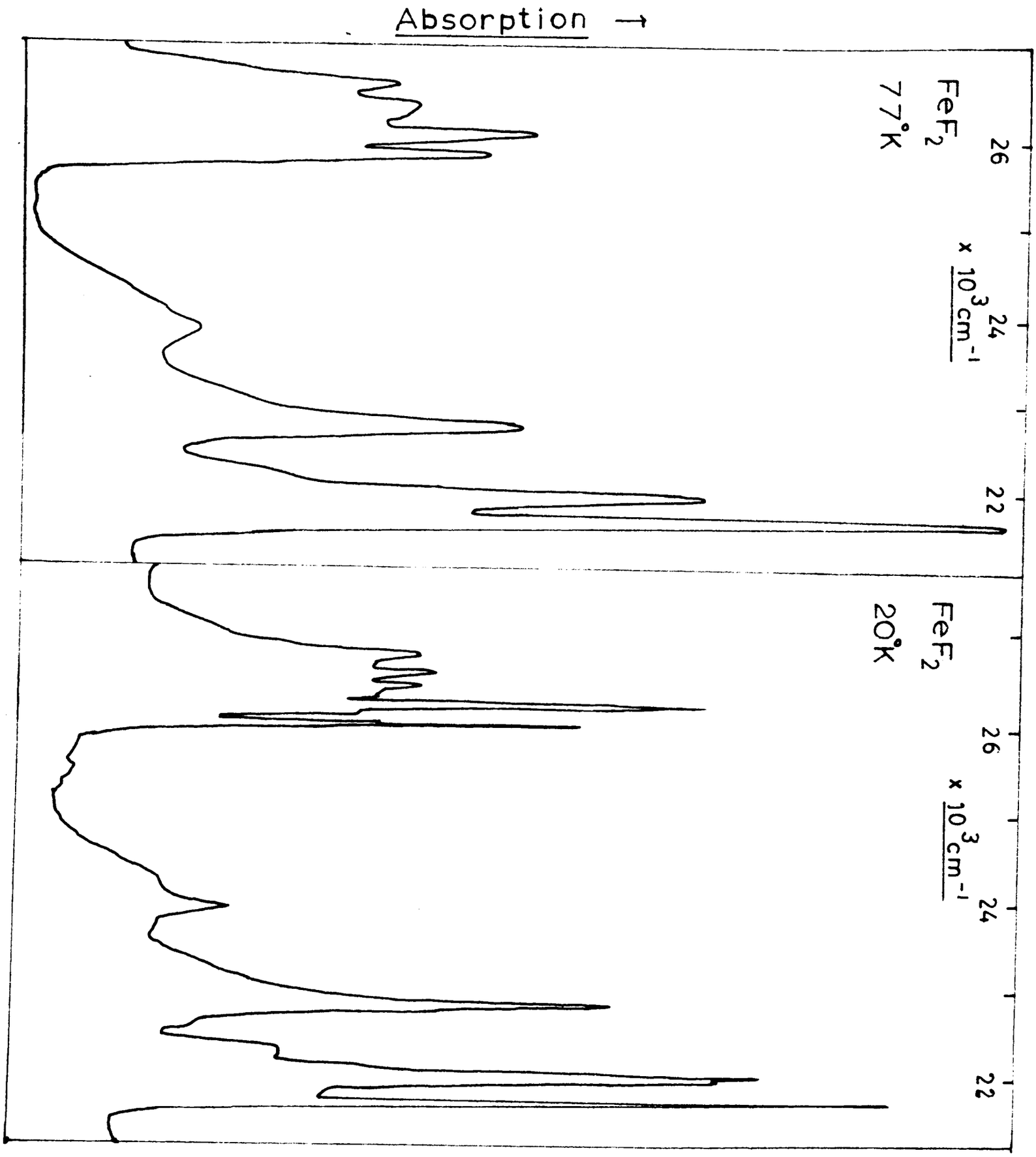

Optical absorption of Ferrous fluoride at 77°K and 20°K temperatures in the 24000cm^{-1} region.

REFERENCES

Baker, J. M., Lourens, J. A. J., and Stevenson, R. W. H., 1961, Proc. Phy. Soc. 77 1038

Beckman, O., and Knox, K., 1961, Phys. Rev., 121, 376

Erickson, R. A., 1953, Phys. Rev., 90, 779

Ferguson, J., Wood, D. L. and Knox, K., 1963, J.Chem.Phys., 39, 881

Finlayson, D. M., Robertson, I.S., Smith, T. and Stevenson, R. W. H., 1960, Proc.Phys.Soc. 76, 355

Foex, M., 1948, Compt. rend., 227, 193

de Haas, W. J., Schultz, B. H., and Koolhaas, J., 1940, Physica 7 57

Hall, T. P. P., Hayes, W., Stevenson, R. W. H., and Wilkens, J. 1963 J.Chem.Phys. 38, 1977

Heeger, A. J., Beckman, O., and Portis, A. M.,1961, Phys.Rev., 123, 1652

Hirakawa, K., Hirakawa, K., and Hashimoto, T., 1960, J. Phys. Soc. Japan, 15, 2063

Hrostowski, H. J., and Kaiser, R. H., 1959, Bull. Amer.Phys.Soc.,4, 167

Jorgensen, C. K. 1955, Acta Chem. Scand., 9, 717

Kanamori, J., 1958, Proc. Theor. Physics, 20, 890

Kanamori, J., 1959, J. Phys. Chem. Solids, 10, 87

Kanamori, J., 1960, J.Appl. Physics Suppl., 31, 145

Knox, K., Schulman, R. G. and Sugano, S., 1963, Phys.Rev., 130, 512

Millar, R. W., 1928, J. Am. Chem. Soc., 50, 1875

Newman, R., and Chrenko, R. M. 1959a, Phys.Rev. 114, 1507

Newman, R., and Chrenko, R. M. 1959b, Phys.Rev. 115, 882, 1147

Okazaki, A., Suemune, Y., and Fuchikami, T., 1959, J.Phys.Soc.Japan 14, 1823

Pratt, G. W. and Coehlo, R., 1959, Phys.Rev. 116, 281

Stout, J. W., 1959, J. Chem. Phys., 31, 709

Sugano, S., and Tanabe, Y., 1963, Tech. Rept. I.S.S.P. Ser. A No. 71

Tsujikawa, I., 1958, J. Phys. Soc. Japan 13, 315

Tsujikawa, I., and Kanda, E., 1959, J. Phys. Radium, 20, 352

CHAPTER FIVE

OPTICAL ABSORPTION BY HOLMIUM IN CALCIUM FLUORIDE

1. Introduction

It has long been known that compounds of the trivalent rare-earth ions have absorption spectra consisting of groups of lines in the near infrared, visible and ultraviolet regions. These arise from transitions within the $4f^n$ configuration. The energy levels of the free rare-earth ion are characterised by total angular momentum J and these are split up by the crystal field to give groups of levels. The line groups observed arise from transitions to these groups.

Calcium fluoride forms an excellent host material for studying the optical absorption of rare earth ions. It is completely transparent from 1200A° to 12μ and it has cubic symmetry. Rare earth ions in both divalent and trivalent form can readily be incorporated in this lattice and these ions substitute for the Ca^{2+} ion. However, the site symmetry around a trivalent ion may be reduced by the presence of charge compensating defects such as interstitial F^- ions (Baker, Hayes and O'Brien (1960)) or substitutional O^{2-} ions (Sierro (1961)). Friedman and Low (1960) have related the occurrence of charge compensating defects adjacent to the impurity ion with the conditions of growth and subsequent quenching of the doped crystals.

The rare earth investigated here was holmium. This was chosen as the electron spin resonance spectrum was being studied by J. W. Twidell of this laboratory and, furthermore, the complete spin orbit matrices

TABLE D.1. Centres of gravity of the bands of Ho^{3+} in CaF_2 at liquid hydrogen temperature. The energy levels of the $4f^{10}$ configuration calculated from the matrices of Reilly (1953) and Crozier and Runciman (1961) are included for comparison.

Experimental Band Position (cm^{-1})	Calculated Energy Levels	SLJ Label
-	0	$^5I_8$
5300	5272	$^5I_7$
8900	8825	$^5I_6$
11500	11344	$^5I_5$
-	13435	$^5I_4$
15700	15624	$^5F_5$
18700	18135	$^5S_2$
	18978	$^5F_4$
	19502	$^3K_8$
20600	21028	$^5F_3$
21500	21133	$^5F_2$
22200	22437	$^5G_6$
	22519	$^5F_1$
24200	23659	$^5G_5$
	24485	$^3K_7$
26200	25813	$^5G_4$

for the f^4 and the complementary f^{10} configuration had been recently published by Crozier and Runciman (1961).

2. Experimental Details

The crystals of calcium fluoride containing 0.1 to 1% molar concentration of holmium were supplied by Mervyn Instruments Ltd. The rare earth was added to the melt in the form of holmium oxide, Ho_2O_3; no scavenging or reducing agents were used.

The spectrophotometer and cryostat described in Chapter 2 were employed here for the optical measurements.

3. Experimental Results and Discussion

The optical absorption of the crystals were investigated in the range 46000 to 4000 cm^{-1} at the three temperatures 20°K, 77°K and room temperature. The spectrum consists of groups separated by several thousand cm^{-1}. Each group consists of lines extending over several hundred cm^{-1}. The wavenumbers of the centres of these groups are listed in Table D.1 together with the level assignments. The structure of the groups is clearly resolved at liquid hydrogen temperature and the lines are resolution limited by the bandwidth (20 cm^{-1}).of the spectrophotometer. Because of these equipment limitations it was not possible to analyse the line structure of each group in detail. The structure observed with the resolution available here showed in general more lines than would be produced by a purely cubic crystal field on the J level of the group and this indicates that the trivalent holmium ion is not in a cubic symmetry site.

The groups of lines can be fitted to the energy level scheme for

Experimental Band Position (cm^{-1})	Calculated Energy Levels	SLJ label
	26799	$^3L_9$
	26899	$^5G_6$
27500	27758	$^5G_5$
	27776	$^5F_2$
	28452	$^3K_6$
	29133	$^3F_4$
28800	29296	$^5G_3$
29800	30861	$^5G_2$
	32120	$^3M_{10}$
	32326	$^3L_8$
	32414	$^3P_1$
	32501	$^3D_3$
	34102	$^1L_8$
	34252	$^3G_3$
34600	34739	$^5G_4$
	34899	$^3P_0$
	35485	$^5G_2$
35600	35721	$^5D_4$
	35940	$^3F_5$
	36015	$^3L_7$
	36553	$^3I_7$
	36863	$^3P_2$

the $4f^{10}$ configuration. Reilly (1953) has given the electrostatic energy matrices for this configuration and these have been extended by Crozier and Runciman (1961) to include the effects of spin orbit coupling. These matrices contain the quantities E^1, E^2 and E^3 (which are appropriate linear combinations of the Slater paramters F_k) and also the spin orbit constant λ. These are regarded as parameters to be determined from the experimental data. In the analysis here a simplification was introduced by assuming hydrogenic wavefunctions and this reduced the number of electrostatic energy parameters to one. The parameters chosen as representing the best fit to the experimental data were $\lambda = -2200cm^{-1}$, $E^1 = 6200cm^{-1}$, $E^2 = 32.5\ cm^{-1}$ and $E^3 = 630\ cm^{-1}$. The energy levels calculated are listed in Table D.1. The agreement between the calculated and experimental data could obviously be improved by considering other than hydrogenic wavefunction ratios for the electrostatic parameters, but in view of the approximately 400 cm^{-1} width of the line groups such refinement was not considered necessary.

In the resonance work, no electron spin resonance was observable in the crystals before X-irradiation and this is consistent with the diamagnetic ground state of Ho^{3+} in CaF_2 (Lea, Leask and Wolf (1962)). After room temperature X-irradiation the crystals show, at 4°K, a spectrum due to Ho^{2+} ions in cubic sites. These ions result from the capture of electrons, produced in the X-irradiation, by the Ho^{3+} ions. The initially yellow crystal, when irradiated, becomes purplish then black and this colour change is due to the growth of two bands at

Experimental Band Position (cm^{-1})	Calculated Energy Levels	SLJ label
	37473	$^3M_9$
	37589	$^3I_5$
	38025	$^3I_6$
38500	38112	$^3F_4$
	39604	$^3D_1$
40000	40339	$^5D_3$
41300	41419	$^5D_4$
	42618	$^5D_2$
42600		
	42784	$^5D_3$
	43576	$^3H_6$
	43605	$^3M_8$
	43858	$^5D_0$
	43972	$^5D_1$
	44241	$^3H_4$
45200 ?	44282	$^5D_2$
	46612	$^3H_5$
	47504	$^3F_3$
	47790	$^1H_5$
	47909	$^1D_2$
	48095	$^1K_7$
	49170	$^1G_4$

27000 cm^{-1} and 18000 cm^{-1} which are associated with the presence of oxygen in the lattice. These bands are formed in pure calcium fluoride crystals that have been additively coloured (Gorlich (1961)) and fine crystals that have been heated in oxygen and subsequently X irradiated. A careful study of the lowest transition ($^5I_8 \rightarrow I_7$) of the Ho^{3+} ion was made to check whether any decrease in the concentration of these ions occurred on irradiation. It was found that even after 60 hours X-irradiation no apparent decrease in the absorption occurred and any decrease must be less than 3% of the total initial intensity. This is in agreement with the electron spin measurements which show that about 0.01% molar concentration of Ho^{2+} is produced by the X-irradiation and so, for a 0.5% concentration sample, represents a conversion of about 2% of the Ho^{3+} ions to divalent form.

REFERENCES

Baker, J. M., Hayes, W., and O'Brien, M. C. M., 1960
Proc.Roy.Soc. A254, 273

Crozier, M. H., and Runciman, W. A., 1961, J.Chem.Phys. 35, 1392

Friedman, E., and Low, W., 1960, J.Chem.Phys. 33, 1275

Gorlich, P., Karras, H., and Lehmann, K., 1961, Physica,
Status solidi, 1, 390

Lea, K. R., Leask, M. J. M., and Wold, P. W., 1962, J.Phys.Chem.Solids
23, 1381

Reilly, E. F., 1953, Phys. Rev., 91, 876

Sierro, J., 1961, J.Chem. Phys., 34, 2183

Table E.1 Frequencies of the quintet-quintet optical transitions for various compounds of divalent iron.

Compound	Temperature (°K)	Mean frequency of the absorption band (cm^{-1})	Splitting (cm^{-1})
FeF_2	290	8800	3600
	77	9050	3500
FeF_2	20	9150	3500
$KFeF_3$	290	8700	2200
	77	9100	2150
$KFeF_3$	20	9100	2150
$KMgF_3:Fe^{2+}$	290	9,250	1800
	77	9,500	1400
$KMgF_3:Fe^{2+}$	20	9,500	1350
$FeSiF_6.6H_2O$	290	9700	1400
	77	10,700*	-
$FeSiF_6.6H_2O$	20	10,700*	-
$FeCl_2$	290	7,000	1400
	77	7,400	800
	20	7,350	700
$MgO:Fe^{2+}$	290	10,300	1800
	77	10,900	1400
	20	10,850	1300

* no clearly resolved doublet structure

APPENDIX 2

MISCELLANEOUS OPTICAL PROBLEMS

Introduction

Several optical research problems that were investigated and yielded some results of interest are described here. The work on them could not be finalised and this forms a report on the present state of the research.

A. Optical Absorption of Divalent Iron

The optical absorption spectra of crystals of ferrous fluoride (FeF_2), potassium ferrous flouride ($KFeF_3$), potassium magnesium fluoride doped with divalent iron ($KMgF_3:Fe^{2+}$), ferrous fluosilicate ($FeSiF_6.6H_2O$), ferrous chloride ($FeCl_2$) and magnesium oxide crystals doped with divalent iron ($MgO:Fe^{2+}$) were measured at 20°K, 77°K and room temperature with the Unicam SP700 spectrophotometer.

The $3d^6$ energy level configuration applies to divalent iron and this is characterised by one spin-allowed transition $^5T_2(^5D) \rightarrow {}^5E(^5D)$ in the 10,000 cm^{-1} region and by several spin-forbidden quintet-triplet transitions at higher energies.

All the observed spectra clearly show the spin allowed quintet-quintet transition as a broad absorption band split into two components separated by frequencies ranging from 700 cm^{-1} to 3600 cm^{-1}. The splitting for the various compounds is listed in Table E.1. Splittings of the same type have been reported by Cotton and Meyers (1960) and by Holmes and McClure (1957) for $Fe(H_2O)_6^{2+}$ present in aqueous solutions.

The splitting was 2000 cm^{-1}.

This splitting is due to the raising of the degeneracy of the upper ^5E_g state of the optical transition. A similar splitting may be present in the ground state, but would not give rise to the spectra observed here as only the lowest component would be populated at low temperatures.

The splitting cannot be due to spin orbit coupling effects as the spin orbit parameter is only 100 cm^{-1} for Fe^{2+} and furthermore only splits the E_g upper state in second order. (Low and Weger (1960)).

The splitting could arise from non cubic crystal fields around the Fe^{2+} ion but such an explanation would not be valid for the cubic $MgO:Fe^{2+}$ crystal and not very likely for the nearly cubic $KMgF_3:Fe^{2+}$ and $KFeF_3$ crystals.

It is suggested that the splitting in these "cubic" crystals is largely due to dynamic Jahn-Teller effects of the type discussed by Longuet-Higgins et.al. (1958), and Liehr and Ballhausen (1958).

The theorem of Jahn and Teller (1937) states that electronically degenerate states of nonlinear molecules are unstable with respect to certain asymmetric displacements of their nuclei and will tend to distort in such a way as to remove the electronic degeneracy. If the stability attained by assuming an asymmetric nuclear configuration is no more than the zero point energy of a typical vibrational mode a special coupling between the electronic and nuclear motions will occur. These interactions constitute the dynamic Jahn Teller effect. The study of this coupling presents a complex problem. Longuet-Higgins et.al.

(1958) have considered the simple model of a doubly degenerate electronic state whose degeneracy is removed in the first order by a doubly degenerate vibration. It displays the essential features of the dynamic Jahn-Teller effect. Using this model Longuet-Higgins et.al. show that, for a vibronic transition from a singlet ground state to a doubly degenerate upper state, the envelope of the absorption band displays two intensity maxima (see their Figure 4). The optical transition of divalent iron corresponds to this vibronic transition so the double peaked absorption band experimentally observed is qualitatively explained.

Of the ferrous compounds studied here only the $MgO:Fe^{2+}$, $KMgF_3:Fe^{2+}$ and $KFeF_3$ have crystal cubic symmetry. All the rest are either orthorhombic (FeF_2) or trigonally distorted ($FeCl_2$, $FeSiF_6.6H_2O$). Electron spin resonance measurements by Low and Weger (1960) show that divalent iron in magnesium oxide is situated at a cubic symmetry site in the lattice. Similar electron spin resonance experiments on the $KMgF_3:Fe^{2+}$ crystals by T. P. P. Hall (1962) of this laboratory failed to reveal absorption due to divalent iron. It is concluded that this crystal is distorted sufficiently to prevent observation of the electron spin resonance spectrum. Wyckoff (1948) gives the symmetry of $KMgF_3$ as monoclinic ($a=b=c=8.00A°$, $\beta = 91°18'$). $KFeF_3$ has the ideal cubic perovskite structure at room temperature ($a = 4.122 \pm 001A°$), but distorts to become rhombodhedral ($a = 4.108 \pm 0.002A°$, $\alpha = 89° 51' \pm 1'$) at 78°K. (Okazaki, Suemune and Funchikami (1959)).

Thus the splittings observed in $MgO:Fe^{2+}$ and in room temperature $KFeF_3$ are the only ones representative of divalent iron in sites of pure cubic symmetry.

The quantitative explanation of these observed splittings is a difficult problem. Liehr and Ballhausen (1958) have calculated the splitting of various transition metal ion compounds and find splittings of several 1000 cm^{-1}, which are in order of magnitude with the experimental values found here. Blankenship and Linn Belford (1962) have performed related calculations for vanadium tetrachloride. It is expected that similar calculations performed for the ferrous iron systems studied here will yield values for the splitting of the magnitude observed.

B. Optical Absorption of the Self trapped hole in Calcium fluoride

Hayes and Twidell (1962) have described the electron spin resonance of the self trapped hole in calcium fluoride. This centre is created by low temperature irradiation of either pure or doped calcium fluoride crystals and it may be described as a molecular F_2^- ion type of centre aligned along <100> directions of the crystal. It is closely related to the F_2^- centre in LiF described by Castner and Kanzig (1957) and Woodruff and Kanzig (1958). It decays with luminescence at 138°K in pure calcium fluoride.

Such a centre would be expected, in analogue to the case of the alkali halides, to possess an optical absorption band. The main optical absorption band of F_2^- occurs in LiF at 348 mμ (28700 cm^{-1})(Delbecq, Hayes and Yuster (1961)) and a search was made for similar bands in

calcium fluoride. Pure calcium fluoride crystals did not colour on low temperature irradiation so thulium doped calcium fluoride crystals were used. X-irradiation at liquid nitrogen temperature produced several absorption bands, some of which corresponded to bands produced also by room temperature irradiation and the others were attributed to divalent thulium ions. On warming this crystal to room temperature the decay of an absorption band centred at 28,000 cm^{-1} (360 mμ) occurred at 140°K. This band forms the shoulder of a strong broad absorption band centred at 32,000 cm^{-1} and so is difficult to detect. To confirm that this band at 28,000 cm^{-1} is related to the electron spin resonance F_2^- centre of Hayes and Twidell (1962) it will be necessary to perform polarised bleaching experiments in which the centres are re-oriented into certain symmetry directions of the crystal, by polarised bleaching radiation of 360 mμ frequency. Such re-orientation of the centres would readily show in the electron spin resonance spectrum. The peak of the absorption band of the F_2^- centres could be determined by studying the rate of orientation with frequency of the bleaching light.

The present state of this research work on the optical absorption band of the F_2^- centre is rather unsettled. The low temperature X-irradiation of hydrogenated calcium fluoride crystals was described in Chapter One and in particular a band at 23000 cm^{-1} was formed. This annealed at 140°K which is the temperature of decay of the electron spin resonance F_2^- centre. It would thus seem that a band at 23000 cm^{-1} in additively coloured calcium fluoride crystals (of which hydrogenated calcium fluoride is an example) is related to this centre. Obviously,

there are several aspects of the problem needing further investigation. Polarised bleaching electron spin resonance experiments, polarised bleaching optical experiments of the type described in Chapter Three and correlated electron spin resonance + optical experiments will have to be performed to definitely identify the optical absorption band of the self trapped hole in calcium fluoride.

REFERENCES

Blankenship, F.A., and Linn Belford, R., 1962, J.Chem.Phys. 36, 633

Castner, T.G., and Kanzig, W., 1957, J.Phys.Chem.Solids, 3, 178

Cotton, F.A., and Meyers, M.D., 1960, J.Am.Chem.Soc. 82, 5033

Delbecq, C.J., Hayes, W., and Yuster, P.H., 1961, J.Chem.Phys., 35, 1521

Hall, T.P.P. 1962, Thesis, Clarendon Laboratory, Oxford

Hayes, W., and Twidell, J.W., 1961, Proc.Phys.Soc., 79, 1295

Holmes, O.G., and McClure, D.S., 1957, J.Chem.Phys., 26, 1686

Jahn, H. A., and Teller, E., 1937, Proc.Roy.Soc. A161, 220

Liehr, A.D., and Ballhausen, C.J., 1958, Annals of Physics, 3, 304

Longuet-Higgins, H.C., Opik, U., Pryce, M.H.L. and Sack,R.A., 1958
Proc. Roy. Soc. A 244, 1.

Low, W., and Weger, M., 1960, Phys. Rev., 118, 1119, 1130

Okazaki, A., Suemune, Y., and Fuchikami, 1959, J.Phys.Soc.Japan, 14, 1823

Woodruff, T.O., and Kanzig, W., 1958, J.Phys. Chem.Solids, 4, 268

Wyckoff, R.W.G., 1948, Crystal Structures (New York: Interscience).